Precision Medicine in early recurrent prostate cancer; identification of metastases by PSMA PET MRI

THESIS

Dr Andre Joshi MBBS

Abstract

Prostate cancer (PCa) is the second most common cause of cancer deaths and 6th leading cause of all male deaths in Australia. Approximately 25 - 50% of all patients undergoing definitive therapy (surgery or radiotherapy) develop biochemical recurrence (BCR). There is a clinical need for more accurate imaging modalities to detect micro-metastatic or low volume disease in early BCR after primary treatment for prostate cancer. Positron emission tomography (PET) using a novel prostate specific membrane antigen (PSMA) ligand has been used to detect localised and metastatic prostate cancer lesions with improved sensitivity and specificity compared with standard imaging. Hybrid PET/magnetic resonance imaging (MRI) systems yielding MRI characterisation of lesions in addition to PET avidity has recently become available. The clinical role and efficacy of this new imaging modality is not yet established.

Precision medicine aims to provide the right treatment, to the right patient for the right cancer at the right time. It is the overall concept of individualising patient management based on their specific tumour characteristics and biology as opposed to traditional histological subtypes. A precision medicine approach has not been explored previously in early recurrent prostate cancer.

Through a prospective clinical trial, we aimed to address this clinical need for more sensitive and specific imaging by evaluating the sensitivity and specificity as well as the clinical implications of PSMA PET/MRI in men with BCR following therapy of curative intent. More sensitive and specific imaging technologies have the potential to detect micro-metastatic and low volume recurrent disease with greater accuracy and could potentially alter standard of care treatment options for patients.

Additionally as a proof of principle we aimed to apply novel organoid culture technology to develop patient derived cell models to allow drug testing and next generation sequencing (NGS) as part of a precision medicine approach to early recurrent prostate cancer. We first tackled the inherent difficulty of in vitro culture of prostate cancer using novel culture technology and then the development of local culture and drug screen protocols. The amplification of patient samples enabled the downstream drug screen and NGS analysis of patient samples.

We have found that PSMA PET/MRI may be useful in staging men with biochemical recurrence, especially when prostate specific antigen (PSA) is low. Our data demonstrates a high detection rate of disease, especially for locally recurrent disease in the pelvis, outperforming standard of care (SOC) imaging. Furthermore, successful culture of a novel patient derived cell line with subsequent patient specific therapeutic screening and NGS has provided proof of principle for a precision medicine approach in the management of early recurrent prostate cancer for the very first time.

With the ability to identify foci of early recurrent disease using PSMA PET/MRI, we are able to treat and sample cancer foci to subsequently allow *in vitro* amplification, therapeutic screening and NGS to allow targeted management for patients. This methodology and findings could have a significant impact on outcomes and potentially alter standard of care treatment options for patients.

Table of Contents

List of Abbreviations

°C	Degree Celsius
μg	Microgram
μl	Microliter
μM	Micromoles
μmol	Micromole/L
2D	Two Dimensional
3D	Three Dimensional
ADT	Androgen deprivation therapy
AR	Androgen receptor
BCR	Biochemical Recurrence
BRAF/RAF1	B-Raf proto-oncogene/Raf-1 Proto-Oncogene
cDNA	Complementary DNA
CM	Conditioned media
CO_2	Carbon dioxide
CRPC	Castrate resistant prostate cancer
CT	Computed tomography
CTC	Circulating tumour cell
DHT	5-dihydrotestosterone
DMSO	Dimethyl sulphoxide
DNA	Deoxynucleic acid
EBRT	External beam radiotherapy
FBS	Fetal bovine serum
Gl	Gleason
HCM	Hans Clever's organoid culture media
HEK293TNog	HEK293T-Noggin
HEK293TR	HEK293T-HA-Rspol-Fc
l	Liters
LDR	Low Dose Rate
mA	Milliamps
mCRPC	Metastatic castrate resistant prostate cancer
MDT	Multi-disciplinary team
mg	Milligrams
min	Minutes
ml	Milliliters
MRAC	MRI-based attenuation correction
MRI	Magnetic resonance imaging
mRNA	Messenger RNA
mRNAseq	mRNA sequencing
MSK3	MSK-PCa 3
mTOR	Mammalian target of rapamycin inhibitor

MW	Molecular weight
n	Number
ng	Nanograms
NGS	Next generation sequencing
nm	Nanometers
nM	Nanomoles
PAH	Princess Alexandra Hospital
PBS	Phosphate buffered saline
PCa	Prostate cancer
PDX	Patient derived xenograft
PET	Positron emission tomography
PIK3CA/B	Phosphatidylinositol-4, 5-bisphosphate 3-kinase catalytic subunit alpha/beta
Poly-O	Poly-L-ornithine
PSA	Prostate specific antigen
PSMA	Prostate specific membrane antigen
qRT-PCR	Quantitative reverse transcription- polymerase chain reaction
RALP	Robotic assisted prostatectomy
RBWH	Royal Brisbane and Women's Hospital
RNA	Ribonucleic acid
rpm	Revolutions per minute
RRP	Retropubic prostatectomy
RTK	Receptor tyrosine kinase
RT-PCR	Reverse transcription- polymerase chain reaction
SOC	Standard of care
SPECT	Single-photon emission computed tomography
SRT	Salvage radiotherapy
SUV	Standardized uptake value
SV	Seminal vesicle
TBS	Tris buffered saline
U	Units
USA	United States of America
v/v	Volume for volume
WBBS	Whole body bone scintigraphy
ZBTB16/PLZF	Zinc Finger and BTB Domain Containing 16/Promyelocytic leukaemia zinc finger protein

List of Tables

List of Figures

Statement of Original Authorship

"The work contained in this thesis has not been previously submitted to meet requirements for an award at this or any other higher education institution. To the best of my knowledge and belief, the thesis contains no material previously published or written by another person except where due reference is made."

Where stated, data has been reproduced with permission from Dr Cheryl Nicholson and Dr Saeid Alinezhad.

QUT Verified Signature

Andre Joshi

October 2018

Acknowledgements

First and foremost I would like to take this opportunity to firstly thank our patients and their families for being a part of this study. Without them none of the following work would be possible.

I would like to show my gratitude to my supervisors, Steve, Jenni, Liz and Prof Nelson for their guidance, ideas, support and patience through my studies. Thank you for pushing me, guiding me and constantly challenging me to be better. Thank you for taking time to answer my many questions, even if they were often drifting.

To Dr Vela, thank you for not only pushing me in the lab but guiding and challenging me clinically, becoming a priceless mentor as I enter formal urology training.

To the Vela team - Handoo, Cheryl and Alex, couldn't have asked for a better group of colleagues and friends, thank you. Without your help I would have been lost during my transition into the lab. Handoo, sorry for eating everything – I stress eat.

I would like to thank everyone at the APCRC-Q for their constant support and the much needed guidance during the initial weeks. I would like to acknowledge Saeid, Anja, Gregor, Lisa, Ellca, Brett, Nataly, Varinder, Lydia and Mei for their constant guidance, collaborations and answering my continuous questions in the lab.

Thank you to all the clinicians at the Princess Alexandra and Greenslopes hospital for referring patients for our trial. I would also like to thank all the staff of the Radiology and Urology Departments of Princess Alexandra Hospital.

Finally I would like to acknowledge my family for their constant support and encouragement to always strive for more. To them I owe more than I could every repay. Thank you.

Chapter 1 - Literature Review

1.1 - Introduction

Prostate cancer (PCa) is the second most common cause of cancer deaths and 6th leading cause of all male deaths in Australia (1). In the year 2016, 18,138 men were diagnosed with PCa, and 3,398 men died as a result of their disease (Table 1.1, Table 1.2). This has increased from 2,666 deaths in 2000, despite a 5 year survival (2008-2012) of 94% (2). Similar trends have been reported worldwide (3).

Table 1.1 *Estimated new cases of cancers in Australia 2017 (1, 2)*

Cancer Type	New Cases	% of all new cancer diagnoses
Prostate (males)	16,665	23.1 (in men)
Melanoma	13,941	10.4
Breast (females)	17,586	28.4 (in females)
Colorectal	16,682	12.4
Lung	12,434	9.3

Table 1.2 *Estimated cancers deaths in Australia 2017 (1, 2)*

Cancer Type	Number of deaths	% of all cancer deaths
Prostate (males)	3,452	12.7
Breast (females)	3,087	14.9
Colorectal	4,114	8.6
Lung	9,021	18.9

PCa diagnosis and staging requires clinical examination, blood tests (prostate specific antigen (PSA), urea, electrolytes, and liver function tests), histopathological confirmation and imaging such as computed tomography (CT), whole body bone scintigraphy (WBBS) or magnetic resonance imaging (MRI). Despite these investigations prior to definitive treatment of localized cancer, up to 50% of patients will develop biochemical or clinical recurrence after surgery or radiotherapy (4). This highlights the inadequacy of our current staging modalities.

1.2 – Biochemical Recurrence

Approximately 25 - 50% of all patients undergoing definitive therapy (surgery or radiotherapy) develop biochemical recurrence, defined as a rise in PSA to 0.2ng/ml post-surgery or a rise in PSA of 2ng/ml from nadir post radiotherapy (4).

When patients have developed biochemical recurrence without evidence of metastatic disease on SOC imaging (CT chest, abdomen, pelvis and WBBS) post-surgery, salvage external beam radiotherapy (EBRT) is often performed. The risk of PSA progression following salvage treatment however is 10%, 50% and 80% for low (PSA doubling time > 15 months, biopsy Gleason score < 7, clinical stage < cT3a and time to BCR > 3 years), intermediate and high (PSA doubling time < 3 months, time to biochemical progression < 3 years, Gleason score 8-10 or clinical stage cT3b-T4) risk groups respectively; again highlighting the inadequacy of current imaging modalities as lesions outside of the radiation field are often not identified and therefore inadequately treated (5, 6).

If further treatment is required, patients progress onto androgen deprivation therapy (ADT) (7). The inevitable consequence of long term ADT in advanced prostate cancer is treatment resistance, with the development of castrate resistant prostate cancer (CRPC). As treatment resistance occurs, second, third and fourth line systemic agents in various sequences and combinations may be utilised. These include androgen receptor (AR) and androgen targeting agents such as enzalutamide and abiraterone or chemotherapy agents, such as docetaxel and cabazitaxel (Figure 1.1) (4, 7). The morbidity associated with these treatments in progressive, advanced metastatic disease is highly significant and therapies are not curative. Therefore, it would be of clinical value to be able to predict failure or success of future treatments in patients with biochemical recurrence.
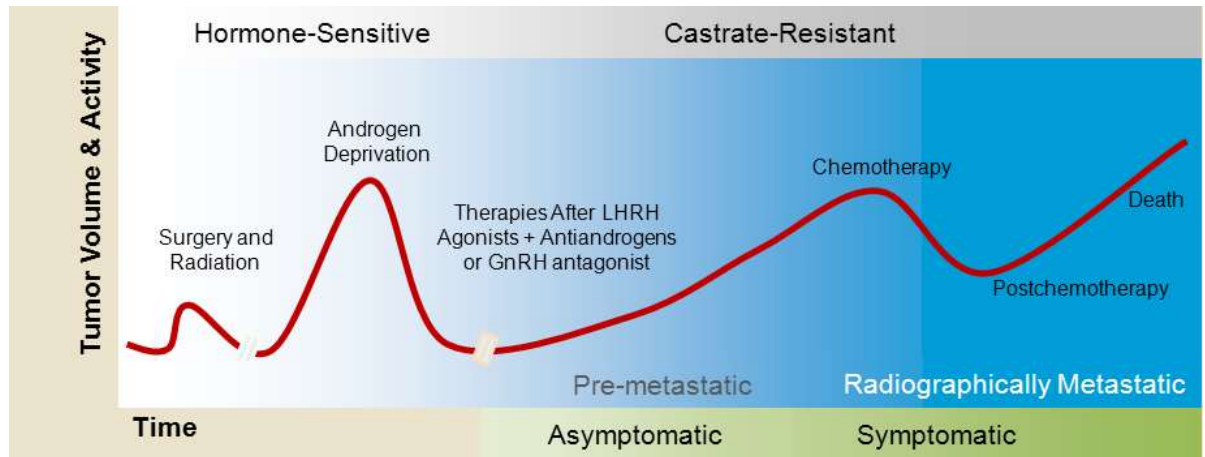
Figure 1.1 *Prostate cancer treatment landscape (8)* Tumour volume is represented by the red line over time, orange boxes represent non-linear time progression. Patients are initially hormone sensitive and asymptomatic and progress onto symptomatic metastatic castrate resistant disease. Initially patients are treated with surgery and or radiation therapy. Once patients have biochemical recurrence they are treated with radiotherapy and/or androgen deprivation therapy before progressing onto second line antiandrogens and eventually chemotherapy. The eventual outcome of this however is treatment resistance and progression, with patients continuing to recur despite these salvage options, leading to death. LHRH: Luteinizing hormone-releasing hormone; GnRH: Gonadotropin-releasing hormone.

Following biochemical recurrence, patients are currently staged with CT, WBBS, single-photon emission computed tomography (SPECT CT) and MRI. In the early phases of biochemical recurrence however, none of these modalities are sensitive enough to routinely detect micro-metastatic, low volume metastatic or locally recurrent disease.

The probability of a positive bone scan is <5% even when the PSA level may be as high as 7ng/mL (normal level post-surgery <0.01 ng/mL) and the mean PSA level associated with a positive CT scan was as high as 27.4 ng/mL in a recent retrospective review (4, 9). There is, therefore, a significant clinical need for more sensitive and specific imaging technologies to detect micro-metastatic and low volume recurrent disease. This could potentially alter SOC treatment options and hopefully lead to improved long term outcomes. Furthermore, patients with negative scans could be managed with more conservative modalities such as watchful waiting, potentially avoiding or delaying the adverse and potentially toxic side effects of treatment.

1.3 – Use of Positron Emission Tomography (PET) in Prostate Cancer

Numerous novel imaging technologies have been introduced to overcome the poor sensitivity and specificity of the current standard imaging modalities. Positron emission tomography (PET) has emerged as a promising imaging tool for cancer with newly developed tracers providing more sensitive and specific imaging for detection of recurrent and metastatic PCa. PET imaging combines radiolabeled tracers using gamma cameras with CT or MRI for anatomical localization. These tracers include monoclonal antibodies against prostate specific membrane antigen (PSMA), 18F-Fluro-Deoxyglucose (18F-FDG), 18F-Fluorocholine (18F-Choline) and 11C-Choline, outlined in Table 1.3 below (10, 11).

Table 1.3 *PET Tracers investigated in prostate cancer*

PET Tracer	Method of Uptake
18F-Fluro-Deoxyglucose (18F-FDG)	Glucose metabolism
18F-Fluorocholine	Lipogenesis in cellular membrane biosynthesis
11C-Choline	Lipogenesis in cellular membrane biosynthesis
68Ga-PSMA	Transmembrane glycoprotein

These various PET tracers are limited in their cancer detecting abilities and are explored widely in the literature. The most commonly used PET radiotracer in cancer detection 18F-FDG, has limited sensitivity for PCa due to the typically low glucose consumption of PCa and artefacts created from high bladder activity due to the urinary excretion of tracer (12, 13). Furthermore it is limited by a relative lack of specificity and does not assess soft-tissue metastases adequately (14). A positive 18F-FDG PET avid lesion has a 62% risk of malignancy (11, 15).

11C-Choline has been used to identify men with oligometastatic disease when diagnosed with biochemical recurrence, with promising results. A retrospective two centre study with 150 patients showed that a major change to a clinical decision was made in 27 patients (18%) as a result of 11C-Choline PET/CT. The study further identified 14 of the 55 (25.5%) patients scheduled for palliative ADT being switched to curative salvage therapy based on 11C-choline PET/CT results. Salvage therapy induced a complete biochemical response in 35.7% of these patients (5 of 14) at the end of a median follow-up of 18.3 months (range, 10-48 months) (16). This study, like most exploring this area, is limited by fairly small population size, retrospective nature, and lack of histologic confirmation affecting the validity of results

These PET tracers have been further evaluated in systematic reviews. The sensitivity and specificity of 11C-Choline was 84% and 79% respectively (17), and 62% and 92% for 18F-Choline (17, 18). This data suggests that PET offers a promising and sensitive imaging modality with the potential to influence treatment choices for patients with biochemically recurrent prostate cancer. These promising findings have led to the investigation and evaluation of other potential PET tracers, in particular the use of 68Ga-PSMA PET imaging.

1.4 – Prostate Specific Membrane Antigen (PSMA)

Prostate-specific membrane antigen (PSMA) also known as glutamate carboxypeptidase II, N-acetyl-a-linked acidic dipeptidase I, or folate hydrolase, is a type II transmembrane protein belonging to the M28 peptidase family (19, 20). It is a cell surface protein, which is highly expressed in normal prostate tissue as well as primary and metastatic PCa. Up to 98% of cases of lymph node metastases have been reported to express PSMA (21, 22). PSMA is located in the cytosol in normal prostate cells and becomes membrane bound in carcinoma. The level of PSMA expression rises with increasing tumour dedifferentiation, rising Gleason grade and in metastatic and hormone-refractory cancers (19, 20). Expression is also up to a thousand times higher in PCa cells compared to other PSMA-expressing tissues, such as kidney or salivary glands and only ~ 10% of prostate cancers do not overexpress PSMA (20, 21, 23). This protein thus provides a promising target for prostate carcinoma-specific imaging and has even been identified as a potential target for delivery of therapeutic agents (Theranostics) such as cytotoxins or radionuclides (23).

Monoclonal antibodies targeting both intra and extracellular domains of PSMA have been developed. One example is the J591 monoclonal antibody targeting the extracellular domain of PSMA that localizes to viable tumour cells (24). The clinical uptake of this antibody however has been limited by a long circulating half-life resulting in high non-specific background activity, poor pharmacokinetics and pharmacodynamics and overall poor tumour penetration (20, 24).

Over the last 24 months, a small molecule ligand targeting PSMA (PSMA HBED-CC) linked to a 68 Gallium isotope (68Ga-PSMA) for PET/CT or PET/MRI has gained widespread popularity in Australia and Europe due to reported high sensitivity and specificity for PCa. Recent large case

series, clinical trials and systematic reviews indicate significantly improved detection compared to other PET tracers.

The 68Ga-PSMA HBED-CC ligand (Glu-NH-CO-NH-Lys(Ahx)-HBED-CC) was initially described by Eder et al. in 2012(25). This molecule binds to the PSMA receptor on the PCa cell surface causing internalization and a high accumulation of the ligand (Figure 1.2). This results in the visualisation of even small metastases with the added benefit of being cleared rapidly from non-target tissues (20, 25).
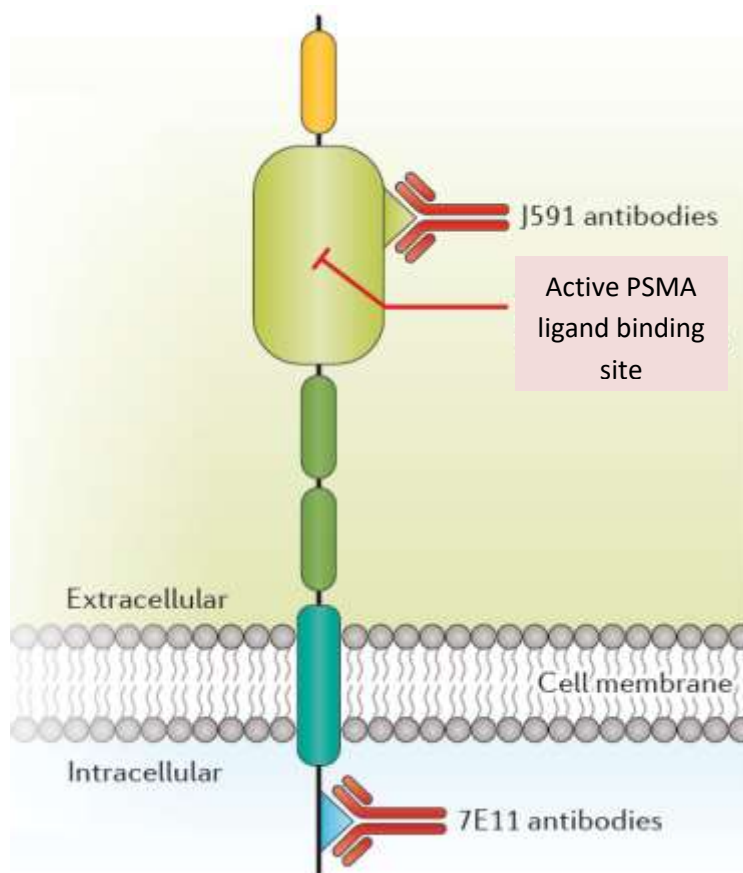
Figure 1.2 *Prostate-specific membrane antigen (PSMA) structure.* The molecule contains intracellular, transmembrane, and extracellular domains. The active site targeted by PSMA ligands used for PSMA PET imaging is located in the extracellular domain. Adapted from Maurer et al (20).

1.5 – The Clinical Uptake of Prostate Specific Membrane Antigen (PSMA) PET in Biochemically Recurrent Prostate Cancer

There is a growing body of evidence supporting the use of 68Ga-PSMA PET in PCa, especially in the biochemically recurrent setting. Initial data suggests 68Ga-PSMA PET/CT significantly improves detection of metastatic prostate cancer lesions, even at very low PSA levels, and could potentially replace current conventional standard of care imaging modalities such as CT, WBBS and MRI.

Retrospective studies, have shown promising results. In a retrospective analysis of 319 patients who underwent 68Ga-PSMA PET/CT from 2011 to 2014, Afshar-Oromieh et al. demonstrated the sensitivity, specificity, negative predictive value, and positive predictive value of 68Ga-PSMA PET/CT to be 76.6%, 100%, 91.4% and 100% respectively on a lesion-based analysis (26). Another large European study of 248 patients with biochemical recurrence demonstrated that 68Ga-PSMA PET/CT had a detection rate of >90% at PSA levels over 1 ng/mL, and positive 68Ga-PSMA PET/CT findings for PSA-values <1 ng/mL in 67% of the patients (27).

Australian data has also demonstrated similar results. Of a cohort of 532 men, the detection rate of metastatic lesions for 68Ga-PSMA PET/CT was 11.3% for PSA 0.01 to <0.2 ng/mL, 26.6% for PSA 0.2 to <0.5 ng/mL, 53.3% for PSA 0.5 to <1 ng/mL, 79.1% for PSA 1 to <2 ng/mL and 95.5% for PSA ≥2 (28). Many of the identified lesions were not confirmed histologically however. This lack of biopsy proven cancer is a current weakness in the literature with potential false positive lesions identified on scans not being histologically confirmed.

In a recent meta-analysis of 68Ga-PSMA PET/CT in 1309 patients the overall percentage of positive 68Ga-PSMA PET scans in the biochemical recurrence cohort in this study was 76%. Positive 68Ga-PSMA PET scans for biochemically recurrent patients increased with PSA level. For PSA ranges of 0-0.2, 0.2-1, 1-2, and >2 ng/ml, 42%, 58%, 76%, and 95% scans, respectively, were positive for lesions. Finally overall on a per-lesion analysis, the sensitivity and specificity were 80% and 97% respectively (29). Another systematic review analysing 1256 patients showed that 68Ga-PSMA PET/CT detected recurrence in 799 of 983 patients (81%). This review also demonstrated a 50% detection rate (74 of 147 patients) for PSA of 0.2–0.49 ng/ml and a 53% detection rate (56 of 195 patients) for restaging PSA of 0.50–0.99 ng/ml (30).

Development of radiolabelled PMSA ligands has shown improved detection rates when compared to other ligands. A recent study has demonstrated the benefits of the 68Ga-PSMA ligand over 18F-fluoromethylcholine PET/CT in the setting of biochemical recurrence post primary therapy (31). This retrospective review of 37 patients revealed 86.5% of the patients had at least one lesion detected in 68Ga-PSMA PET/CT compared to only 70.3% using 18F-Fluoromethylcholine PET/CT. The study further revealed that at PSA values of 2.82ng/ml and less, at least one lesion was identified in 68.8% of patients, while all patients presented with pathological lesions at PSA values greater than 2.82ng/ml with 68Ga-PSMA (31). Using the same threshold for 18F-fluoromethylcholine PET/CT, only 43.8% of patients presented with at least one lesion at PSA levels of 2.82ng/ml and less. Furthermore all lesions detected by 18F-fluoromethylcholine PET/CT were also detected by 68Ga-PSMA PET/CT. A patient in the series even had a positive 68Ga-PSMA PET/CT with a PSA of 0.01ng/ml (31). Thus 68Ga-PSMA PET was found to detect foci of recurrent cancer with greater sensitivity when compared to 18F-fluoromethylcholine, even at low PSA levels (31).

Similarly in a large cohort of 4426 scans, the optimal PSA cut-off value of a positive 11C-Choline PET/CT scan was 1.16 ng/ml (32). This suggests that 68Ga-PSMA is substantially more sensitive at low PSA levels than choline PET/CT. Therefore 68Ga-PSMA PET/CT can potentially be used to substantially improve detection of PCa lesions even at low PSA levels.

Hybrid PET/MRI scanners utilizing the 68Ga-PSMA ligand have recently been reported. This new hybrid PET/MRI imaging has now been introduced in select centres in Australia and internationally to potentially provide improved anatomical characterization of lesions through MRI with the added benefits of PSMA PET avidity. Small retrospective studies (n=20) have demonstrated promising results with 68Ga-PSMA PET/MRI for the detection of biochemical recurrence of PCA over 68Ga-PSMA PET/CT (33). PCa foci were detected with higher contrast with Ga-PSMA PET/MRI than with PET/CT. PET/MRI systems have the potential added benefit of lower radiation coupled with higher anatomical definition provided by MRI. This reduction in radiation exposure may be especially important in younger patients and those requiring multiple follow-up examinations (33). The study did however reveal that the PET/MRI frequently produced a reduced signal ("halo" artefact) around the urinary bladder and at the level of the kidneys, making image interpretation difficult and requiring special attention in interpretation (33).

PSMA PET/MRI may provide increased diagnostic accuracy as a result of the combination with multi parametric MRI, which has a higher detection efficacy for locally recurrent tumours than CT (20). This combination might be able to improve detection rates in patients with very low serum PSA values (<0.5 ng/ml) (20).

With ongoing studies investigating the benefits of hybrid PET/MRI, clinicians may be able to stage men locally and systemically with a single scan, with lower radiation for patients at PSA levels as low as <1 ng/ml. This modality has the potential to significantly improve PCa staging even further and allow earlier identification of recurrent/distant disease when compared to SOC imaging. The clinical role and efficacy of this new imaging modality however is still to be established.

1.6 – Precision Medicine in Prostate Cancer

Precision medicine aims to provide the right cancer treatment, to the right patient at the right time. It is the overall concept of individualising patient management based on their specific tumour characteristics and biology as opposed to traditional histological subtypes. This aims to improve clinical outcomes, decrease morbidity and improve survival in men with advanced PCa.

In order for precision medicine to become a reality, identification of predictive biomarkers is necessary. Unfortunately, in biochemical recurrence and in particular the metastatic CRPC (mCRPC) setting, there has been difficulty in obtaining clinical samples and a subsequent lack of genomic data to identify potentially targetable alterations or biomarkers for responses or resistance to therapies (34-36).

A recent, large-scale study has attempted to significantly add to the body of knowledge in order to identify potential therapeutic targets. Robinson et al and the Stand up To Cancer (SU2C/PCF) Prostate Cancer Dream Team described how metastatic lesions from 150 patients with mCRPC were biopsied for DNA and RNA sequencing (34). The biopsies sequenced were from lymph node (42%), bone (28.7%), liver (12.7%), and other soft tissues (16.7%). Using next generation sequencing (NGS) technologies such as whole genome and whole exome

sequencing, approximately 90% of patients with advanced disease had actionable aberrations (34). This rate of actionable aberrations was a lot higher than previously reported in PC (34).

The study reported that aberrations of androgen receptor (AR), ETS genes, TP53, and Phosphatase and tensin homolog (PTEN) were frequent in up to 40%–60% of cases (34). Furthermore, multiple new genomic alterations were identified in phosphatidylinositol-4, 5-bisphosphate 3-kinase catalytic subunit alpha/beta (PIK3CA/B), R-Spondin, B-Raf proto-oncogene/Raf-1 Proto-Oncogene (BRAF/RAF1), APC, β-catenin, and Zinc Finger and BTB Domain Containing 16/Promyelocytic leukaemia zinc finger protein (ZBTB16/PLZF). Aberrations of BRCA2, BRCA1, and ATM were observed at substantially higher frequencies (19.3% overall) when compared to primary PCa. Indeed, 89% of affected individuals harboured a clinically actionable aberration, including 62.7% with aberrations in AR, 65% in other cancer-related genes, and 8% with actionable pathogenic germline alterations (34).

In identifying these clinically actionable aberrations, this study provides valuable information that could impact treatment decisions for affected individuals (Figure 1.3). For example, a patient with an AR-V7 splice variant of the androgen receptor, (which has been implicated in abiraterone acetate and enzalutamide resistance), could benefit from alternate therapeutic options, such as up front chemotherapy (37, 38). Furthermore SPOP, CHD1 and ERG status can be used for segregation, as they suggest future AR loss and possibly aggressive cancer development. Tumours with loss of RB on the other hand may require aggressive treatment as RB loss has been shown to increase AR expression (38, 39). As outlined in figure 1.3, further applications of this approach could include patients receiving dovitinib (a pan receptor tyrosine kinase (RTK) inhibitor) or everolimus (a mammalian target of rapamycin (mTOR) inhibitor), on the basis of gain-of-function mutations in RTKs, or PTEN/AKT respectively in individual's tumours. Tumours with unregulated protein kinase B (AKT) or gain-of- function mutations in AKT can be treated with everolimus, to inhibit mTOR, a downstream target of AKT (34, 38).

Neuroendocrine PCa is a highly aggressive subtype of prostate cancer with a low median survival (40, 41). It is considered to most commonly evolve from pre-existing prostate adenocarcinoma entering an AR independent state. The management of neuroendocrine PCa is difficult with poor understanding of this disease process clinically, histologically, and at a molecular level. As such there are no established management standards for patients with this

variant. Recent work has led to the identification of altered N-myc signalling and the upregulation of aurora kinase A. These aberrations, in particular aurora kinase A are targetable aberrations with ongoing clinical trials (40, 41). This highlights the potential to treat based on targetable molecular aberrations rather than on traditional histological subtypes.

However, it is important to appreciate that the identified target aberrations may in fact be non-functional or not driver mutations. Consequently, many of these "targets" in the patient may not be therapeutically relevant and therefore when targeted with drugs, not produce a clinical response. Thus *in vitro* therapeutic screening of patient derived cultures is required to show a functional effect of identified aberrations via NGS.
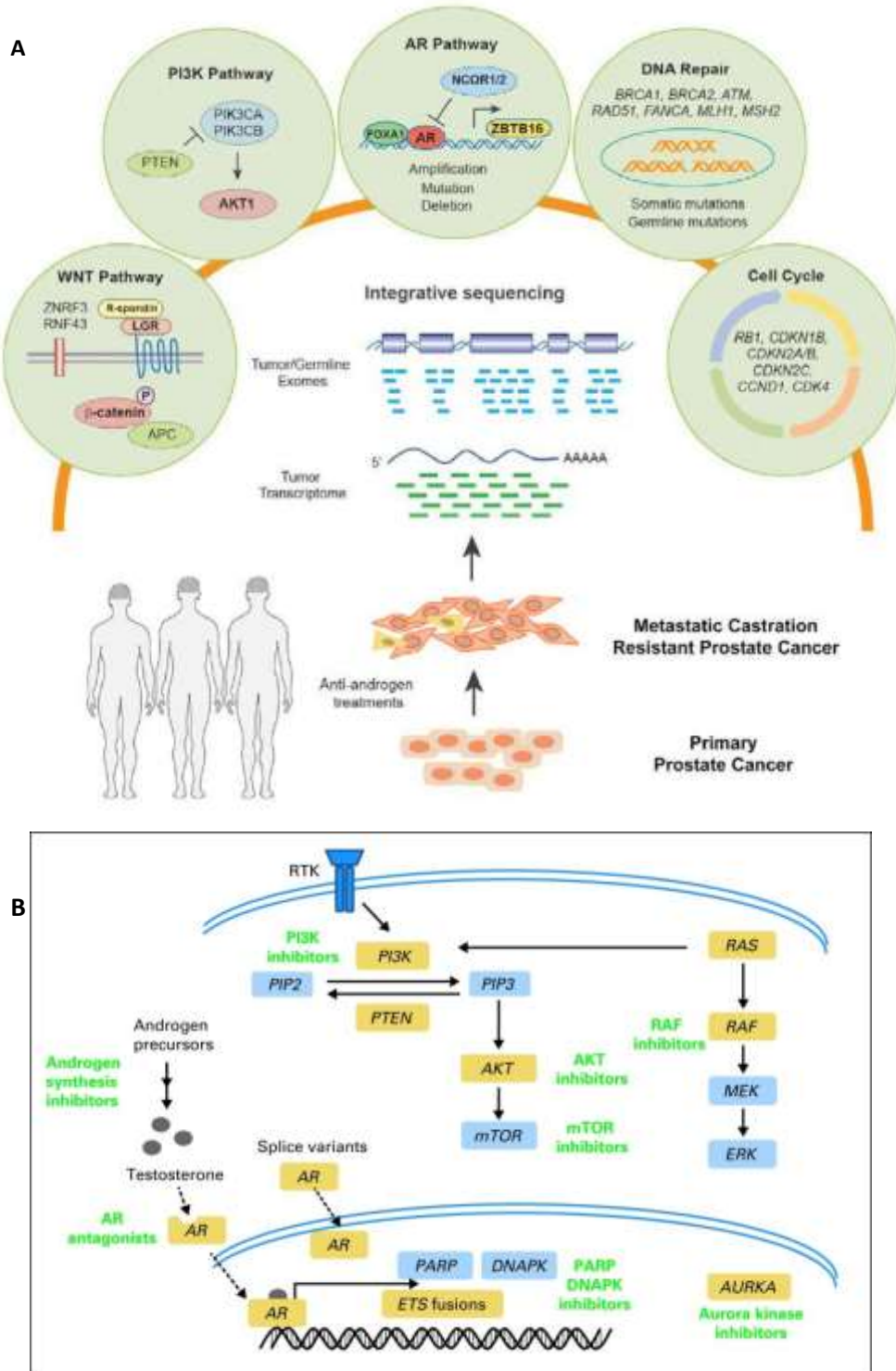
Figure 1.3 *Precision Medicine in Prostate Cancer* **(A)** Various examples of clinically targetable aberrations identified by sequencing individual metastasis samples. Reproduced from Robinson et al. (34) **(B)** Pathway guided management in prostate cancer. Reproduced from Roychowdhury et al. (36).

1.7 – Organoid Media Technology

Prostate cancer has remained challenging to culture *in vitro*, as demonstrated by the limited number of clinically relevant available cell line models despite multiple attempts internationally to establish models (42-49). This has hindered the study of tumour pathogenesis and the therapeutic responses of PCa. This under-representation of prostate cancer cell lines is due to the difficulty in propagating PCa cells *ex vivo* for extended periods whilst maintaining prostate tumour characteristics (50). Although various *in vivo* models are available, these are limited due to their expense, and are time-consuming and technically challenging (51).

Androgen receptor (AR) signalling is essential for prostate development, homeostasis, initiation and progression. Unfortunately, many established cell lines do not have an intact AR signalling pathway, thus making them poor models for clinically relevant research (50, 51) . Furthermore, these cells do not represent the common presentation of clinical disease, lacking many of the known genomic aberrations that underlie prostate tumourigenesis for example SPOP mutation, FOXA1 mutations and CDH1 loss (52-55).

1.7.1 Summary of available prostate cancer cell lines

As mentioned above, the establishment of PCa cell lines has been difficult. Several lines are available; however none fully represent the spectrum of clinical PCa. Many also are either androgen independent or do not express PSA again limiting their relevance to the most common forms of the clinical disease.

PC3

The PC3 cell was derived from a bony metastatic deposit in 1979 from a 62 year old Caucasian male (43). It has become one of the most widely utilised PCa cell lines. Despite this however the cell line does not represent the common clinical presentation. The cell line is both AR and PSA negative, and is androgen independent. The cell line also produces osteolytic bone metastasis, instead of the classical osteoblastic prostatic bone metastases seen most commonly in patients (43, 48).

LNCaP

The LNCaP cell line was derived from a left supraclavicular lymph node metastatic PCa deposit from a 50 year old male in 1977 (42). The cell line is hormone responsive with a mutated AR and expresses PSA (42). It is very slow growing in comparison to PC3 cells and is less tumorigenic, requiring a higher cell concentration for formation of tumours.

DU-145

The DU-145 cell line was derived from a central nervous system metastasis of a 69 year old Caucasian male with PCa and lymphocytic leukaemia at time of parieto-occipital craniotomy (48, 49). The tumour was described to be a moderately differentiated adenocarcinoma. DU-145 cells do not express AR or PSA. The line is also hormone insensitive like PC3 and also forms atypical osteolytic bone metastases (48).

DuCaP

The DuCaP cell line was derived from dura mater tissue taken at autopsy of a 60-year-old Caucasian male with hormone refractory widespread bony metastases. The line was initially propagated in SCID mice and the resultant patient derived xenograft (PDX) harvested and cultured *in vitro* to generate the cell line (47, 48). DuCaP cells are androgen sensitive and PSA and AR positive.

VCaP

The VCaP cell line was derived from the same patients as the DuCaP line (44, 48). Tissue was harvested at autopsy from a metastatic lesion in a lumbar vertebra. The tissue was xenografted into SCID mice, and later harvested and converted to in vitro culture. VCaP cells express AR and large quantities of PSA (44, 48).

MSK-PCa 3 (MSK3)

The novel MSK3 cell line described by Gao, Vela et al was derived from a retroperitoneal lymph node from a patient with castrate resistant metastatic prostate cancer previously treated with ADT, bicalutamide, docetaxel and carboplatin (5). The cell line expresses low levels of PSA and AR compared to LNCaP cells (5).

Table 1.4 *Summary of available prostate cancer cell lines*

Cell Line	AR	PSA	Androgen Response
PC3	Negative	Negative	Independent
LNCaP	Mutate AR	Positive	Dependant
DU-145	Negative	Negative	Independent
DuCaP	Positive	Positive	Dependant
VCaP	Positive	Positive	Dependant
MSK3	Low Positivity	Low Positivity	Weaklly dependant

AR: androgen receptor, PSA: prostate specific membrane antigen

1.7.2 Development of novel organoid media technology

Clevers and colleagues recently developed a novel androgen-responsive organoid culture system (50, 51). The use of this media has led to the development of additional prostate cancer cell lines, including the first PCa circulating tumour cell (CTC) cell line (50). Seven patient-derived PCa organoid lines were described. These lines express a wide range of common PCa genetic aberrations including SPOP mutation, PTEN loss, TMPRSS2- ERG interstitial deletion, TP53 and FOXA1 mutations (50).

An intrinsic issue with *in vitro* cell culture is the limit of the number of passages before cells undergo senescence and stop growing. This is the so-called "Hayflick limit", first described in 1965 (56). The Hayflick limit can be bypassed using artificial immortalisation of cells through reactivation of telomerase and the inactivation of the p53 and RB tumour suppressor pathways (57). The organoid culture technology developed by Clevers and colleagues and more specifically the PCa culture media utilised in this thesis allows for the indefinite propagation of both benign and malignant prostate cells without the need for artificial transformation as a result of the various constituents added to the media. Furthermore the culture technology appears to maintain the integrity of the genome without evidence of genetic drift and potentially allows development of new clinically applicable cell lines with a high success rate (58). The constituents of this novel media are described in Chapter 2, and the media subsequently utilised in the laboratory to generate patient derived cell models.

1.8 – Conclusion

As seen by the preceding review personalised medicine is a potentially achievable and clinically viable goal in managing men with PCa. 68Ga-PSMA PET is a novel imaging modality demonstrating superior performance for the detection of PCa recurrence and metastasis in patients with biochemical recurrence. This modality hopes to address the clinical need for improved imaging in this cohort of patients, with high sensitivity and specificities in comparison to the current 'standard of care' (SOC) modalities. Despite its recent development and lack of large scale studies, it has been rapidly and widely adopted throughout Australia due to its clinically evident superiority to current SOC imaging.

The role of PET imaging with 68Ga-PSMA in aiding treatment decisions in men with biochemical recurrence or improving clinical outcomes by changing the natural history of the disease due to superior staging is yet to be established. Recent advancements have demonstrated actionable aberrations in advanced prostate cancer. It is however currently unknown whether a similar incidence and profile of actionable aberrations are present in the setting of early biochemical recurrence, or if a precision medicine approach will improve patient outcomes. The current study aims to provide preliminary data to investigate these possibilities.

1.9 – Project Outline

There are 3 main issues that the proposed study aims to address. Firstly, the inability of current imaging and staging to accurately identify early recurrent and metastatic PCa. There is therefore, a significant clinical need for more sensitive and specific imaging technologies to detect micro-metastatic and low volume recurrent disease, which could potentially alter SOC treatment options for patients. Secondly, the inherent difficulty of *in vitro* culture of PCa from clinical samples in order to amplify tumour material to allow downstream molecular and functional analysis of patient samples and for the potential generation of novel cell lines. Lastly, if a precision medicine approach can be used to predict failure or success of future treatments in patients with biochemical recurrence.

Hypotheses

I hypothesise that enhanced imaging technology in the form of PSMA PET/MRI allows identification of sites of cancer recurrence/metastasis with improved sensitivity and specificity compared to standard imaging technologies. Transcriptomic, genomic and *in vitro* drug sensitivity analyses of metastatic tissue samples, cultured from patients with recurrent disease will highlight biological pathways under-pinning treatment response to these agents, mechanisms of resistance to these agents, and predict effective therapeutic strategies in individual patients.

Aims

- To evaluate the sensitivity and specificity of 68Ga-PSMA PET/MRI in detecting metastatic or locally recurrent lesions in patients with biochemical recurrence post primary treatment compared to staging CT, bone scan/SPECT CT and standard MRI and the relative contribution of each imaging modality to the recurrence site (bone vs soft tissue or both).
- To assess the utility of hybrid PET/MRI scan compared to standard imaging modalities in altering the management of patients from the standard of care (salvage pelvic radiation or ADT).
    - Major change in management – diagnosis of metastatic disease outside of the pelvis leading to palliation if wide spread or targeted treatment if oligometastatic (radiation or surgery).
    - Minor change in management – diagnosis of localised recurrence within the prostatic fossa/bed or pelvis leading to targeted/high dose therapy or surgery in addition to salvage pelvic radiation.
- Utilise novel *in vitro* culture technology to amplify and culture biopsy and circulating tumour cell (CTC) samples from individual patients to allow NGS technologies and *in vitro* drug sensitivity screening in clinically meaningful timeframes to identify therapeutic strategies, markers of resistance/sensitivity and enrich patient populations for clinical trials.

In order to investigate these aims, a prospective clinical trial was established and performed at the Princess Alexandra Hospital.

Chapter 2 - Methods and Materials

2.1 – PSMA PET/MRI Biochemical Recurrence Trial

A multi-centre, prospective, one-arm study was approved for recruitment at the Princess Alexandra Hospital (PAH) (HREC/15/QPAH/355, ACTRN12616000186459). Thirty patients with biochemical recurrence (BCR) post primary treatment (surgery or radiotherapy) were recruited. The trial was funded by a PAH Research Foundation New Appointment Grant and the 2016 ANZUP/TOLMAR Clinical Research Fellowship awarded to principal supervisor Dr Vela. Potential patients were identified from the PAH Urology multi-disciplinary team (MDT) meeting or referred from clinic for consideration for the trial. All potential patients were reviewed and assessed for eligibility. Inclusion and exclusion criteria are outlined in Table 2.1 below.

Table 2.1 PSMA PET/MRI BCR Trial Inclusion and Exclusion criteria

Inclusion Criteria	Exclusion Criteria

• Male patients with pathologically diagnosed prostate cancer
• Biochemical Recurrence defined as
   o PSA > 0.2ng/ml on at least 2 occasions post radical prostatectomy
   o PSA 2.0 ng/ml above nadir 2 years post radiotherapy
• History of primary treatment for prostate cancer no sooner than 3 months post-surgery and 2 years post radiotherapy
• No known problems with peripheral intravenous or central line access
• Able to provide informed signed consent
	• Age under 18 years
	• Administered a radioisotope within 5 physical half-lives prior to study enrolment
	• Unable to lie flat during or unable to tolerate PET/MRI
	• Prior history of any other malignancy within last 2 years
	• Contraindication to PET scan or [68Ga]Gallium-labelled PSMA ligand
	• Claustrophobia not manageable by oral sedatives i.e. Temazepam
	• Renal impairment or haemodialysis
	• Contraindication to biopsy of identified lesion
	• Contraindication to MRI such as implantable medical devices
	• Body weight above 150kg or axial diameter larger than 60cm

BCR: biochemical recurrence; PSA: prostate specific antigen; PET/MRI: positron emission tomography/magnetic resonance imaging, PSMA: prostate specific membrane antigen

2.1.1 Study Protocol and Trial Design

Eligible patients proceeded to 68Ga-PSMA (HBED-CC) PET/MRI imaging. 68Ga -PSMA (HBED-CC) (HBED-CC, ABX AG, Germany) was manufactured at the specialised PET Services Queensland Radiopharmaceutical Laboratory at the Royal Brisbane and Women's Hospital (RBWH) as per Eder et al. (59). 68Ga-PSMA (HBED-CC) was transported to PAH for injection on day of imaging. All PET images were acquired within 45-60 minutes following administration of 150 MBq of 68Ga-PSMA. SOC CT abdomen/pelvis and whole body bone scans were also performed for enrolled patients for comparison (Figure 2.1).

Following imaging, comparison of results between imaging modalities was performed. Results of SOC and PSMA PET/MRI Identified lesions in individual patients were discussed at the PAH Urology MDT meeting to allow future treatment planning. Following discussion patients were offered surgery, radiotherapy, hormone therapy, watchful waiting or entry into additional clinical trials depending on the patient/tumour characteristics, life expectancy, expected adverse effects of any treatment provided, and technical feasibility.

Patients with amenable identified target lesions underwent image guided biopsy or surgical excision. Samples were taken fresh for in vitro culture and processed for histopathological analysis. Findings from culture or downstream analyses were not used to direct patient care.

In discussion with the Princess Alexandra Hospital and Transitional Research Institute in house statisticians this study was powered as a pilot study to include 30 patients.
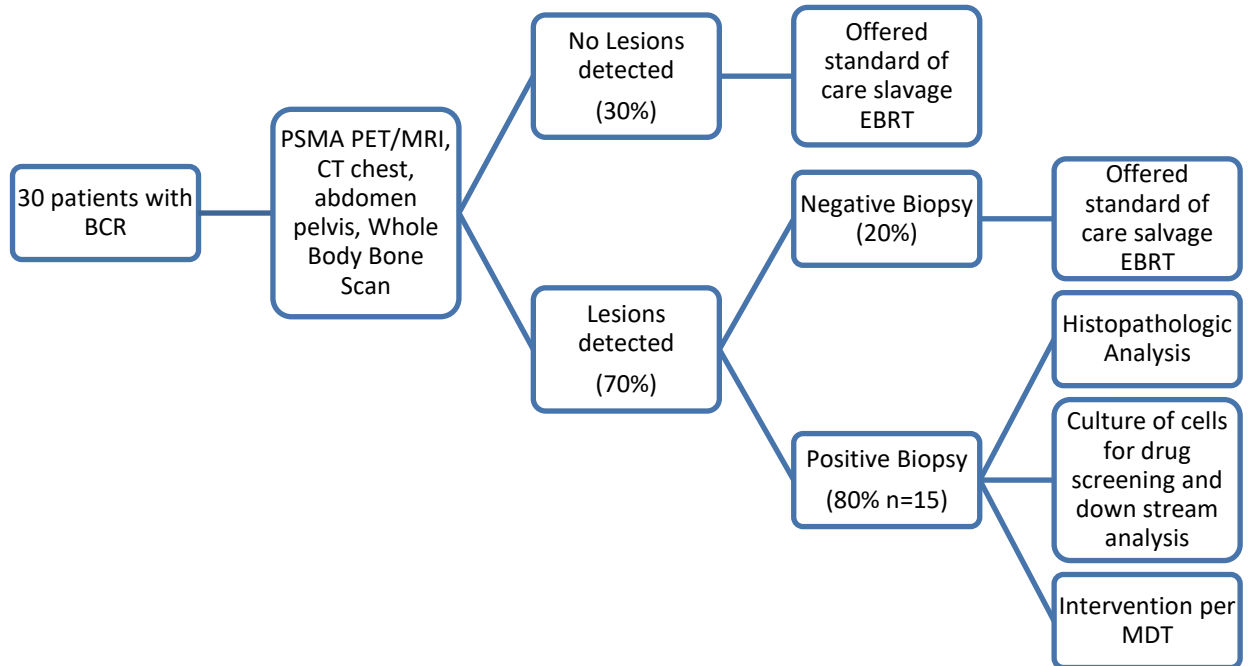
Figure 2.1 *PSMA PET/MRI BCR Trial Study Design with estimated numbers.* 30 Patients with BCR (Biochemical Recurrence) were recruited and underwent PSMA PET/MRI as well as SOC CT and WBBS. Detected lesions amenable to biopsy were sampled for histological analysis, *in vitro* culture for drug screening and NGS as well as for MDT discussion to guide treatment. Patients with negative imaging proceeded to SOC EBRT (external bean radiotherapy). Patients with negative lesions on biopsy were discussed in MDT and offered SOC EBRT.

2.1.2 Image Acquisition and Protocol

All PSMA PET/MRI scans were performed at the PAH. Each scan was assessed subjectively by 3 clinicians independently. A positive lesion was identified as a lesion with suspicious PSMA uptake when compared to background activity (measured as standardized uptake value [SUV]). PET lesions were then correlated with MRI findings. An identified lesion with a SUV max above background uptake and a corresponding MRI lesion was considered suspicious. There was no threshold SUV max value set for a positive scan.

PET/MRI scans were performed in two parts. The first series of images (VTAD - Vertex to Thigh Arms Down), were acquired first with a MRI and MRI-based attenuation correction (MRAC) series with in, out, fat and water phases. Next Diffusion/Short tau inversion recovery (a fat

signal suppression technique) and Transverse series were acquired. PET imaging was performed over 5 stations at 3 mins per station (segments of the body that are imaged separately then combined in post image processing). Following these initial image acquisitions, patients were asked to empty their bladder and 20mg of Buscopan was administered.

The second phase of imaging was then performed with Pelvis/Prostate phases acquired. An MRI 'fast view' of the pelvis, followed by a MRAC series with in, out, fat and water phases were acquired with Sagittal T2, Axial T2 and Coronal T2 series. PET imaging was performed in conjunction with the above sequences over 1 pelvic station for 15mins. MRI Diffusion series images were then acquired. Contrast was injected (7.5ml of Gadovist made up to 15mls with normal saline) and a final T1 Vibe Dynamic phase was acquired. Post processing of the images included a Diffusion weighted B2000 series and perfusion colour map generation.

2.2 – Imaging Analysis and Comparison

Sensitivity and specificity analysis of 68Ga PSMA PET/MRI in detecting metastatic or locally recurrent lesions in patients with biochemical recurrence compared to standard of care imaging was calculated. A positive MRI lesion was defined as a pathological lesion greater than or equal to 1cm. The primary end points were PSMA avid lesion detections rates, detection rates compared to SOC, and histological correlation of avid lesions. Analysis on how PSMA PET/MRI changed clinical management compared to SOC, quality of life analysis and cost analysis were performed as per secondary objectives. Statistical analysis was performed using Pearson's Chi-squared test to compare the two imaging modalities per patient.

2.3 – Hans Clever's Organoid Culture Media

Hans Clever's organoid culture media (HCM) was based on established published protocols (50, 51). Table 2.2 describes the additives added to Advanced DMEM (Dulbecco's Modified Eagle Medium)-F12 serum free base media (Gibco) to make HCM (50, 51).

Table 2.2 *HCM additives in Advanced DMEM-F12 serum free base media*

Additive	Supplier	Final Concentration in 100ml
R-Spondin conditioned media		10% v/v
Noggin conditioned media		10% v/v
Glutamax	Invitrogen	2mM
EGF	Sigma	5ng/ml
FGF 10	Peprotech	10ng/ml
FGF2	Lonza	5ng/ml
HEPES	Gibco	10mM
Nicotinamide	Sigma	10mM
N-acetyl-L-cysteine	Sigma	1.25mM
A83-01	BioScientific	0.5um
SB202190	Selleckchem	10uM
Y-27632 dihydrochloride	Selleckchem	10uM
B27	Gibco	50x diluted
Primocin	InvivoGen	1:100 v/v
Dihydrotestosterone (DHT)		1nM or 0.1nM

DHT: dihydrotestosterone; EGF: epidermal growth factor; FGF: fibroblast growth factor

2.4 – R Spondin and Noggin Conditioned Media

A key constituent of HCM is Noggin and R Spondin. Due to the expense of the respective recombinant proteins we utilised conditioned media from HEK293T-HA-RspoI-Fc (HEK293TR) cell line (60) and HEK293T-Noggin (HEK293TNog) cell line both of which overexpress and secrete R-Spondin and Noggin, respectively and can be collected and purified (described in Section 2.4.1). These cell lines were previously developed by Dr Vela (60).

2.4.1 Developing R Spondin and Noggin Conditioned Media for use in HCM

Initially HEK293TR and HEK293TNog cell lines, that had been stored in liquid nitrogen were thawed and seeded in flasks with Advanced DMEM-F12 (Gibco, Gaithersburg, Maryland, USA) + 10% foetal bovine serum (Gibco, Gaithersburg, Maryland, USA) containing penicillin/streptomycin (ThermoFischer Scientific, Waltham, Massachusetts, USA). Cells were subsequently propagated and passaged (split ratio ~1:3) to establish large population numbers. Once cells reached 70% confluency, media was replaced with 25mls serum free DMEM. After 24 hours, media was collected and stored at 4°C. Serum free media was once

again added to cells and media collected after 24 hours and pooled with stored conditioned media. The pooled conditioned media was filter sterilised using Merck MILLIPORE Stericup® 0.2 micron Filter Units (Merck Millipore, Burlington Massachusetts, USA). Filtered conditioned media was collected, aliquoted, and stored at −20°C for up to 6 months avoiding repeated freeze-thaw cycles.

2.4.2 Validating R Spondin Conditioned Media

The Wnt pathway controls a large and diverse set of cell fate decisions in embryonic development, adult organ maintenance and their dysregulation in cancers/disease (61). Wnt proteins bind to receptors on the cell surface, initiating a signalling cascade that leads to stabilization and nuclear translocation of Beta-catenin. Beta-catenin then binds to TCF/LEF transcription factors in the nucleus, leading to transcription and expression of Wnt-responsive genes (61).

The Wnt Signalling Pathway TCF/LEF Reporter (Luc) – HEK293 Cell Line is designed for monitoring the activity of the Wnt/β-catenin signalling pathway (62, 63). This cell line contains a firefly luciferase gene under the control of TCF/LEF responsive elements stably integrated into HEK293 cells. This cell line is validated for the response to the stimulation of mouse Wnt3a and to the treatment with an inhibitor of the Wnt/β-catenin signalling pathway. Therefore, Wnt target genes associated with a luciferase plasmid saw an increase in relative luciferase activity when appropriate activation of Wnt occurs. If Wnt signalling is inhibited, a loss of luciferase expression is measured.

R-Spondin proteins are agonists of the canonical Wnt/β-catenin signalling pathway. These proteins are necessary and sufficient for Wnt signal potentiation, and although R-Spondin is unable to initiate Wnt signalling, it has the potential to enhance responses to low-dose Wnt proteins. Therefore, wells with added recombinant R-Spondin and R-Spondin conditioned media should enhance the Wnt3a substrate and luminesce brighter than Wnt3a alone and controls.

HEK 293TR cells were seeded at $3x10^{4}$ cells per well in 96 well plate with 100μl of media per well. Mouse Wnt3a (Abcam, Cambridge, United Kingdom) and various concentrations of conditioned media were prepared and added to wells. Steady-Glo® Luciferase Assay Reagent

(Promega, Madison, Wisconsin, USA) was prepared as per the Manufacturer's protocol and 100μl was added to each well. Plates were covered with aluminium foil for 5 minutes while cell lysis occurred. Luminescence was subsequently measured at 560nm. Validation results of R Spondin Conditioned Media are outlined in Appendix 1.

2.4.3 Validating Noggin Conditioned Media

Noggin conditioned media was validated using a Western blot comparing Recombinant Noggin to various dilutions of conditioned media.

BIORAD MiniProtean TGX stain-free pre cast gels (10 well, any kD, 30μl wells; BIORAD, Hercules, California, USA) were used with a Page Ruler Plus Pre-stained protein ladder (ThermoFischer Scientific, Waltham, Massachusetts, USA) for comparison.

For each 10 ml sample of conditioned media/recombinant Noggin, 5 μl of 4x loading buffer and 5μl MilliQ Water were added into 1 ml tubes. Samples were boiled for 5 mins at 95°C and spun down before being loaded onto gel. Electrophoresis was carried out at 25 amps for 60 minutes. Gels were transferred using the semidry trans-blot Turbo transfer system (BIORAD, Hercules, California, USA).

Membranes were blocked in 5% skim milk in phosphate buffered saline (PBS) for 1 hour before incubation with primary Noggin antibody (1:2500, Pierce TM Noggin Antibody, ThermoFischer Scientific, Waltham, Massachusetts, USA) and incubated at 4°C overnight. Membranes were then washed with TBS-Tween (0.1% Tween 20, SIGMA, USA product code: 1001649544) three times for 10 mins each. Membranes were incubated with anti-rabbit secondary antibody conjugated to horse radish peroxidase (1:2500; NA934V-1ml, anti-rabbit IgG – HRP; GE Healthcare, United Kingdom) and incubated at room temperature for 1 hour on a rocker. Finally the antibody solution was aspirated; the membrane washed with TBS-T and developed with Thermo Scientific Pierce enhanced chemiluminescence Western Blotting Substrate (ThermoFischer Scientific, Waltham, Massachusetts, USA). Membranes were imaged using the BIORAD developer platform (Gel Doc XR+ System, BIORAD, Hercules, California, USA).

Validation results of Noggin Conditioned Media are outlined in Appendix 2.

2.5 – Culture Conditions

All monolayer and 3D cell cultures were grown in HCM media containing 1nM DHT for hormone sensitive and patient derived cell lines or 0.1nM DHT for castrate resistant lines. All cultures were maintained in a humidified incubator at 37°C and 5% CO_2. Media was changed every 2 to 3 days.

Monolayer cell cultures were passaged by washing with PBS and detaching the cells with TrypLE™ Select Enzyme (1X) (no phenol red, Gibco, Gaithersburg, Maryland, USA). Cell pellets were re-suspended in fresh media and plated.

2.6 – Primary Tissue Culture Protocol

Acquiring patient samples

Patients were consented and enrolled into the PSMA BCR trial. Patients with PSMA PET MRI avid lesions which were safely accessible either via core biopsy or operative approaches were consented for biopsies. De-identified and coded patient samples were transported to the lab fresh on ice in Advanced DMEM-F12 base media. Concurrent samples were sent to the PAH pathology department for formal histology. A portion of tissue was placed in a sterile Eppendorf tube and snap frozen in liquid nitrogen to enable genomic and transcriptomic analysis of fresh frozen tissue.

Preparation of sample biopsies for *in vitro* culture

Following biopsy, samples were immediately placed in Advanced DMEM-F12 media on ice and transferred to the laboratory. Under sterile conditions, tissue was minced with a scalpel in a 60mmx 50mm dish containing Advanced DMEM-F12 media before being transferred to a sterile 1.5ml Eppendorf tube and centrifuged at 130 x g for 3 minutes (37°C). Media was aspirated and 1ml of 5mg/ml collagenase type II (Gibco, Gaithersburg, Maryland, USA) per 50mg of minced tissue was added and incubated and shaken at 37°C for a minimum of 1.5 hours for metastatic tissue. Following digestion, cells were centrifuged at 130 x g for 3 minutes (37°C), supernatant aspirated, and cells washed twice in PBS. Finally, cells were resuspended in pre-warmed HCM media containing 1nM DHT and plated onto collagen type 1 (Corning, New York, USA) coated 24-well plates. Cells were incubated at 37°C in a humidified 5% CO_2

incubator. Media was changed every 2 to 3 days. Samples were cultured *in vitro* for a minimum of 2 weeks prior to validation methods described in section 2.7.

Patients were also consented and asked to provide blood samples. Vacutainer® Blood tubes (Becton Dickinson, Franklin Lakes, New Jersey, USA) were centrifuged at 1200 x g for 10 minutes. 500µl aliquots of serum and plasma was transferred a cryovial and repeated until all serum and plasma was banked. Buffy coat was aspirated in a circular motion from plasma tubes and were similarly aliquoted to cryovials for storage. Samples were labelled and subsequently stored at -80°C.

2.7 – Patient Derived Cell Line Validation Methods

Validation of tissue of origin is required to confirm that *in vitro* samples generated were from PCa cells, as tissue cores often contain surrounding benign tissue. It is not possible to determine this based on phenotypic appearance of isolated cells. PSA levels in conditioned media were assessed using a PSA ELISA (GenWay Biotech, San Diego, California, USA) as per the manufacturer's protocol to indicate the presence of prostate cells. Furthermore quantitative real time PCR (RT-qPCR) was performed to compare various prostatic genes of interest (PSA, AR, FKBP5, TMPRSS2) between cultured patient samples and established prostate cancer cell lines (LNCaP and VCaP - authenticated by Genomics Research Centre @ QUT - Institute of Health and Biomedical Innovation 2017; Original source ATCC, Manassas, Virginia, United States).

2.7.1 RNA extraction and synthesis of cDNA

RNA was extracted using the Norgen RNA/DNA/Protein Purification Plus Kit (Norgen Biotek Corp, Thorold, Canada) as per the manufacturer's protocol. RNA was subsequently used immediately for Complementary DNA (cDNA) synthesis or stored at -80°C for subsequent analysis. RNA concentration was determined by Nanodrop (Nanodrop 1000, Thermo Scientific), before being diluted to 250ng with RNAse free water (Gibco, Gaithersburg, Maryland, USA) in a total volume of 15µl. A 5µl 'master mix' (Bioline, Alexandria, NSW, Australia) of 5x reverse transcriptase buffer and reverse transcriptase were added to RNA,

mixed with gentle pipetting then placed in a thermal cycler (C1000 Touch™ Thermal Cycler, BIORAD, Hercules, California, USA). Contents were incubated at 25°C for 10 minutes, 42°C for 15 minutes and 85°C for 5 minutes. cDNA products were stored at -20°C for use in subsequent analyses.

2.7.2 Quantitative Real Time PCR (RT- qPCR)

Forward and reverse primers of target genes PSA, AR, TMPRSS2 and FKBP5 (Appendix 3) were used to validate the presence of prostate cancer cells. To analyse target gene expression, gene-specific primer pairs were added to 1µl of cDNA and SYBR Green (Life Technologies, Carlsbad, California, USA). RT- qPCR reactions were performed in a 384 well plate with triplicates. The ViiA 7 Real-time PCR System (ThermoFischer) was used to perform RT- qPCR. PCR amplification was performed following an initial 10 minute denaturation step at 95°C followed by 40 cycles of 95°C for 15 seconds and 60°C for 60 seconds. A dissociation curve was included in each run to confirm amplification of a single gene product. Gene expression was quantified using the ΔΔCt method (64). Samples were normalised to the expression of the housekeeping gene RPL32.

2.7.3 Summary of mRNA sequencing (mRNAseq) methodology

For mRNAseq, total cellular RNA was extracted using the Norgen RNA Purification PLUS kit #48400 (Norgen Biotek Corp) according to the manufacturer's instructions, including DNase treatment. RNA quality and quantity were determined on an Agilent 2100 Bioanalyzer (Agilent Technologies, Santa Clara, USA) and Qubit®. 2.0 Fluorometer (Thermo Fisher Scientific Inc, Waltham, USA). Library preparation and sequencing was performed at the Kinghorn Centre for Clinical Genomics (KCCG, Garvan Institute, Sydney) using the Illumina TruSeq Stranded mRNA Sample Prep Kit with an input of 1 ug total RNA (RIN>8), followed by paired-end sequencing on an Illumina HiSeq2500 v4.0 (Illumina, San Diego, USA), multiplexing 6 samples per lane and yielding about 30M reads per sample. Raw data was processed through a custom designed pipeline. Raw reads were trimmed using 'TRIMGALORE' (65), followed by parallel alignments to the genome (hg38) and transcriptome (Ensembl v77) using the 'STAR' (66) aligner and read quantification with 'RSEM' (67). Differential expression between the two conditions was calculated after between sample trimmed mean of M-values normalization method (TMM) normalization (68) using 'edgeR' (69) and is defined by an absolute fold change of >1.5 and a

false discovery rate (FDR) corrected p-value <0.05. Quality control of raw data included sequential mapping to the External RNA Control Consortium (ERCC) spike-in controls, rRNA and a comprehensive set of pathogen genomes as well as detection and quantification of 3'bias. For each gene list supplied, the significance of enrichment was determined using the one-tailed Fisher exact test. P values are Benjamini-Hochberg (BH) adjusted across all cell/tissue types. The final score reported in CTen was the -log10 of the BH-adjusted P value. An enrichment score of 2 or greater was considered significant.

2.7.4 Whole Exome Sequencing methodology

Whole exome sequencing and somatic mutation detection was performed using National Association of Testing Authorities (NATA) accredited protocols by the Australian Translational Genomics Centre (ATGC) based at the PAH. Whole exome sequencing was performed using the Integrated DNA Technologies (IDT) exome capture kit plus xGen Pan-Cancer Panel. Libraries were sequenced on an Illumina NextSeq 500 machine to an average depth of 95.01x. Data were aligned to the GRCh37 reference sequence using the ATGC Bioinformatics Pipeline version X. Somatic variants were called using the Mutect2 function of the Genome Analysis Toolkit version 3.7. Filter PASS variants were annotated using Variant Effect Predictor (VEP) release version 86. Copy number variations (CNVs) were identified using Canvas version 1.11 (Illumina; San Diego, United States).

2.8 Therapeutic Drug Screen

Patient derived cancer cells were utilised for both 2D and 3D *in vitro* drug sensitivity screening for various therapeutic agents. The effect of enzalutamide, biclutamide, ARN509, docetaxel and cabazitaxel were evaluated. 2D drug screens were performed using Incucyte live cell imaging and 3D drug screen using CellTiter-Glo® Luminescent Cell Viability Assay (Promega Corporation, Madison, Wisconsin, USA).

2.8.1 2D Cell culture and Drug Screen techniques

LNCaP cells were plated and treated according to established lab APCRC-Q/MRTA protocols (version 25-Jun-2014, Appendix 4). HCM was used instead of RPMO+ FBS in this protocol.

Established and patient derived cell models were plated onto 96-well ImageLock^{TM} plates (Essen BioScience, Michigan, USA) and these were used to perform all 2D *in* vitro drug screen experiments. Cells were plated at 5000 cells per well onto rat tail type 1 collagen coated plates (Corning, New York, USA).

Cells were subsequently incubated for 3 days. After 3 days, media was aspirated and various drug treatments added. Anti-androgens (bicalutamide, enzalutamide, ARN509) were administered at 10µM. Docetaxel and cabazitaxel were used at concentrations of 0.5nM and 1nM respectively. All treatments were plated as technical triplicates, with each experiment repeated as indicated in the results. Two dimensional drug screens were performed using the IncuCyte ZOOM cell imaging system (Essen BioScience, Michigan, USA) which images cells every 2 hours and determines confluence as a reflection of cell growth and proliferation. Data was analysed after 5 days of drug therapy.

2.8.2 3D Cell culture and Drug Screen techniques

Three dimensional cell culture has been shown to be more representative of the *in vivo* environment and may produce different results in cells compared to 2D culture (50, 51, 70). Three dimensional drug screens were carried out using similar seeding density and drug concentrations as the 2D (2.8.1). The primary differences were in cell seeding methodology.

ImageLock^{TM} Plates (96-well) were precooled and placed on ice. Diluted Matrigel™ (Corning, New York, USA), 50% diluted with Advanced DMEM-F12 was added to each well (30µL per well) and centrifuged at 200g for 10mins at 4°C. The plate was then incubated for 60 mins at 37°C to allow the Matrigel to polymerise. Another 30µL layer of 25% diluted Matrigel™ with 5000 suspended cells was added to each well and centrifuged at 100g for 10mins at 4°C. The plate was then incubated for another 60 mins at 37°C for the Matrigel to set. Each well was topped up with 130µL of warmed media. Plates were incubated for 5 days to allow growth of cell colonies.

After 5 days, media was aspirated and treatments were added to wells. Wells were treated for 5 days prior to analysis with CellTiter-Glo® Cell Viability Assays as per manufacturer's protocol. Media and drugs were replenished at day 3.

2.8.3 Statistics

Statistical analysis comparing two means was done using the students T-test. Further statistical analysis was performed using Pearson's Chi-squared test to compare percentage of positive scans for both imaging modalities per patient. All statistics were done using the 'Analysis ToolPack' add-on for Microsoft Excel 2010 (Microsoft, Redmond, Washington, USA).

Chapter 3 - Evaluation of the performance of PSMA PET/MRI hybrid imaging vs Standard of Care imaging in biochemical recurrence

3.1 - PSMA PET/MRI biochemical recurrence trial

Current imaging and staging does not accurately identify early recurrent and metastatic prostate cancer with high sensitivity. There is therefore a significant clinical need for more sensitive and specific imaging technologies to detect micro-metastatic and low volume recurrent disease, which could potentially alter standard of care treatment options for patients. 68-Ga PSMA PET/MRI hybrid imaging is a new technique that may provide the potential answer to this clinical need with promising outcomes reported, but limited by a small number of published retrospective studies (33, 71, 72). The aim of this project was to evaluate the sensitivity and specificity of this new imaging modality in comparison to standard of care (SOC) staging CT and whole body bone scan. Specifically, the ability to detect metastatic or locally recurrent lesions in patients with biochemical recurrence post primary treatment and the relative contribution of each imaging modality to the identified recurrence site (bone vs soft tissue or both) was evaluated. A further aim was to assess the utility of the hybrid PET/MRI scan compared to standard imaging modalities in altering the management of patients from the SOC therapy (salvage pelvic radiation) defined as:

a) Major change: diagnosis of metastatic disease outside of the pelvis leading to palliation if wide-spread, or targeted treatment if oligometastatic (radiation or surgery).

b) Minor change: diagnosis of localised recurrence within the prostatic fossa/bed or pelvis leading to targeted/high dose therapy or surgery in addition to salvage pelvic radiation.

A multi-centre, prospective, one-arm study was ethically approved (HREC/15/QPAH/355, ACTRN12616000186459) for recruitment at the Princess Alexandra Hospital (PAH). A total of 30 patients were recruited between March 2016 and July 2017. Patients had a median age of 68 years, median Gleason Score of 7 and a median PSA of 0.69ng/ml at the time of investigation. A total of 23 patients were previously treated with definitive surgery (open retropubic prostatectomy (RRP) or robotic assisted prostatectomy (RALP)), 6 patients were

previously treated with external beam radiotherapy (EBRT) with neoadjuvant androgen deprivation therapy (ADT) and 1 patient had previously been treated with Low Dose Rate (LDR) brachytherapy. The median time from primary therapy to PSMA PET/MRI was 4 years.

3.2 – Trial Outcomes

All thirty patients recruited underwent SOC and PSMA PET/MRI imaging for analysis. Twenty one of thirty patients (70%) had clinically significant findings on PSMA PET/MRI. The median PSA of a positive scan was 1.5ng/ml, with the lowest positive scan at 0.23 ng/ml. This overall detection rate in biochemical recurrence is comparable to large published PSMA PET/CT detection rates as outlined in Table 3.1 (28-30). It is important however to note that PSMA PET/MRI is a novel cutting-edge imaging modality thus there is little extant data for comparison, especially in patients with early biochemically recurrent disease. PSMA PET/CT on the other hand, is widely used internationally with a larger body of published evidence. PET/CT however provides a CT component coupled with PSMA avidity which provides lesser anatomical characterisation and detail, especially in the pelvis, when compared to MRI. Therefore the comparison in Table 3.1 is to PSMA PET/CT and should be taken into consideration as these are different imaging modalities.

Table 3.1 *Detection Rates of PSMA PET/MRI in this study compared to published PSMA PET/CT Literature*

PSA (ng/ml)	Detection Rate (%)			
	Meredith et al.	Perera et al.	Von Eyben et al.	PSMA PET/MRI
	Retrospective Study	Systematic Review	Systematic Review	This Prospective Study
0.01 to <0.2	11.3	42	50	nil patients
0.2 to <0.5	26.6	58		40
0.5 to <1	53.3		53	42.9
1 to 2	79.1	76		66.7
>2	95.5	95		90
Overall Detection Rate	76			70.4

Based on comparison to published PSMA PET/CT data, detection rates in this study using PSMA PET/MRI are comparable (28-30). It is important to consider however that this is a comparison of two different imaging modalities. No patients enrolled in this study had PSA levels <0.2ng.ml due to inclusion criteria. Only 9 patients were able to be biopsied in our study to confirm histology as outlined below in detail in section 3.3.

In this current study, all MRI detected lesions had corresponding PSMA avidity (100%
concordance if MRI positive). There were however two examples of false positive PSMA avid
lesions in the study cohort. The first example was a PSMA avid rib lesion which was identified
as benign bone following histologic correlation. The second example was a focus of PSMA
avidity in the left pelvis, which on T2 weighted MRI, was identified as a dilated portion of
ureter. This case is further discussed below. Table 3.2 summarises baseline characteristics and
imaging data for all trial patients, with representative images from all positive scans in
appendix 5.

Table 3.2 *Patient baseline demographics, Gleason Score (Gl) and ISUP Grade Group at diagnosis, previous treatment (and margin status if surgery), PSA levels at time of imaging and outcome of imaging modalities.*

Trial ID	Age	Initial Histology	ISUP Grade Group	Initial Treatment	Margin	PSA (ng/ml)	PSMA PET/ MRI	CT	Bone Scan
BCR001	72	Gl 3+4=7	2	EBRT + ADT		0.24	Positive	Positive	-
BCR002	67	Gl 4+5=9	5	RRP		1.5	Positive	Positive	-
BCR003	64	Gl 5+3=8	4	EBRT + ADT		32	Positive	Positive	-
BCR004	63	Gl 3+4=7	2	RALP		0.52	Positive	-	-
BCR005	68	Gl 4+4=8	4	RRP		0.62	Positive	-	-
BCR006	75	Gl 4+5=9	5	RRP + PLND		0.23	Positive	-	-
BCR007	70	Gl 3+4=7	2	RALP		2.4	Positive	-	-
BCR008	67	Gl 4+4=8	4	RRP + PLND		0.2	-	-	-
BCR009	63	Gl 3+4=7	2	RRP		0.91	-	-	-
BCR010	68	Gl 4+3=7	3	RRP + PLND		0.29	-	-	-
BCR011	70	Gl 4+5=9	5	RRP + PLND	Positive	0.76	-	-	-
BCR012	66	Gl 2+2=4	1	LDR Brachytherapy		10	Positive	-	-
BCR013	64	Gl 3+4=7	2	RRP + PLND		5	Positive	-	-
BCR014	69	Gl 4+3=7	3	RRP	Positive	1.2	Positive	Positive	-
BCR015	60	Gl 3+4=7	2	EBRT + ADT		3.3	Positive	-	-
BCR016	57	Gl 4+5=9	5	RALP	Positive	0.6	Positive	Positive	-
BCR017	59	Gl3+4=7	2	RRP + partial nodes	Positive	0.26	Positive	-	-
BCR018	68	Gl 4+4=8	4	RRP	Positive	7.8	Positive	-	-
BCR019	66	Gl 3+4=7	2	RALP + PLND		0.28	-	-	-
BCR020	68	Gl 3+4=7	2	EBRT + ADT		8.4	Positive	Positive	-
BCR021	73	Gl3+4=7	2	EBRT + ADT		4.1	Positive	-	-
BCR022	72	Gl 3+4=7	2	EBRT + ADT		2.3	Positive	Positive	-
BCR023	70	Gl 4+3=7	3	RRP		0.44	Positive	-	-
BCR024	59	Gl 3+4=7	2	Laparoscopic RP	Positive	0.28	-	-	-
BCR025	71	Gl 4+3=7	3	RRP		0.59	Positive	-	-
BCR026	58	Gl 4+5=9	5	RRP		0.25	-	-	-
BCR027	68	Gl 3+4=7	2	RRP	Positive	0.24	-	-	-
BCR028	73	Gl 4+3=7	3	RRP		35	Positive	Positive	-
BCR029	76	Gl 4+5=9	5	RALP	Positive	0.63	Positive	Positive	Positive
BCR030	73	Gl 3+3=6	1	RRP		1.1	-	-	-
Median	68	7	4			0.69	21	9	1

- : negative scans; RRP: radical retropubic prostatectomy; RALP: robotically assisted laparoscopic prostatectomy; EBRT: external beam radiotherapy; ADT: androgen depravation therapy. Representative images of positive scans in Appendix 5.

3.2.1 Comparison of PSMA PET/MRI to SOC imaging

SOC contrasted CT chest/abdomen/pelvis and whole body bone scan identified only 9 of 30 patients (30%) with positive findings (Table 3.2). These cases were all identified on CT imaging and there was only one positive bone scan in this study. There were two presumed false positives on SOC imaging (80% concordance of PSMA PET/MRI with SOC imaging), with two discordant lesions on SOC CT compared to PSMA PET/MRI (Table 3.3).

The first patient was reported to have an enlarged 11mm pre-sacral node which was stable in size on imaging since 2014 and a borderline right common iliac node measuring 6mm. These lesions were reported as suspicious on CT imaging. On PSMA PET/MRI imaging however local recurrence inferior to the left seminal vesicle was identified with no PSMA avidity noted in the pre-sacral node or in the right common iliac node identified on CT. No histologic confirmation was made with either node.

The second patient was reported to have a small sclerotic focus in his right superior pubic ramus on CT. Bone scan was negative for the identified lesion on CT. This lesion was not identified on either the PET or MRI component of the PSMA PET/MRI scan. PSMA PET/MRI however, identified PSMA avid lesions in the right pre-sacral and left common iliac nodes.

Both of these individual patient CT-identified lesions were presumed as false positives following PSMA PET/MRI imaging and were not biopsied for histological confirmation; however these scans have been considered as positive SOC CT scans in this analysis.

Table 3.3 *Correlation of positive PSMA PET/MRI to positive SOC imaging.*

Trial ID	Age	PSA (ng/ml)	PSMA PET/ MRI	CT	Bone Scan	Correlation of PSMA PET to SOC imaging
BCR001	72	0.24	Positive	Positive	-	Yes
BCR002	67	1.5	Positive	Positive	-	Yes
BCR003	64	32	Positive	Positive	-	Yes
BCR014	69	1.2	Positive	Positive	-	No - lymphadenopathy on CT with no corresponding PSMA avidity
BCR016	57	0.6	Positive	Positive	-	No – sclerotic bone lesion no identified on both MRI and PSMA PET component of PSMA PET/MRI scan
BCR020	68	8.4	Positive	Positive	-	Yes
BCR022	72	2.3	Positive	Positive	-	Yes
BCR028	73	35	Positive	Positive	-	Yes
BCR029	76	0.63	Positive	Positive	Positive	Yes

PSMA PET/MRI scans had a 100% concordance rate; all lesions identified on MRI had PSMA positivity. Two patients did not have correlating scans between PSMA PET and SOC imaging. Patient BCR014 had lymphadenopathy on CT, which did not have correlating PMSA avidity in these nodes. Patient BCR016 had a sclerotic bone lesion on CT which was not identified on either the MRI or PSMA PET components of PSMA PET/MRI. - : negative scans.

When detection rates of PSMA PET/MRI and CT by location were compared (Table 3.4a), PSMA PET/MRI detected local recurrence (p=0.005; Pearson's Chi-squared test) and lesions in the pelvis (p=0.06; Pearson's Chi-squared test) more accurately than SOC imaging, in a per-patient analysis. It is possible that other locations, in particular lymph node detection and lesions outside the pelvis did not reach statistical significance as a result of the small sample size. This analysis could be confounded by the fact that two CT lesions were false positives, as discussed above, and could improve the results of CT imaging adding bias. When adjusted for this however, PSMA PET/MRI appears to have better detection rates; reaching statistical significance for both local recurrence and lesions within the pelvis (Table 3.4b). Furthermore PSMA PET/MRI accuracy of detecting lesions outside the pelvis also showed a trend towards statistical significance (p=0.073; Pearson's Chi-squared test). Furthermore, when comparing the detection rates for the number of lesions present (Table 3.4c) PSMA PET/MRI not only identified more patients with recurrence, but also more sites of recurrence per patient, although this only reached statistical significance for locally recurrent lesions (p=0.027; Pearson's Chi-squared test). Differences in bone lesions did not reach statistical significance.

Table 3.4a *Comparison of positive PSMA PET/MRI and SOC scans by recurrence site and tissue type by*

patient numbers.

	PSMA PET/MRI	CT	P Value
Lymph Nodes	10 (33.3%)	6 (20%)	0.247
Bone	2 (6.67%)	2 (6.67%)	1
Local Recurrence	11 (36.7%)	2 (6.67%)	0.005
Pelvic Recurrence	14 (46.7%)	7 (23.3%)	0.060
Outside Pelvis	7 (23.3%)	3 (10%)	0.169

PSMA PET/MRI detected more patients with lesions than SOC imaging. When compared to SOC, PSMA

PET/MRI detected local recurrence and pelvic lesions with greater efficacy. Statistical analysis was

performed using Pearson's Chi-squared test to compare percentage of positive scans for both imaging

modalities per patient

Table 3.4b *Adjustment for false positive CT scans.*

	PSMA PET/MRI	CT	P Value
Lymph Nodes	10 (33.3%)	5 (16.6%)	0.1393
Bone	2 (6.67%)	1 (3.33%)	0.5569
Local Recurrence	11 (36.7%)	2 (6.67%)	0.005
Pelvic Recurrence	14 (46.7%)	6 (20%)	0.0298
Outside Pelvis	7 (23.3%)	2 (6.67%)	0.073

When this data is adjusted for two false positive CT scans, PSMA PET/MRI outperforms SOC imaging

with statistical significance for both local recurrence and lesions within the pelvis. Statistical analysis was

performed using Pearson's Chi-squared test to compare percentage of positive scans for both imaging

modalities per patient

Table 3.4c *Comparison of the number of avid lesions on PSMA PET/MRI and SOC scans by recurrence site*

and tissue type.

	PSMA PET/MRI	CT	P Value
Number of Lesions	42	26	
Lymph Nodes	24 (30.7%)	18 (41.9%)	0.322
Bone	6 (7.70%)	6 (14.0%)	0.359
Local Recurrence	12 (15.4%)	1 (2.32%)	0.04
Pelvic Recurrence	14 (18.0%)	3 (6.98%)	0.211
Outside Pelvis	22 (28.2%)	15 (34.9%)	0.211

PSMA PET/MRI not only identified more patients with recurrence, but also more sites of recurrence per

patient. Once again local recurrence and pelvic recurrences were identified with greater sensitivity than

SOC imaging. Statistical analysis was performed using Pearson's Chi-squared test to compare percentage

of positive scans for both imaging modalities per patient

3.3 – Histologic Confirmation of PSMA PET/MRI Identified Lesions

From 21 positive PSMA PET/MRI scans, 9 patients had lesions amenable for biopsy. The remaining lesions were in anatomical locations deemed unsafe to biopsy by the Interventional Radiology Service at the PAH. The biopsy rate of positive scans in this study was 42.8%. There were 8 positive biopsies and 1 negative biopsy (Table 3.5), yielding an 88.9% histological correlation rate. In 8 cases there was only one focus of PSMA uptake for biopsy. In the 9th patient (BCR006), there were two avid lesions, the biopsied rib lesion and a pelvic lymph node not amenable to biopsy. The negative biopsy (BCR006) resulted from a PSMA avid lesion in a rib which returned benign bone in a patient post RRP + PLND with a PSA of 0.23ng/ml. On subsequent MDT review of the biopsied lesion, the MRI component of the scan suggested a likely benign lesion, with only low PSMA avidity. Recent evidence and growing local experience has identified that rib lesions are frequently sites of false positive PSMA uptake (73). As such our current clinical practice is to consider isolated rib lesions as false positives when there are no correlating lesions identified on CT or MRI. Overall PSMA PET/MRI has a positive predictive value of 95.2% and a sensitivity of 68.9%.

Table 3.5 *Summary of final tumour histology following biopsy of PSMA avid lesion.*

Pt	PSA (ng/ml)	Previous Treatment	Initial Pathology	Lesion	Histology
BCR001	0.24	EBRT + ADT	Gl 3+4=7	Pelvic side wall lesion	Dedifferentiated prostate adenocarcinoma resembling lung adenocarcinoma
BCR002	1.5	RRP	Gl 4+5=9	External Iliac lymph node	Metastatic prostate cancer
BCR006	*0.23*	*RRP + PLND*	Gl 4+5=9	*Rib*	*Benign*
BCR007	2.4	RALP	Gl 3+4=7	Residual prostate bed tissue	Prostatic tissue
BCR013	5	RRP + PLND	Gl 3+4=7	Small recurrence adjacent to prostate bed	Prostate adenocarcinoma Gl 4+3=7
BCR015	3.3	EBRT + ADT	Gl 3+4=7	Prostate	Prostate adenocarcinoma Gl 4+4=8
BCR018	7.8	RRP	Gl 4+4=8	Small recurrence adjacent to prostate bed	Prostate adenocarcinoma Gl 4+5=9
BCR020	8.4	EBRT	Gl 3+4=7	Prostate	Prostate adenocarcinoma Gl 3+4=7
BCR023	0.44	RRP	Gl 4+3=7	Prostatic bed	Prostate adenocarcinoma Gl 4+4=8

RRP: radical retropubic prostatectomy; RALP: robotically assisted laparoscopic prostatectomy; EBRT: external beam radiotherapy; ADT: androgen depravation therapy. False positive lesion highlighted in red. Images of biopsied lesions are provided in Appendix 5.

3.4 – Comparison of Clinical Management Following PSMA PET/MRI vs SOC

In this study, SOC therapy (post SOC CT abd WBBS) in patients with biochemical recurrence post-surgery was defined as prostate fossa and seminal vesicle (SV) salvage radiotherapy (SRT) for local recurrent disease and initiation of ADT for patients with biochemical recurrence post radiotherapy or widely metastatic disease. In patients with Following PSMA PET/MRI, biopsy and subsequent MDT discussion, all patients with a positive scan (21 patients, 70% overall) had a change in their management as a result of imaging. In comparison, based on SOC imaging alone, only 5 patients (16% overall) would have had a change in their planned management, 4 of these patients with disease outside the pelvis leading to ADT. All of these 5 patients had a positive PSMA PET/MRI scan and there were no patients who had lesions identified on SOC imaging alone.

Changes to clinical management due to the imaging results were defined as 'Major' and 'Minor'. Patients identified with disease outside of the pelvis leading to palliation if wide spread, or targeted treatment if oligometastatic (radiation or surgery), were defined as a 'Major' change, whereas patients identified with localised recurrence within the prostatic fossa/bed or pelvis leading to targeted/high dose therapy or surgery in addition to salvage pelvic radiation, were defined as having a 'Minor' change. As a result of PSMA PET/MRI there was a statistically significant difference in patients having a 'Minor' change in management ($p=0.0001$, Pearson's Chi-squared test) when compared to SOC imaging (Table 3.6). This is likely the result of improved sensitivity of detection for local and pelvic recurrence with PSMA PET/MRI. There was no difference in patients having a 'Major' change in management; however this is likely a result of the small sample size and patient selection with the target group of patients with "early" biochemical recurrence in this study having a median PSA of 0.69 at the time of imaging. Table 3.5 outlines the difference between PSMA PET/MRI and SOC in changing patient management.

Table 3.6 Change in clinical management following PSMA PET/MRI or SOC imaging

Change in management	PSMA PET/MRI positive	SOC positive	P value
Minor (pelvis)	14 (46.7%)	1 (3.33%)	0.0001
Major (outside pelvis)	7 (23.3%)	4 (13.3%)	0.3209

Statistical analysis was performed using Pearson's Chi-squared test to compare percentage of positive scans for both imaging modalities per patient.

3.5 –Discussion

Based on our data, there appears to be substantial potential clinical benefit of hybrid PSMA PET/MRI imaging over SOC imaging. Firstly, hybrid scans with MRI add important high definition anatomical information to the PSMA PET component. This has the potential to improve specificity and as such reduce false positive results.

PSMA PET/MRI improves detection of locally recurrent disease, reducing the incidence of false negative scans. In early biochemically recurrent disease, patients may have locally recurrent prostatic fossa or anastomotic site recurrences. These lesions are not identified on SOC imaging and are detected and characterised more accurately with PSMA PET/MRI. The MRI component of the scan can characterise with superior anatomical definition areas of low PSMA avidity and therefore improve detection of anastomotic recurrences. Furthermore, lesions close to the bladder are better identified with the MRI component, due to the difficulty in identifying lesions hidden behind the 'halo' of PSMA avidity within the bladder due to urinary excretion of tracer (Figure 3.1).
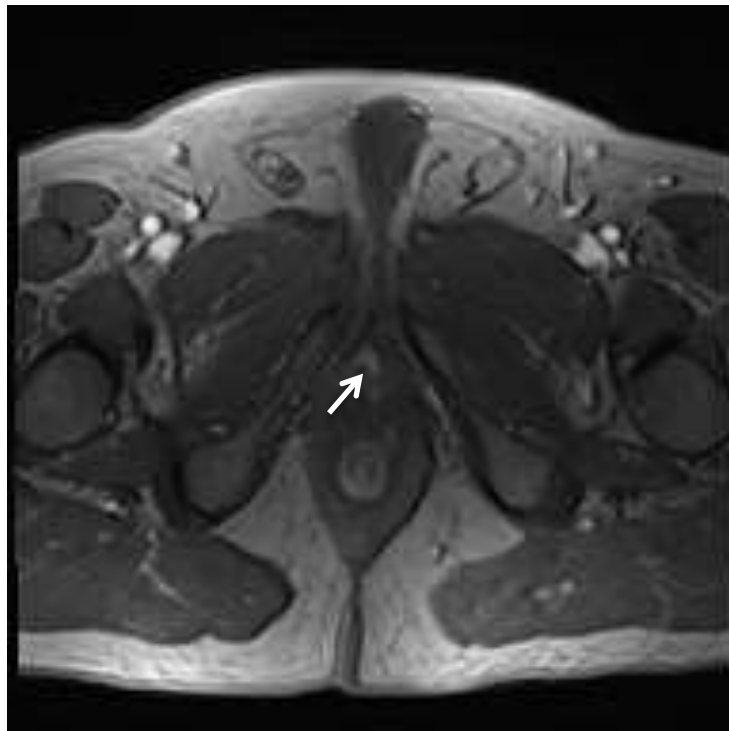
Figure 3.1 Axial dynamic contrast-enhanced MRI image for patient BCR004 showing tumour recurrence at vesicourethral anastomosis (white arrow).

The benefits of MRI are also outlined by BCR006, who was found to have a PSMA avid rib lesion. On the MRI component of the hybrid scan this lesion was characterised as benign, allowing the radiologists to call this a false positive result. This lesion was subsequently biopsied and confirmed as benign. To ensure accuracy of biopsy, a live CT guided biopsy was performed targeting the suspected area seen on CT (Figure 3.2B).
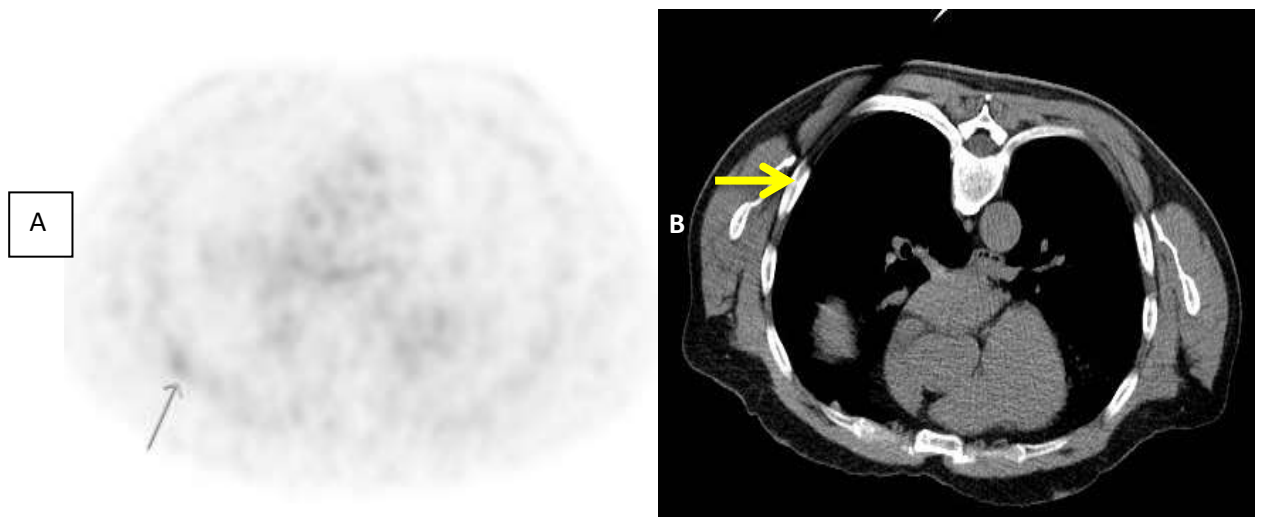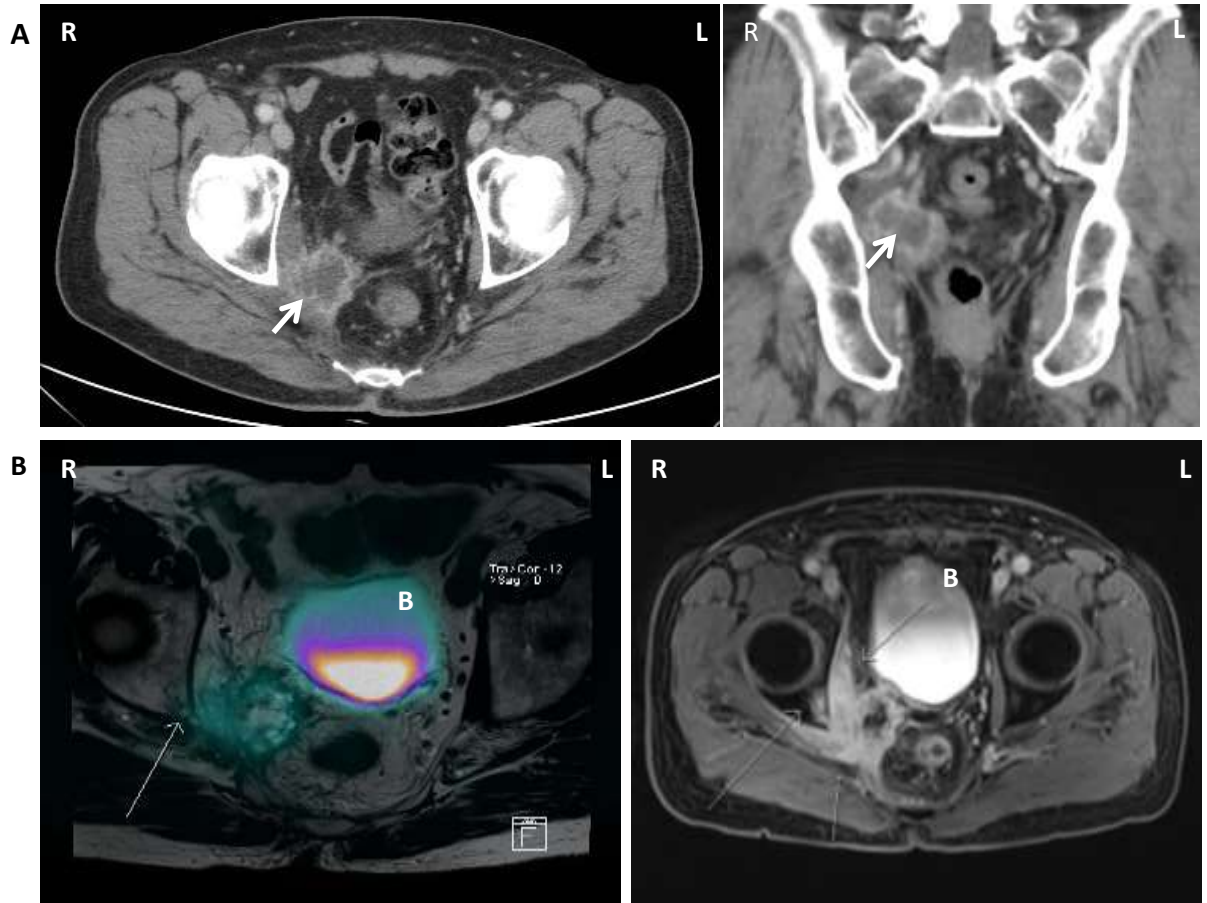

Figure 3.2 PSMA PET MRI imaging for patient BCR006 demonstrating an avid rib lesion (**A**) Axial PSMA PET/MRI showing an avid Rib lesion (black arrow) (**B**) CT guided biopsy of avid lesion (yellow arrow pointing to intended biopsy target on CT at time of biopsy).

Another example of the improved anatomical characterisation provided by the MRI component of the hybrid scan is demonstrated in patient BCR001. BCR001 is a 62 year-old patient treated previously with neo-adjuvant ADT + EBRT for Gl 3+4=7 prostate cancer. His PSA at the time of enrolment was 0.24 ng/ml but he was symptomatic with increasing lower back pain with symptoms suggestive of nerve compression.

Following standard of care imaging, 'necrotic lymphadenopathy' was noted in the pelvis on CT scan (Figure 3.3A). PSMA PET/MRI showed this mass to have moderate peripheral PSMA avidity, in keeping with local recurrence/necrotic metastatic lymphadenopathy. This lesion was identified as far more extensive than suggested on SOC imaging and was further able to be characterised with MRI. It demonstrated involvement of the right obturator internus muscle, right ureter, right seminal vesical, right sciatic nerve, right ischium and extended through the mesorectal fascia without extension to the rectum, all previously not appreciated on CT imaging (Figure 3.3B).

This extensive recurrence explained the patient's symptoms and due to the better definition of the lesion and understanding of the extent of involvement, his symptoms were better palliated appropriately with the implementation of docetaxel chemotherapy and the insertion of a ureteric stent to maintain patency of the involved right ureter.

Figure 3.3 Comparison of standard CT and PSMA PET MRI for patient BCR001 (**A**) Standard computer tomography (CT) image showing axial [left panel] and coronal [right panel] views of a right pelvic sidewall mass (white arrows). (**B**) Prostate Specific Membrane Antigen Binding Ligand Positron Emission Tomography/ Magnetic Resonance Imaging (PSMA PET/MRI) demonstrating PSMA avidity of same lesion (white arrow) [left panel]; lesion on T2 weighted MRI demonstrating degree of invasion, not identifiable in (A) (white arrows) [right panel] R: right, L: left, B: bladder.

Hybrid PSMA PET/MRI imaging also significantly improves characterisation of PSMA avid lesions in the pelvis and at distant sites, differentiating between true PSMA avid lesions and areas of benign/ background expression. This benefit of the T2 weighted MRI sequence is demonstrated in the case of patient BCR005 (PSA 0.626 ng/mL biochemical recurrence post

radical prostatectomy, Gleason 4+4=8). A focus of PSMA avidity was reported in the left pelvis, which on T2 weighted MRI was seen to correspond to a localised dilatation of the left ureter which was therefore considered to represent urinary excretory PSMA activity as opposed to tumour recurrence (as initially reported on the PSMA PET imaging component) (Figure 3.4)
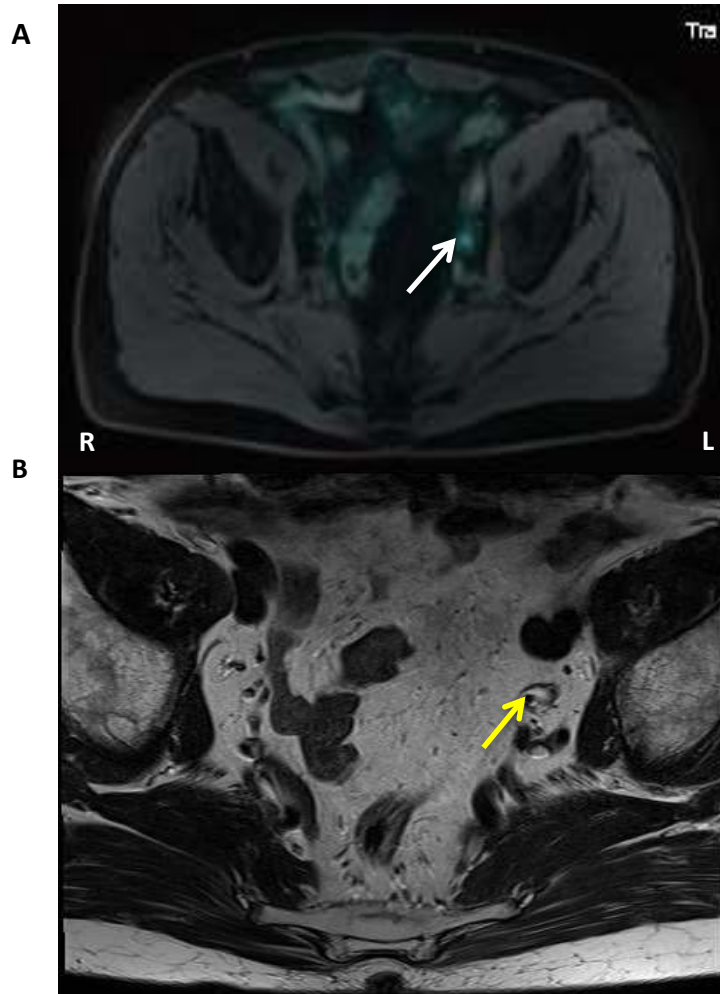
Figure 3.4 PSMA PET/MRI for patient BCR005 demonstrating the benefit of the T2 MRI component of the PET/MRI scan (**A**) PSMA PET/MRI demonstrating PSMA avidity in left pelvic side wall (white arrow) (**B**) T2 weighted MRI correlating avidity with urine in a dilated left ureter (yellow arrow). R: right, L: left

3.6 –Conclusion

In conclusion hybrid PSMA PET/MRI may be useful in staging men with biochemical recurrence, especially when PSA levels are low. Based on our study data, PSMA PET/MRI has a positive predictive value of 95.2% and a sensitivity of 68.9%. Our data demonstrates a high detection rate, especially for locally recurrent disease in the pelvis, outperforming SOC imaging, even at PSA <1.0ng/mL. This is similar to the reported sensitivity of PSMA PET/CT; however in suspected cases of biochemical recurrence, PSMA PET/MRI imaging provides improved detection rates and reduces false positives and false negatives. The superior anatomical definition provided by the MRI component of the hybrid scan adds valuable information and, as demonstrated by the data above, outperforms SOC imaging. The MRI component adds additional information to the PSMA component over and above that of a PSMA PET/CT due to the discussed advantages in this clinical setting. We have thus shown that PSMA PET/MRI not only outperforms SOC imaging, but has clinically significant benefits over PSMA PET/CT; however a clinical trial comparing the two modalities would be required to definitively confirm this. The benefit of combining the high definition of MRI imaging with PSMA avidity is highlighted by the examples above. By using PSMA avidity in combination with MRI, areas of interest or those potentially missed or overlooked can be better characterized.

PSMA PET/MRI has the potential to significantly improve recurrent prostate cancer detection and allow early identification and management of recurrent disease. This may have implications for earlier salvage treatment, avoidance of futile local therapy in patients with distant disease and change patient management which could potentially translate to better outcomes for our patients.

Chapter 4 – Organoid Culture and Precision Medicine Techniques

4.1 - Introduction

Precision medicine aims to individualise patient management based on their specific tumour characteristics and biology, treating on the basis of the targetable tumoral aberrations rather than traditional histologic subtypes. This aims to improve clinical outcomes, with decreased morbidity and improved survival in men with prostate cancer.

In order for precision medicine to become a reality, identification of predictive biomarkers is necessary. Most of the initial work in precision medicine in prostate cancer has been in mCRPC patients, who have undergone multiple previous rounds of therapy. Whilst multiple potentially actionable aberrations have been identified in this group of patients (34), at this stage, use of this technology in the routine care of patients or as biomarkers for response or resistance to therapies have not been established except in the investigative setting (34-36).

To our knowledge there have been no previous investigations of the potential for precision medicine in the early recurrent prostate cancer population and thus it is currently unknown if identification of actionable aberrations in this early recurrent setting will predict future responses or resistance to therapies or indeed if a precision medicine approach is possible to improve patient outcomes.

This chapter outlines novel *in vitro* culture technologies (described in Chapter 2) used to amplify and culture biopsy samples from individual patients. It was hypothesised that these technologies would allow adequate growth of tumour cells to allow next generation sequencing technologies and *in vitro* drug sensitivity screening in clinically meaningful (6 to 8 week) timeframes. If successful, it is anticipated that this information may be used to identify therapeutic strategies, markers of resistance/sensitivity and enrich patient populations for clinical trials.

Prior to experimenting with patient samples, we aimed to apply novel media technology to cell lines (LNCap, MSK3) and patient-derived xenograft (PDX) *in vitro* models in order to develop streamlined protocols to apply to subsequent clinical samples.

## 4.2 – Development of 2D Culture Drug Screening Protocol

Prior to testing patient-derived tumour samples, 2D and 3D culture drug screening protocols were established using LNCaP (42) and MSK-PCa 3 (MSK3) cell lines (50) to establish a methodology for patient samples. LNCaP and MSK3 cells were plated and treated according to established lab protocols (outlined in Appendix 4). As discussed in Section 2.8 above, the effect of drugs was monitored by cell confluency using the IncuCyte ZOOM cell imaging system (Essen BioScience). All treatments were plated as technical triplicates, with each experiment repeated up to three times where possible.

A panel of drugs, representing those used clinically for the treatment of biochemical recurrence was selected for developing the screening protocols including bicalutamide, enzalutamide, ARN509, docetaxel and cabazitaxel.

4.2.1 Establishment of protocols for MSK3 cell lines

MSK3 is a novel cell line recently developed at the Memorial Sloane Kettering Cancer Centre that has only been utilised in a limited number of studies (5). Therefore, in order to facilitate *in vitro* 2D drug screening, it was necessary to establish specific plating protocols to ensure reproducible experimental conditions.

Initially MSK3 cells were plated at 5000 cells per well onto type 1 collagen (Corning Rat Tail Collagen Type 1), Poly-L-ornithine (0.01%, Sigma-Aldrich) coated or un-coated 96-well ImageLock^{TM} plates. Plates were analysed using the IncuCyte ZOOM cell imaging system to determine which coating conditions would allow for the most efficient cell growth. Collagen coating of plates allowed an adherent monolayer of cells to be established to provide optimal conditions for Incucyte analysis to be performed compared to uncoated plates where cells aggregated. The marked effect of collagen coating is highlighted in figure 4.1 and 4.2 below.
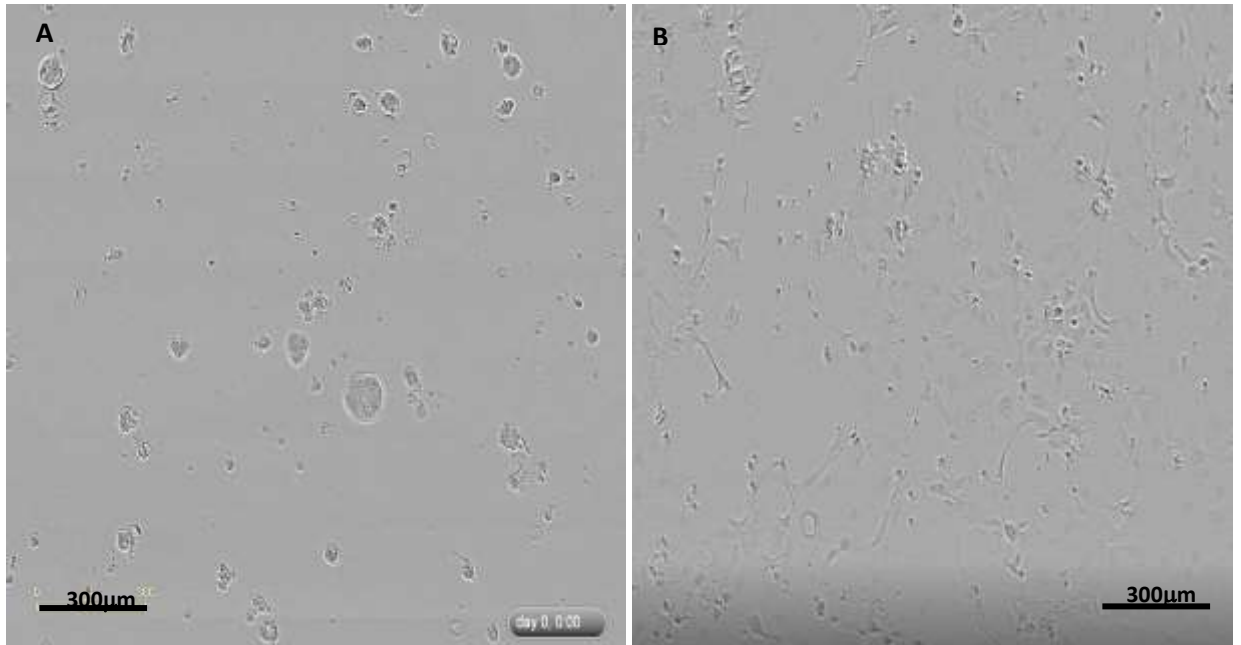
Figure 4.1 Collagen coating of 96 well plates prevents cell clustering allowing Incucyte analysis **A:**
Uncoated plates showing clustering of MSK3 cells not suitable for analysis with Incucyte, **B:** Collagen
coated plate at 36 hours showing an adherent monolayer of MSK3 cells which allows Incucyte analysis
to be performed and a comparison of cell confluency (scale bar 300µm).
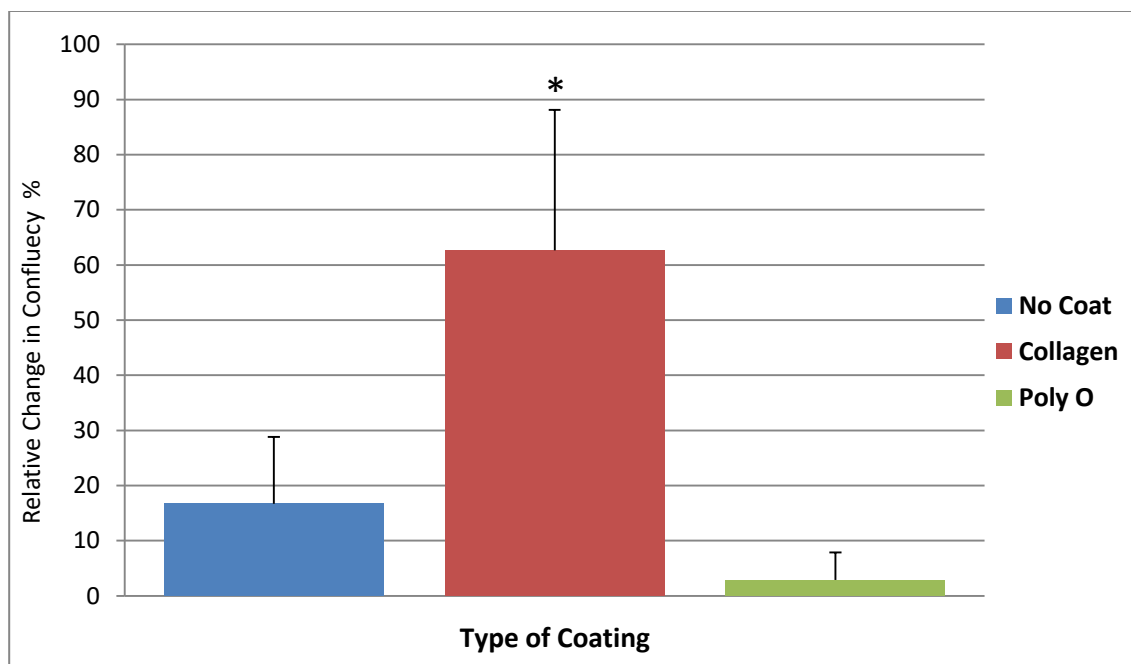
Figure 4.2 Collagen coating increases confluency of MSK3 cells. The effect of various coating agents on MSK 3 growth after 72 is demonstrated in this figure. A significant difference (*) in confluency at 72 hours is seen with collagen coating compared with no coating (p=0.0074) or poly-L-ornithine (Poly O) coating (p= 0.0051), using the Incucyte system. This marked increase in confluency with collagen coating is likely a representation of an adherent monolayer of cells which allows Incucyte analysis to be performed more accurately [n=3 technical repeats, error bars represent standard error of the mean, cells seeded at 5000 cells per well grown in HCM with 0.1nM DHT].

4.2.2 Establishment of optimal doses for 2D Drug screen protocol

Once the 2D culture protocol was established for MSK3 cells, the conditions for *in vitro* drug screening were optimised in preparation for patient-derived samples. MSK3 cells were plated onto collagen coated 96-well ImageLock™ plates and incubated for 3 days. After 3 days, media was aspirated and various drug treatments added at pre-determined concentrations (Appendix 4). Anti-androgens (bicalutamide, enzalutamide, ARN509) were administered at 10 µM. A dose range for Docetaxel Cabazitaxel was determined using MSK3 cells and concentrations of 0.5 nM and 1 nM were subsequently used – maximal benefit doses (Figure 4.3). These doses resulted in approximately 50% decrease in relative confluency. Plates were subsequently returned to the IncuCyte and imaged for up to a further 5 days. From these preliminary experiments a therapeutic drug screening panel was developed (Table 4.1).
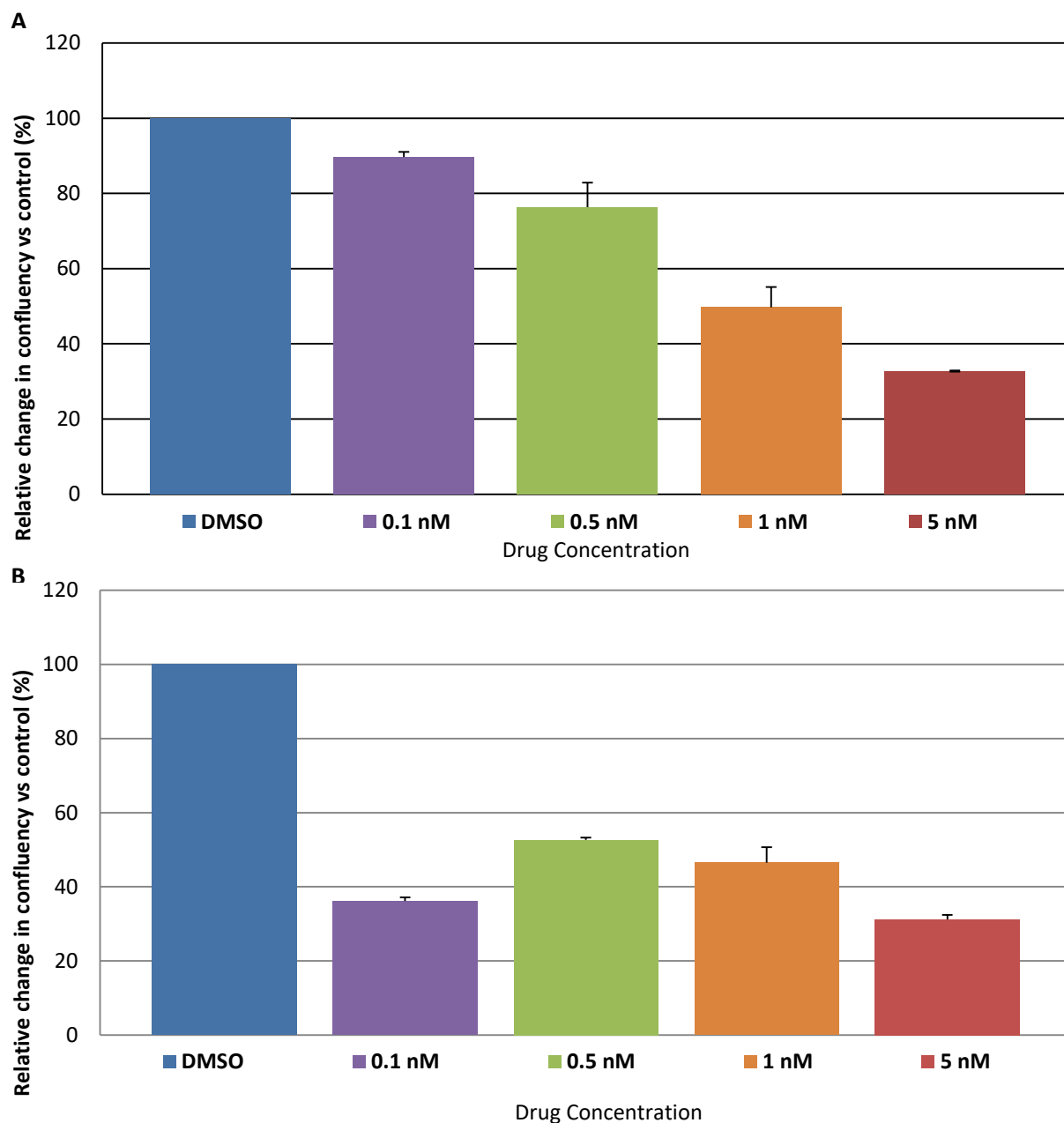
Figure 4.3 *The dose effect of docetaxel and cabazitaxel on MSK3 cell line.* A: The effect of docetaxel on MSK cells after 72 hours; B: The effect of cabazitaxel on MSK 3 cells after 72 hours. Both panels demonstrate an approximately 50% decrease in relative confluency at 1 nM concentration for both treatments [n=3 biological repeats, error bars represent standard error of the mean, cells seeded at 5000 cells per well grown in HCM with 0.1nM DHT, DMSO control].

A therapeutic drug screening panel was developed using these concentrations, the drug doses used are summarised below in Table 4.1.

Table 4.1 *In Vitro Therapeutic Drug Screen Panel*

Drug	Concentration
DMSO control	1%
Bicalutamide	10 µM
Enzalutamide	10 µM
ARN 509	10 µM
Docetaxel	0.5 nM, 1 nM
Cabazitaxel	0.5 nM, 1 nM

### 4.2.3 MSK3 cells show apparent resistance to antiandrogens in 2D culture conditions

2D drug screen results for MSK3 and LNCaP are displayed in figure 4.4 below. In a 2D system, MSK3 cells appear to show resistance to anti-androgen treatments when compared to control treated DMSO cells as no statistical change in confluency was observed with any anti-androgen treatments (Figure 4.4). This is likely due to the MSK3 cell line being castrate resistant with low AR expression (as previously discussed). Chemotherapy appears to reduce cell confluency in both cell lines as non-significant reductions in confluency were observed in both cell lines with both chemotherapy agents (0.5nM dose). However significant effects on confluency were observed in LNCaP cells treated with docetaxel. In 2D, LNCaP cells responded to Enzalutamide treatment (p=0.025), whereas Bicalutamide and ARN 509 treatments did not reach statistical significance. The absence of significant effects of bicalutamide and ARN509 is surprising, although possible trends towards reduced confluency suggest that increased treatment time might result in both statistical and biological significance being achieved with these compounds. As confluency is determined by the combination of cell proliferation, death, morphology and movement these parameters might be altered by antiandrogens or chemotherapeutic compounds to different degrees at different rates and thus further experimentation should have been done to look at these parameters in further detail. However, having demonstrated the ability to induce significant changes to cell growth with chemotherapy drugs and Enzalutamide, we decided to investigate further using a 3D drug screen model due to its greater resemblance to *in vivo* conditions.
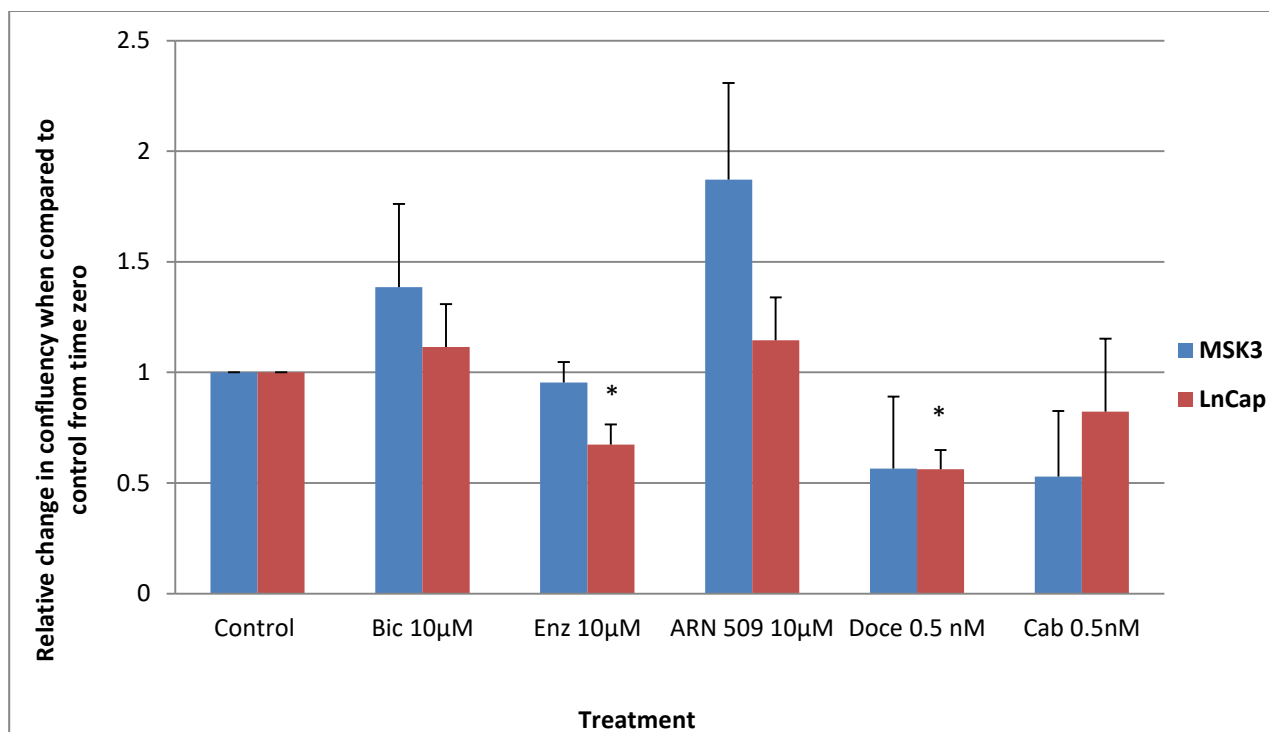
Figure 4.4 *MSK 3 cells demonstrate apparent resistance to anti-androgen treatment - MSK 3 and LNCaP cell lines 2D drug screen results after 5 days in culture.* Cells seeded at 5000 cells per well grown in HCM with 0.1nM DHT for MSK3 cells and with 1.0nM DHT for LNCaP cells. MSK3 cells (blue) show an apparent resistance to anti-androgen treatments as expected given their castrate resistant nature compared to androgen sensitive LNCaP (red) cells. Chemotherapy reduces cell confluency in both cell lines. Bic: bicalutamide, Enz: enzalutamide, Doce: docetaxel, Cabi: cabazitaxel. [n=3 biological repeats, data represents means, error bars representing standard error of the mean; * $p < 0.05$ when comparing the effect of treatment to control DMSO for each cell line; statistical analysis and p values were calculated using Students T-test].

4.3 – Development of 3D Culture Drug Screening Protocol

3D cell culture is more representative of the *in vivo* environment and may produce different results in cells compared to 2D culture (50, 51, 70). 3D drug screens were carried out using similar seeding density and drug doses as the previously described 2D protocol. Plates were prepared for 3D culture as described in section 2.8.2 above. Plates were incubated for 5 days (Figure 4.5).
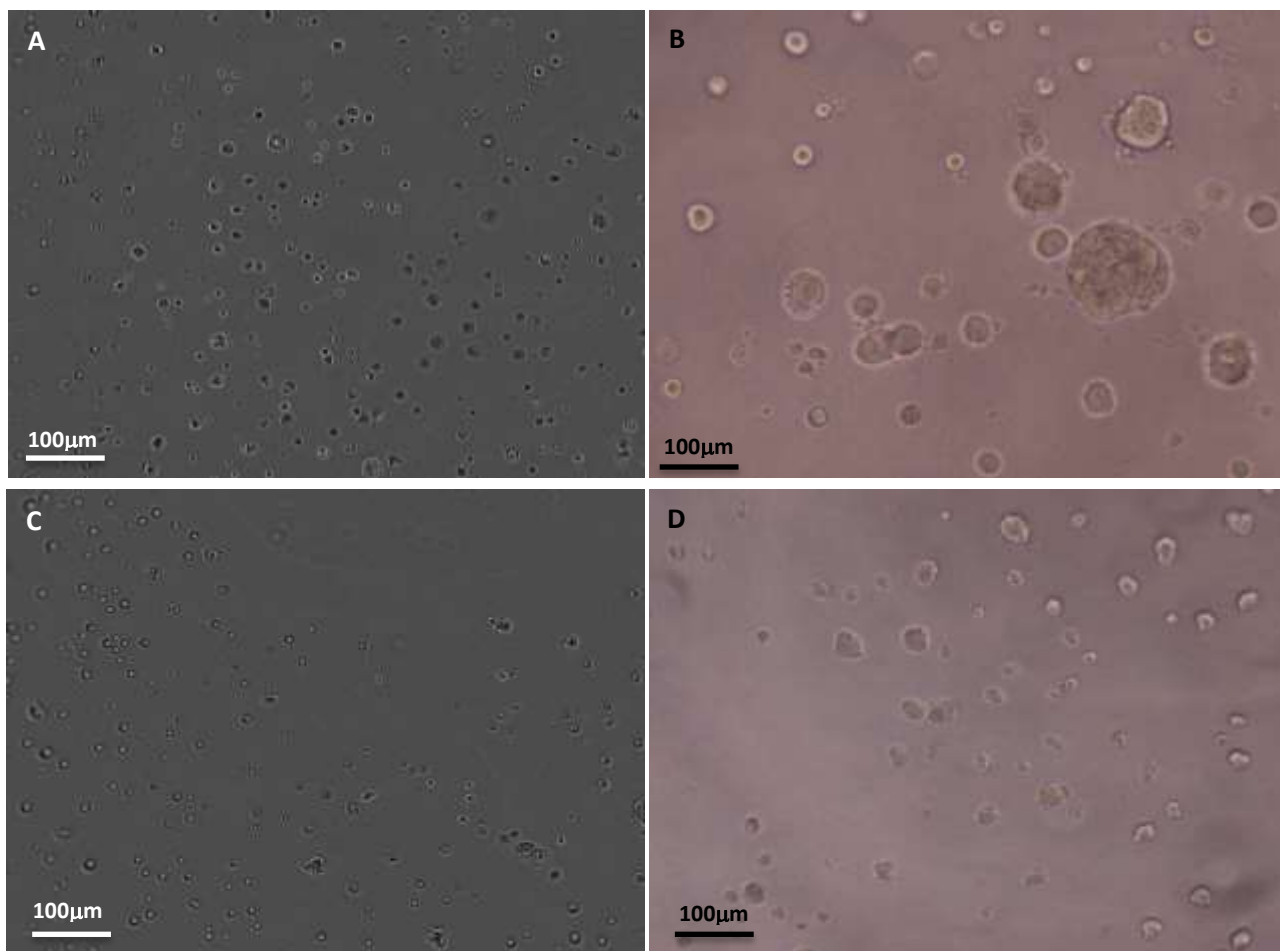
Figure 4.5 *Cell growth in 3D forming "organoids" after 3 days of culture **A:** MSK3 cells at time of seeding (T0); **B:** MSK3 cells after 3 days; **C:** LNCaP cells at T0; **D:** LNCaP cells after 72 3 days (Scale bar 100μm)*

After 5 days, media was aspirated and drugs were added to wells for 3 days before media and treatments were replenished. After 5 days of treatment CellTiter-Glo® Cell Viability Assays were performed as per manufacturer's protocol to determine viability (Figure 4.6).

In this 3D system, MSK3 cells once again showed an apparent resistance to anti-androgen treatments when compared to DMSO treated control cells, not reaching statistical significance. Although MSK appeared sensitive to Enzalutamide, the effect of this drug did not reach statistical significance (Figure 4.6). Antiandrogen treatment had no significant effect on LNCaP however, chemotherapy significantly reduced cell viability in both cell lines (MSK docetaxel $p=0.012$, cabazitaxel $p=0.036$; LNCaP docetaxel $p<0.01$, cabazitaxel $p<0.01$). The effect of chemotherapeutics agents was particularly marked for MSK3 cells, reducing viability by ~50% vs vehicle control, whereas LNCaP showed a ~70% reduction. Treatment with

chemotherapeutics not only reduced cell viability of MSK3 cells but also resulted in visually identifiable disruption of organoids in culture (Figure 4.7), a response not observed in LNCaP cells. Chemotherapeutic drugs preferentially affect rapidly dividing cells, such as the rapidly proliferating MSK3 cells compared to LNCaP cells which may explain the marked disruption seen in treated MSK3 organoids.

It also appears that the vehicle control (DMSO) has a relative reduced effect on cells in 3D than in 2D culture, when compared to media alone (Figure 4.4). The effects seen in 3D culture are thus more likely due to added treatments, as opposed to DMSO.
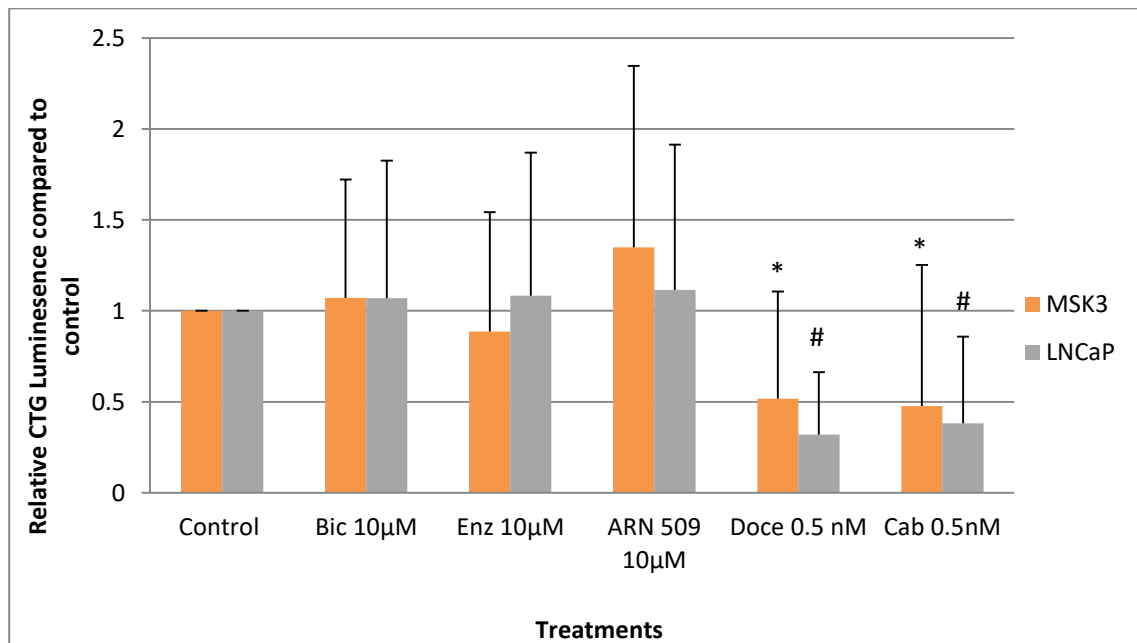
Figure 4.6 *MSK 3 and LnCaP cells are significantly affected by chemotherapy agents in 3D culture after 5 days.* MSK3 cells (orange) show an apparent resistance to anti-androgen treatments. Chemotherapy significantly reduces cell viability in both cell lines. Control: DMSO, Bic: bicalutamide, Enz: enzalutamide, Doc: docetaxel, Cabi: cabazitaxel. [n=3 biological repeats, data represents means, error bars representing standard error of the mean; * $p<0.05$ when comparing the effect of treatment to control DMSO for MSK3 cells and # $p<0.05$ for LNCaP; statistical analysis and p values were calculated the students T-test].
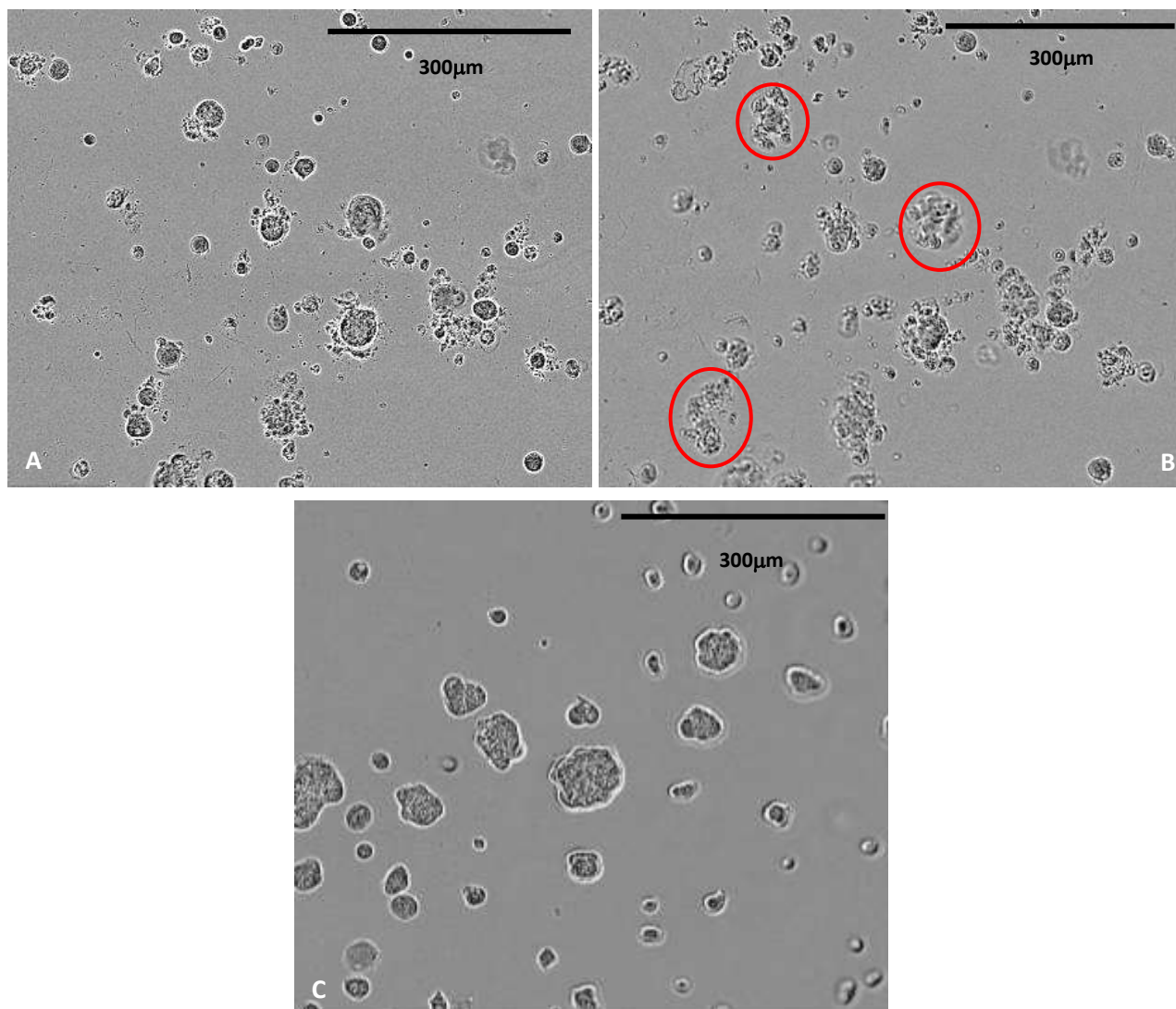
Figure 4.7 *Effect of docetaxel chemotherapy on 3D cell culture after 5 days of treatment.* **A:** MSK3 cells in 3D treated with DMSO (vehicle control); **B:** Disrupted MSK3 organoids following treatment with docetaxel (red circle). **C**: LNCaP cells after treatment showing intact organoids. (Scale bar 300μm).

4.4 – Preclinical Applications of Organoid Media Technology and Establishment of Techniques

To optimise culture techniques from patient-derived biopsy specimens prior to 2D and 3D drug testing, organoid media technology was first used to convert the prostate cancer PDXs, BM18 (74) and LuCap 35 (75) into *in vitro* cultures. PDX lines, whilst useful models, are limited by the inability to be manipulated genetically via over-expression, knockdown or silencing of genes of

interest. The BM18 and LuCaP 35 PDX models have never previously been successfully cultured *in vitro* (personal communication Dr Elizabeth Williams, APCRCQ).

PDX tissues were collected fresh at the time of passage. These tumours were digested in Type II Collagenase (Gibco) for 30 minutes before being seeded in 150 µL Matrigel™ or directly onto Collagen Type I coated plates in HCM. Using this protocol, both PDX lines were successfully maintained continuously in *in vitro* culture for up to 6 weeks for the first time (Figure 4.8).
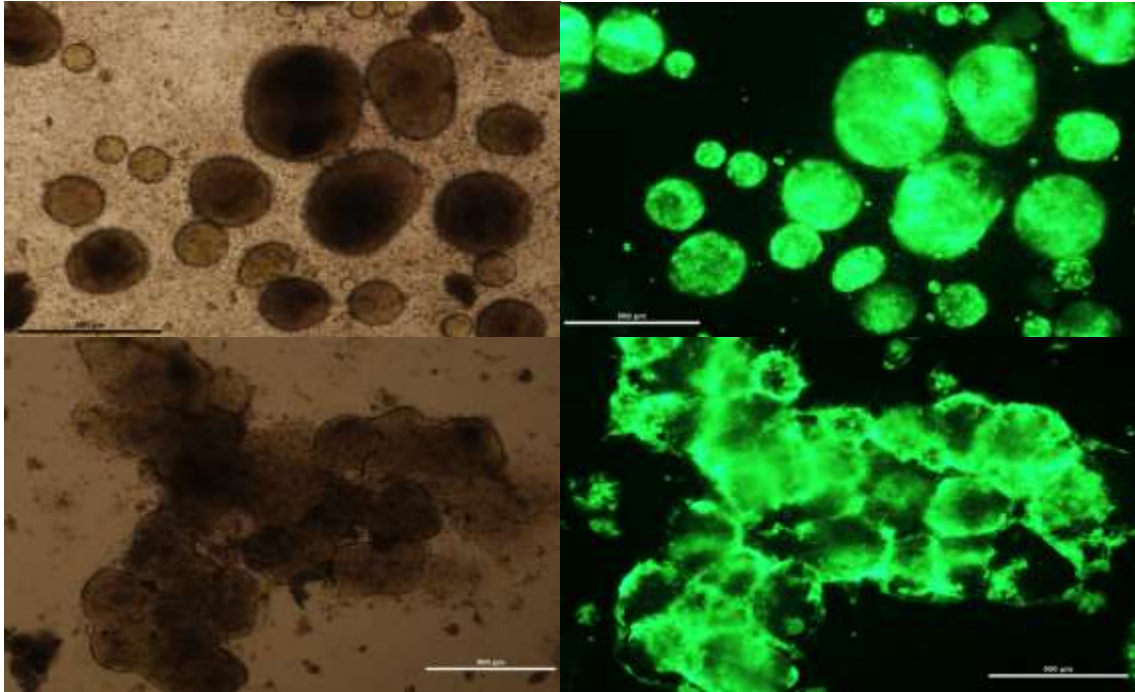
Figure 4.8 Successful in vitro culture of PDX and proof of principle genetic manipulation **A&B**: Organoid culture of LuCaP 35 PDX. **A** Brightfield image of organoid culture and **B** successful expression of GFP following Lentiviral infection to produce LuCaP 35-GFP model. **C&D**: Organoid culture of BM18 PDX. **C** Brightfield image of organoid culture and **D** successful expression of GFP following lentiviral infection to produce BM18-GFP model.

Fresh frozen tumour samples of each PDX line, and the associated culture samples were collected for RNA analysis as biologic triplicates. cDNA was analysed using specific primers for genes of interest (AR, PSA, TMPRSS2; primers listed in Appendix 3) as technical triplicates and comparisons between culture and PDX samples were performed. This experiment was conducted by Dr Cheryl Nicholson at the APCRC-Q (data reproduced with permission). There does not appear to be substantial alteration of phenotypes based on this limited gene

expression analysis, however some changes due to relative expression of selected genes are observed, especially from PSA and TMPRSS (Figure 4.9).
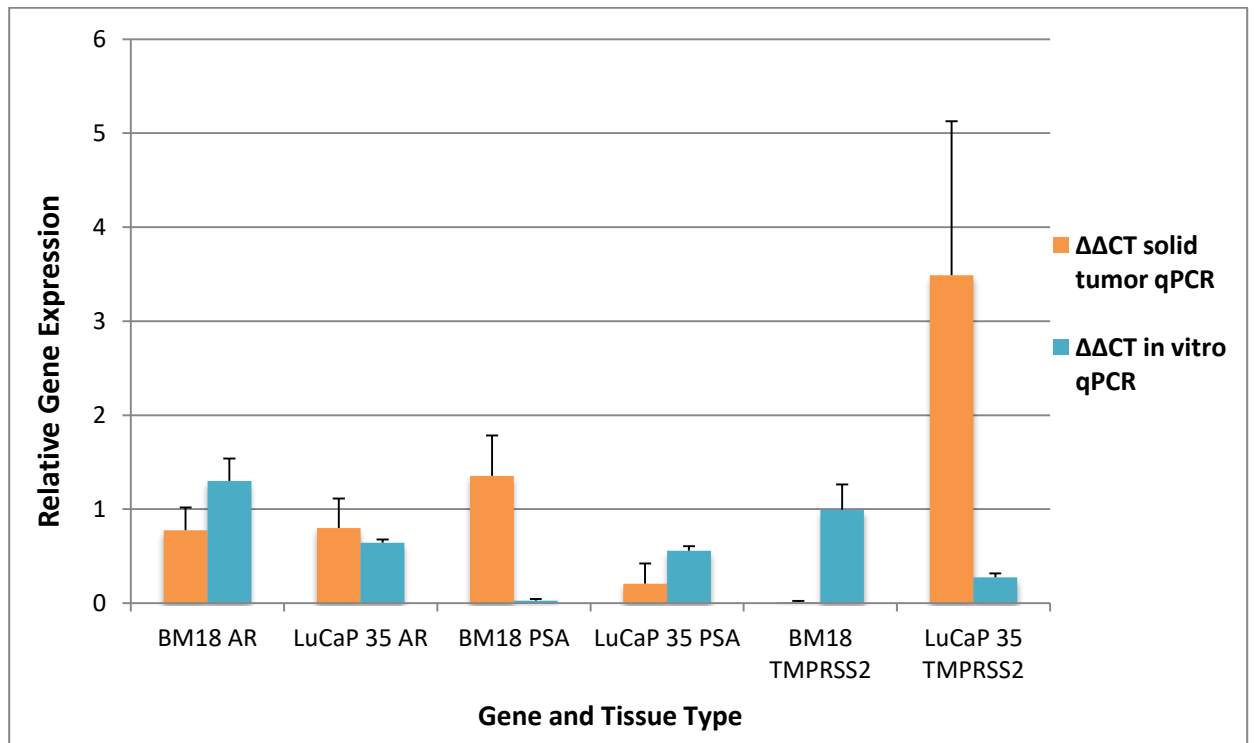
Figure 4.9 *RT-qPCR analysis of selected genes comparing Fresh Frozen PDX tissue vs in vitro cultured cell expression.* Organoid in vitro culture of LuCaP 35B PDX and BM18 PDX does not appear to alter the expression of selected genes as assessed by qPCR (normalized expression relative to COXIV housekeeping gene). Data and conclusions reproduced from Dr Cheryl Nicholson with permission.

4.4.1 Genetic manipulation of PDXs

Given the apparent successful *in vitro* culture of these PDX lines for the first time, genetic manipulation of the cultured cells was performed as proof of principle for potentially increasing the utility of PDX models or of future patient-derived organoid models. Transient lentiviral transfection of *in vitro* cultured cells was performed using a pGIPZ lentiviral vector with a non-silencing hairpin targeting Fire Fly Luciferase and expressing Turbo GFP (ThermoScientific) as per manufacturer's protocol. LuCaP 35 and BM18 lines were successfully labelled with GFP for the first time, creating LuCaP 35 GFP and BM 18 GFP PDX models (Figure 4.8).

BM18-GFP and LuCaP 35B-GFP cells from *in vitro* culture were then injected subcutaneously at $1x10^5$ cells in 200µL Matrigel™ into NOD SCID Gamma mice demonstrating stable and persistent expression of GFP *in vivo* and were able to reconstitute PDX tumours with similar phenotype to the parental lines (macroscopically at dissection and microscopically when cultured) and demonstrated stable expression of GFP *in vivo* (Figure 4.10). Tumours were imaged using epi-fluorescence on subsequent *in vivo* passage to identify stable GFP expression and demonstrated persistent GFP expression (Figure 4.11).
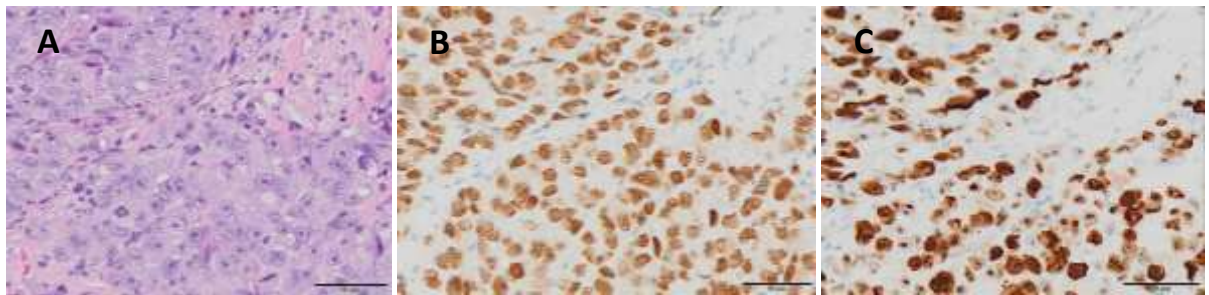
Figure 4.10 Genetically *Modified PDX lines showing maintenance of AR and PSA expression.* **A:** H&E of successful subcutaneous tumour regrowth of organoid culture of LuCaP 35 PDX. **B:** AR expression is maintained in the regrown organoid culture tumours of LuCaP 35 PDX. **C:** PSA expression is maintained in the regrown organoid culture tumours of LuCaP 35 PDX. (Scale 50µm)
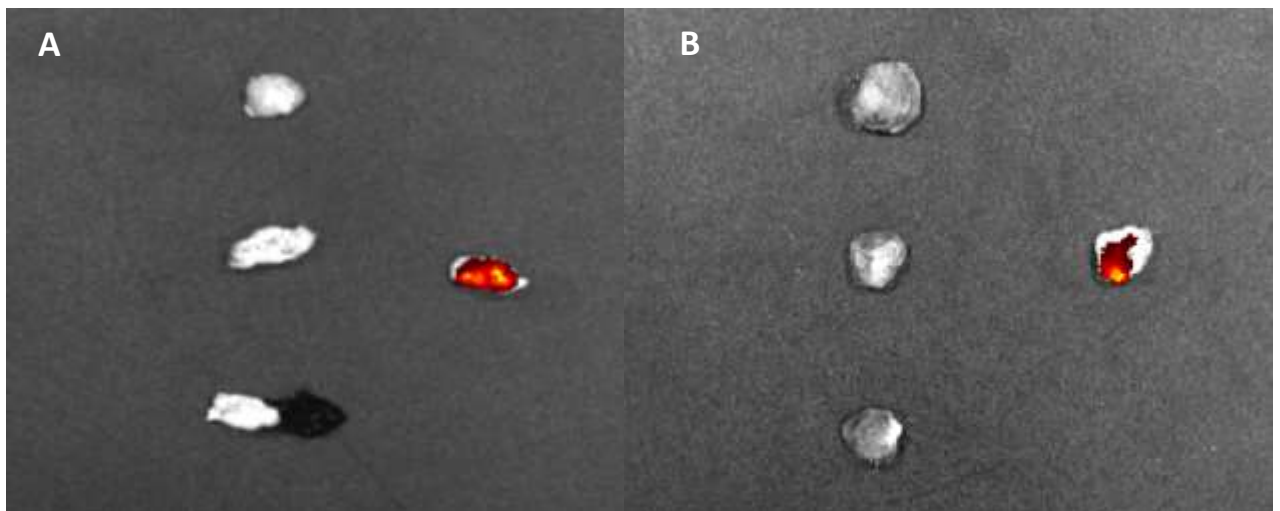
Figure 4.11 *Stable GFP expression on subsequent passage of in vivo tumours using epi-fluorescence; (***A)** LuCaP35 PDX; **(B)** BM18 PDX. Control tumours are on the left, GFP labelled tumour with persistent expression are on the right of each panel.

4.5 – Conclusion

The 2D and 3D protocols described above were applied to enable *in vitro* drug screening of a novel patient-derived cell line (MSK3) for the first time and establish protocols for future *in vitro* drug screening of patient-derived organoid lines as part of the larger PCa clinical trial. The MSK3 cell line, derived from a retroperitoneal lymph node, was used to model potential future patient-derived cell line models from metastatic deposits in biochemical recurrence. These developed methods and techniques were then applied to patient-derived cell models. 2D and 3D drug screen results demonstrated expected outcomes when experimenting with MSK3 and LNCaP cell lines. The castrate resistant MSK3 cell line, developed from a patient with disease progression whilst on anti-androgen therapy had an apparent resistance to anti-androgen therapies in both 2D and 3D *in* vitro drug screening when compared to androgen-sensitive LNCaP cells. This outlines the ability of *in vitro* drug screening and culture system to produce expected results based on prior *in vivo* treatment exposures and clinical responses and therefore suggests that the *in vitro* system maintains the prior clinical phenotype of the cancer and is potentially a robust system to model therapeutic efficacy and resistance.

Prostate cancer cells remain difficult to culture *in vitro*, however through the use of HCM and techniques outlined in this chapter we have been able to culture novel *in vitro* cell lines to allow drug screening and genetically manipulate multiple well established PDX models, for the first time. Furthermore this suggests that *in vivo* tumours can be excised, subsequently cultured *in vitro* and returned to *in vivo* environments for drug testing with no change between the original and re-implanted cells.

Substantial experience was gained with the initial studies described in this chapter along with optimisation of techniques. Initial attempts at conversion of these PDX tumours to *in vitro* models were unsuccessful due to low input tumour volumes. Furthermore, not all PDX line trialled were able to be successfully converted into an *in vitro* model such as the BM18 and LuCaP35 models. Reasons for this failure have not been readily apparent but are likely due to specific differences in PDX tumour models. However, once the methodology was established and experience was gained, successful replication of this work was achieved at our institute.

This proof of principle study has demonstrated how this technology could increase the utility of PDX models for the broader scientific community by permitting genetic manipulation of

these tumours for the first time *in vitro* and then reconstitution in the complex *in vivo* environment as a manipulated PDX model. This potentially facilitates novel findings, studies and investigations with PDX models and using patient-derived tissue rather than established cell lines. With collaborators within our institute we are generating further PDX *in vitro* models, genetically manipulating these models with inducible over-expression or knockdown of AR in a complex *in vivo* model for the very first time. The preliminary experience gained through this work has therefore established techniques to be used with clinical tissues samples for a precision approach to early recurrent prostate cancer as discussed in the following chapters.

Chapter 5 – Precision medicine in the management of early recurrent prostate cancer

5.1 – Introduction

Following the establishment of protocols and successful utilisation of novel *in vitro* culture media as described in Chapter 4, we aimed to utilise this technology with clinical samples to allow propagation of patient-derived *in vitro* cell lines for next generation sequencing technologies and *in vitro* drug sensitivity screening in clinically meaningful timeframes. As discussed previously, the SU2C East Coast Dream Team has previously explored the concept of precision medicine in advanced prostate cancer. Robinson et al., prospectively carried out whole-exome and transcriptome sequencing of tumour biopsies from 150 metastatic castrate resistant patients (mCRPC) and found that approximately 90% of mCRPC harbour clinically actionable molecular alterations (34). This was significantly higher than previously believed, thus indicating the applicability of precision medicine in prostate cancer. This study however did not include organoid culture technology or *in vitro* therapeutic screening in order to demonstrate if any of those identified aberrations were actually functional.

The role of precision medicine in early recurrent disease has not been investigated previously thus it is not known if this approach is possible and, if so, would change patient outcomes. Use of organoid culture technology for *in vitro* therapeutic screening has also not been performed in the clinical setting as a functional assessment of targetable aberrations identified by NGS of tumour/metastatic samples. This chapter highlights a proof of principle approach to precision medicine in managing men with early recurrent prostate cancer.

5.2 – Precision Medicine in biochemically recurrent prostate cancer

Patient derived metastatic tissue samples were collected as part of the larger clinical trial at the time of confirmatory diagnostic biopsy. These samples were prepared and cultured *in vitro* using protocols described in Chapter 2 section 2.6 for a minimum of 2 weeks prior to validation of prostate origin. Phenotypic assessment alone is insufficient to determine the cell type of origin, as cells were not sorted for culture, and thus further validation is required.

PSA ELISA (GenWay Biotech) of conditioned media and RT-qPCR comparison of various gene products of interest between cultured patient samples and established prostate cancer cell lines was performed to confirm prostatic origin of cultured cells. Samples, identified as of prostatic origin, were subsequently utilized for therapeutic screening and next generation sequencing technologies.

A total of 6 tissue samples from 6 patients with histologically proven metastatic prostate cancer were available for culture. Three patient samples were successfully grown in vitro. One sample did not propagate to sufficient quantities to allow downstream analysis; two patients will be discussed in detail demonstrating the application of precision medicine in the management of prostate cancer.

5.2.1 Patient 1

Tissue from a 72 year old male, previously treated with neo adjuvant ADT + EBRT for Gleason score 3+4=7 prostate cancer was collected at time of percutaneous biopsy from a PSMA avid pelvic lymph node (PSA 0.24 ng/ml). Histology revealed adenosquamous carcinoma, staining positive for P40, CK5/6, CK 7 and TTF-1. Interestingly PSA and CK20 staining was negative. After radiologically ruling out any other malignancies, the final histology was considered as a de-differentiated adenocarcinoma initially of prostatic origin. Cells were grown in culture for 2 weeks and showed clear evidence of organoid formation but had very low PSA secretion, possibly due to its histological subtype, lack of PSA staining and the patient's low PSA at recurrence with extensive disease (Figure 5.1). Unfortunately, this patient sample did not propagate to sufficient quantities for sequencing and *in vitro* drug screen analysis.
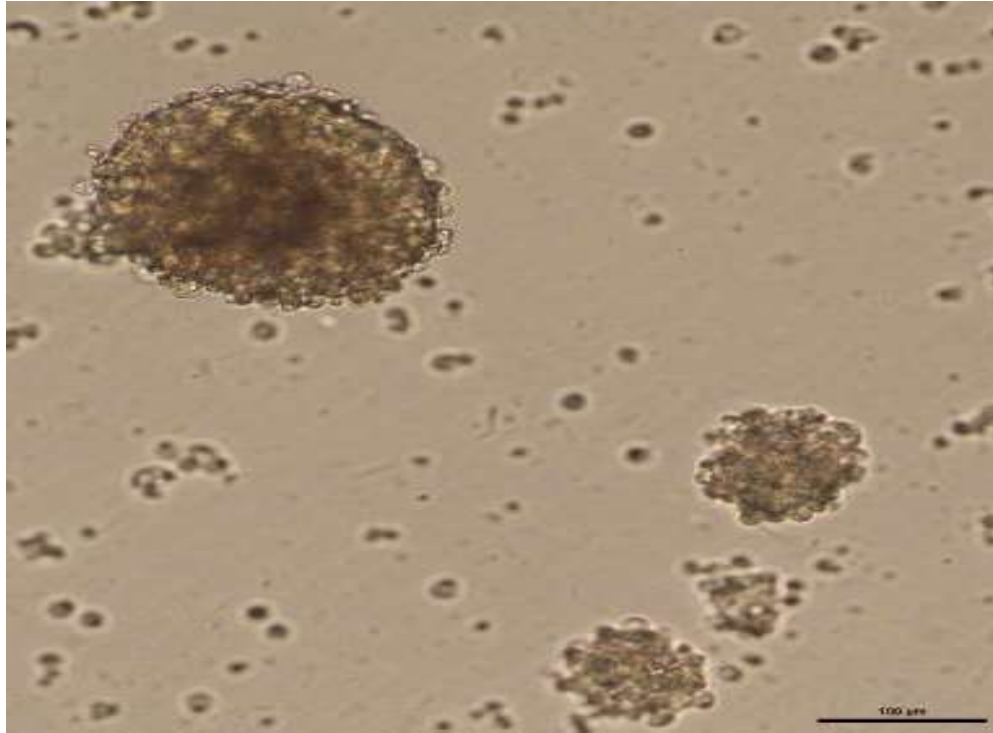
Figure 5.1 _Patient derived organoids cultured from BCR001 after 2 weeks in culture._ Bright field image of patient-derived organoid culture from pelvic lymph node biopsy; Scale bar: 100μm

5.2.2 Patient 2 – "BCR002"

A 67 year old male with a PSA of 1.5 ng/mL following open radical retropubic prostatectomy in 2014 (Histology: Gleason 4+5=9 pT3bNxMx) was enrolled in the clinical trial. The patient had not received any adjuvant, salvage or systemic therapies prior to enrolment. Standard of care bone scan was negative and CT chest/abdomen/pelvis revealed a suspicious equivocal node in the right pelvis. Subsequently PSMA PET/MRI was performed revealing a PSMA avid pelvic lymph node (Figure 5.2). No other PSMA avid lesions were identified.
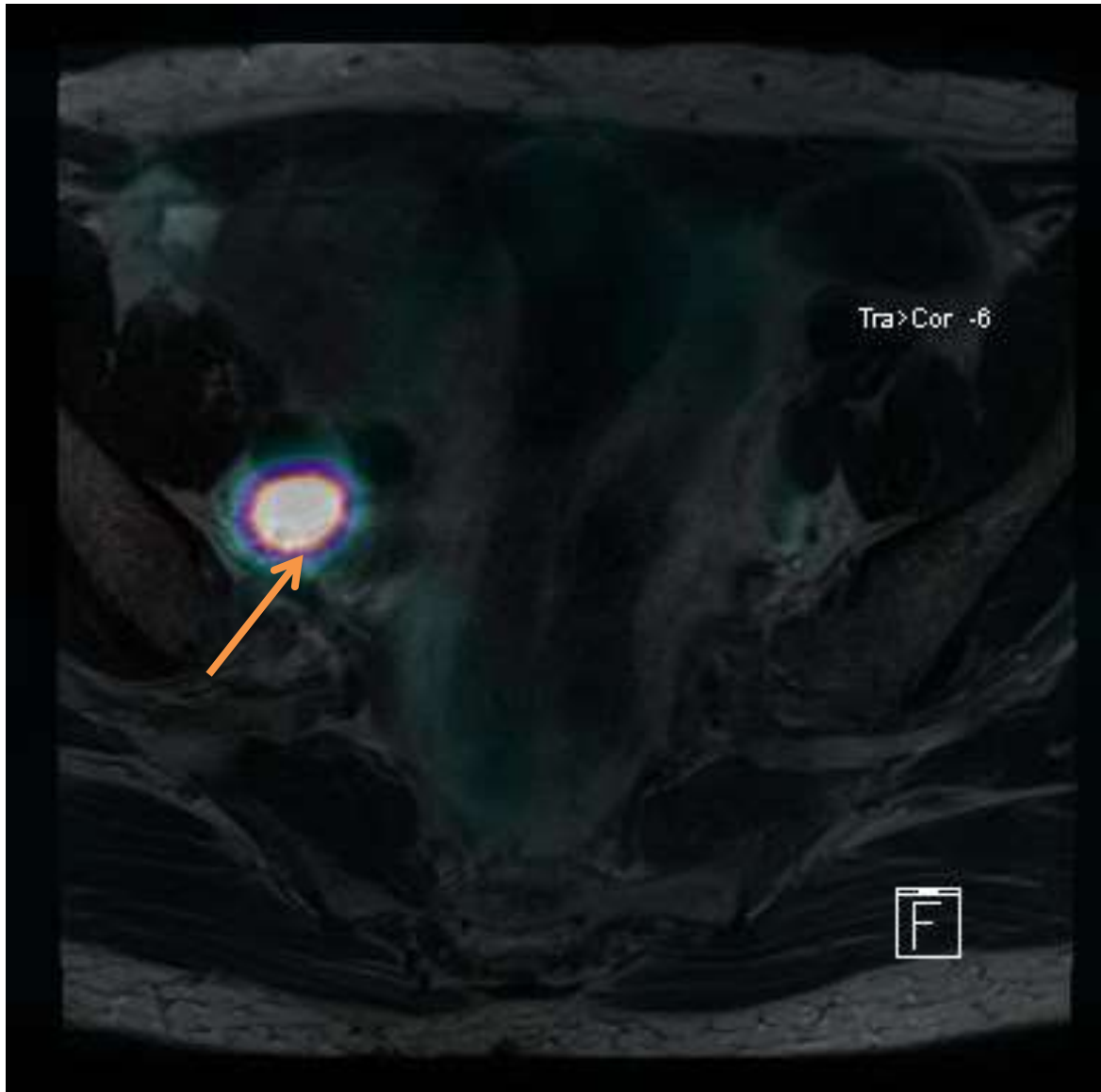
Figure 5.2 *PSMA PET/MRI of patient BCR002:* Imaging demonstrates an isolated PSMA avid right external iliac lymph node (orange arrow).

Following discussion at a multidisciplinary team meeting the patient underwent a salvage lymph node dissection. Tissue from the PSMA avid lymph node was obtained fresh intra operatively, with some retained as fresh frozen tissue and the remainder cultured as previously described (Figure 5.3).
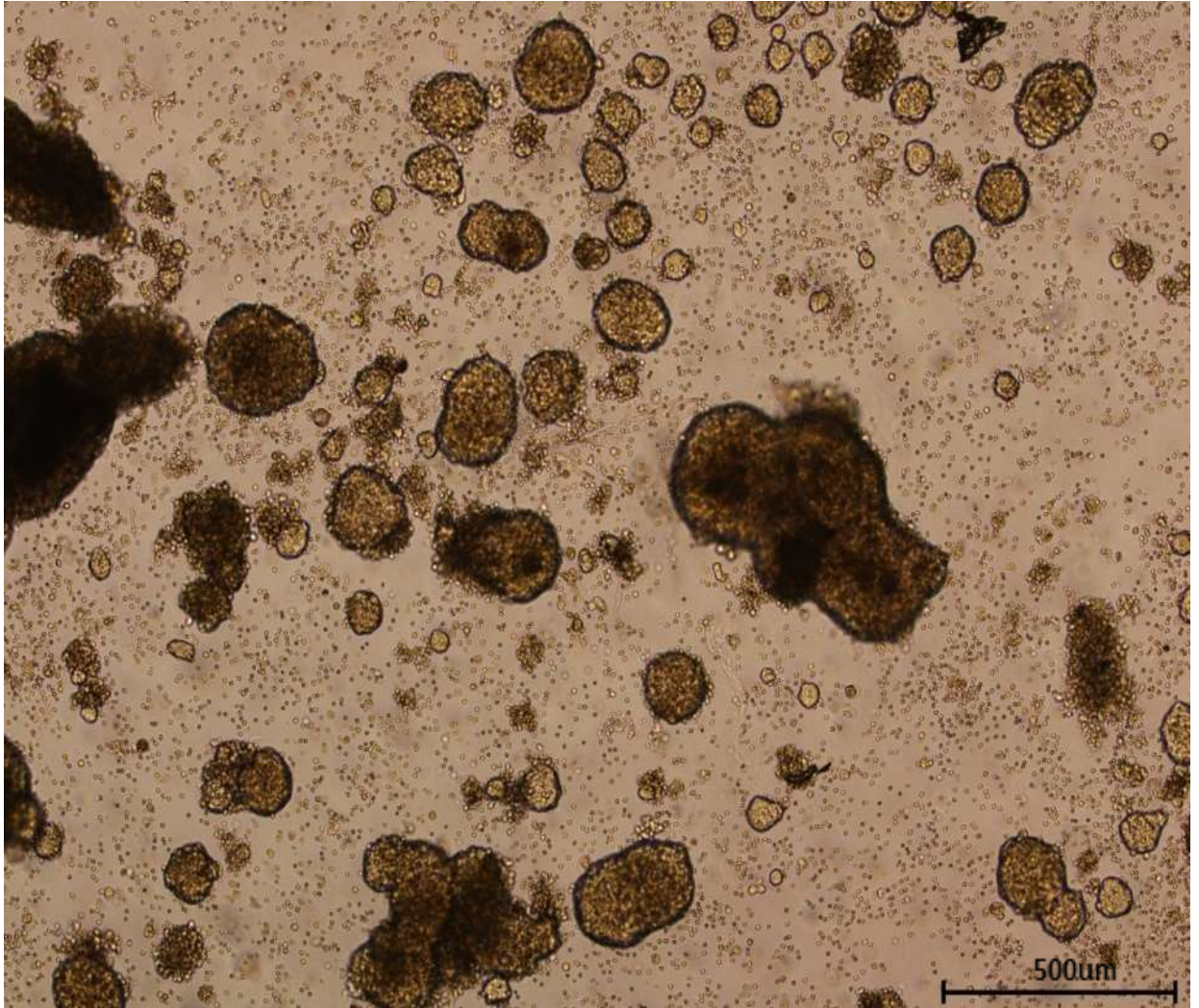
Figure 5.3 *Patient BCR002-derived in vitro culture derived from excisional lymph node biopsy of PSMA avid lymph node.* Bright field image of patient-derived 3D organoid culture after 2 weeks in culture; Scale bar: 500µm.

PSA ELISA (GenWay Biotech) of conditioned media from the *in vitro* culture was positive with a value up to 31 ng/ml. RT-qPCR using gene specific primers for prostate associated genes (AR, PSA, FKBP5 and TMPRSS 2) also suggested prostatic origin of the cells growing in culture (Figure 5.4).
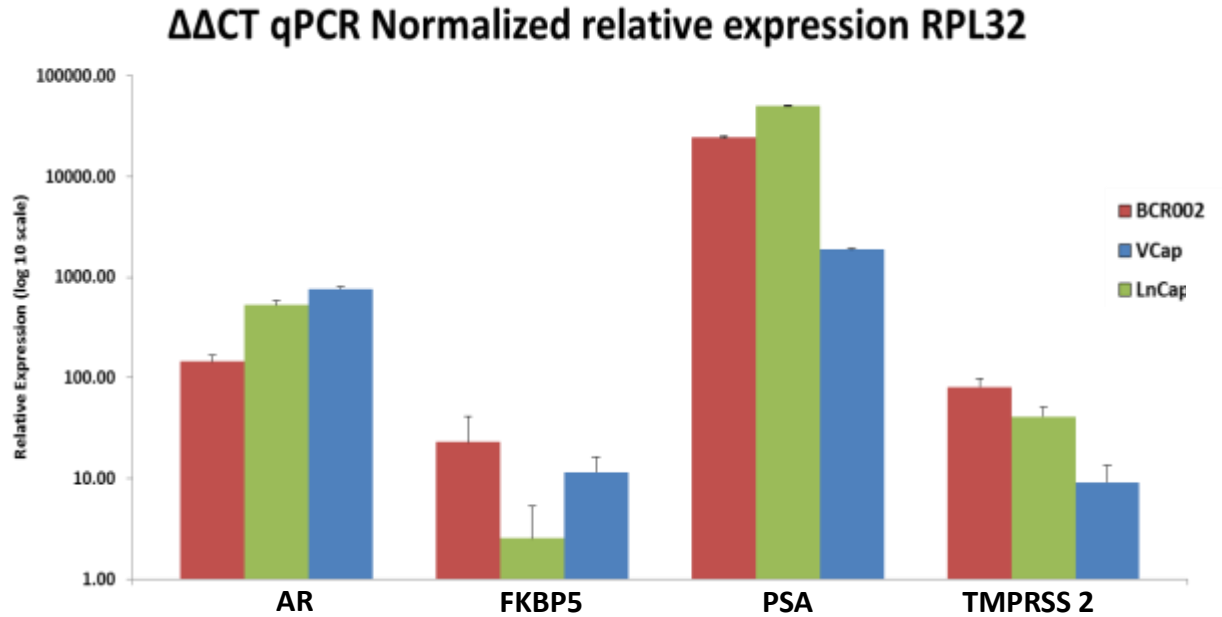
Figure 5.4 *RT-qPCR of prostate specific genes in BCR002 organoid cultures.* Comparable expression of AR, FKBP5, PSA and TMPRSS 2 of BCR002 patient-derived sample (red) to LNCaP (green) and VCaP (blue), normalized to RPL32. BCR002 expressed prostate-associated genes AR, FKBP5, PSA and TMPRSS 2 in similar magnitude to established prostate cancer cell lines LNCaP and VCaP. This suggests that BCR002 cells might be prostatic in nature. [n=3 technical repeats; error bars represent standard deviation].

Whole exome and RNA sequencing was performed on fresh frozen and *in vitro* samples after 6 weeks in culture. RNA sequencing was performed at the Kinghorn Centre for Clinical Genomics (KCCG) – Garvin Institute of Medical Research NSW. Samples were processed using Illumina TruSeq Stranded mRNA LT Sample Prep Kits. RNA was sequenced with 500 ng inputs on the mRNA Deep Depth (Illumina HiSeq 2500) v4.0 system. A read length of 125 base pairs was used.

As prostate cancer lymph node metastases contain heterogeneous cell types, our first aim was to determine if we had successfully cultured PCa cells from the patient *in vitro.* Based on cell-type enrichment analysis conducted using Cten software (76), the transcriptomic profile produced by RNAseq of *in vitro* cultured cells appeared to become enriched for a prostate signature in comparison to the fresh-frozen patient sample, which would contain both cancer cells and benign lymph node cell populations (Figure 5.5). This result implies that the media

culture technology is in fact selecting for prostate cancer cells as previously described (50). The

in vitro sample demonstrated a significantly enriched score for prostate cells, which in the

fresh frozen sample ranked 24 with a very white cell/lymph node biased signature. Culture

conditions appear to decrease many of the contaminating cell types present in the fresh

sample (Fig 5.5A and B). Based on this, the BCR002 cell line was assessed as 'prostate' in origin

with a reduction in contamination by other cell types. It is possible that with prolonged culture

conditions cleaner samples could be isoloated. Due to this apparent enrichment of target

cancer cells, it was also inferred that sequencing results of both the RNA and DNA were more

likely to be a true reflection of the transcriptomic and genomic landscape of the metastastic

cancer.

Rank	Cell ID	Enrichment
1	Lymph Node	43.72
2	CD4+ T Cells	40.03
3	BDCA4+ Dentritic Cells	36.72
4	CD8+ T Cells	34.36
5	CD14+ Monocytes	29.31
24	Prostate	0.84

Rank	Cell ID	Enrichment
1	Smooth Muscle	37.68
2	Cardiac Myocytes	18.59
3	Bronchial Epithelial Cells	18.51
4	Adipocyte	14.54
5	Prostate	6.81

Figure 5.5: *Fresh Frozen and In Vitro sample RNA enrichment maps;* **A**: Fresh frozen sample showing high

expression of lymphoid tissue and cell types in keeping with a lymph node, **B**: In Vitro sample showing

enrichment for 'prostate' cells.

RNA sequencing suggested very low AR expression in this patient sample in both the fresh frozen sample and the enriched *in vitro* culture (Table 5.1). Further analysis of AR transcript variants showed that this patient sample did not express clinically significant AR variants, such as AR3/AR-V7, which have been associated with resistance to both enzalutamide and abiraterone (37). This low level of AR expression is likely as a result of this patient's systemic treatment naïve state. RNA analysis also revealed expression of PSA, TMPRSS 2 and FKBP 5 in keeping with RT-qPCR findings above. PSMA expression was also confirmed by RNA sequencing of this patient's tumour.

Table 5.1 *Baseline expression of genes androgen responsive genes and analysis of AR variants.*

	LNCaP	MSK3	Fresh Frozen	In Vitro
Full length AR	44	5	5	5
KLK 3	1837	0.56	1374	2387
TMPRSS 2	318	15	123	500
FKBP 5	34	17	19	75
PSMA	730	0.67	209	112
AR45/AR-V2	18	0.26	0	0.57
AR3/AR-V7	0.5	0.1	0.24	0.09
AR4/AR-V1	0.075	0	0	0
AR567es	0	0.4	0.64	0.01

In vitro RNA sequencing suggests very low expressions of the androgen receptor in this patient sample (expressed as Transcripts per million).

Whole exome sequencing was performed by the Australian Translational Genomics Centre (ATGC) based at the based at the Princess Alexandra Hospital.

Sequencing data revealed 2 somatic point mutations in the AR gene that may be clinically relevant. The first of the identified point mutations occurs at codon 877 of the androgen receptor and changes the encoded amino acid from Threonine (T) to Alanine (A) resulting in T877A (Table 5.2). This mutation has previously been commonly detected in castrate-resistant prostate tumours and alters the androgen receptor ligand binding specificity. This clinically results in activation of the AR by certain antiandrogens, due to the conformational change in the ligand binding domain (77). The presence of this mutation in a tumour could potentially confound the ability of anti-androgen receptor targeting agents to impact on growth of the patients PCa cells and provide intrinsic resistance to their therapeutic effect. This mutation was identified in the fresh frozen sample however and not in the *in vitro* sample that was

sequenced. A second AR point mutation, in the 3'UTR region of AR was detected in both fresh frozen and *in vitro* sample DNA sequences however the possible effect of this is unknown.

Furthermore, sequencing of both fresh frozen tissue and cultured cells demonstrated a somatic BRCA 1 mutation in this patient (Table 5.2). This mutation occurs in an intron in Chromosome 17 in both samples. A second BRCA1 gene mutation was further identified in the *in vitro* sample, at a different intron region in Chromosome 17. The significance of this mutation however is unknown and may potentially be a silent or passenger mutation. However it can be hypothesised that due to the mutations occurring in this DNA repair gene, clinically this patient may benefit from treatment with the PARP inhibitor such as olaparib (78).

Table 5.2 Clinically actionable mutations on whole exome sequencing.

Sample	Chromosome	Region	Mutation Type	Gene	Clinical Significance
Fresh Frozen	X	Missense Mutation "T877A"	SNP	AR	Intrinsic resistance to anti-androgen therapy
	X	3'UTR	SNP	AR	Unknown
	17	Intron	DEL	BRCA1	Response to PARP inhibitor
In Vitro	X	3'UTR	SNP	AR	Unknown
	17	Intron	DEL	BRCA1	Response to PARP inhibitor
	17	Intron	DEL	BRCA1	Response to PARP inhibitor

In vitro DNA sequencing suggests a point mutation in the androgen recepter as well as a BRCA 1 mutation in both fresh frozen and *in vitro* samples for this patient. It is unknown if this BRCA 1 mutation is functional or if it is a silent or passenger mutation. There appears to be concurence between fresh frozen and *in vitro* samples, highlighting the ability for this method to result in a patient derived tumour culture that is reflective of an expected in vivo tumour response. SNP: Single-nucleotide polymorphism, DEL: deletion, AR: androgen receptor; BRCA 1: Breast-Cancer susceptibility gene 1.

These sequencing findings were further investigated and validated with 2D and 3D cell culture as a measure of functional relevance using previously described protocols in Chapter 2 and 4.
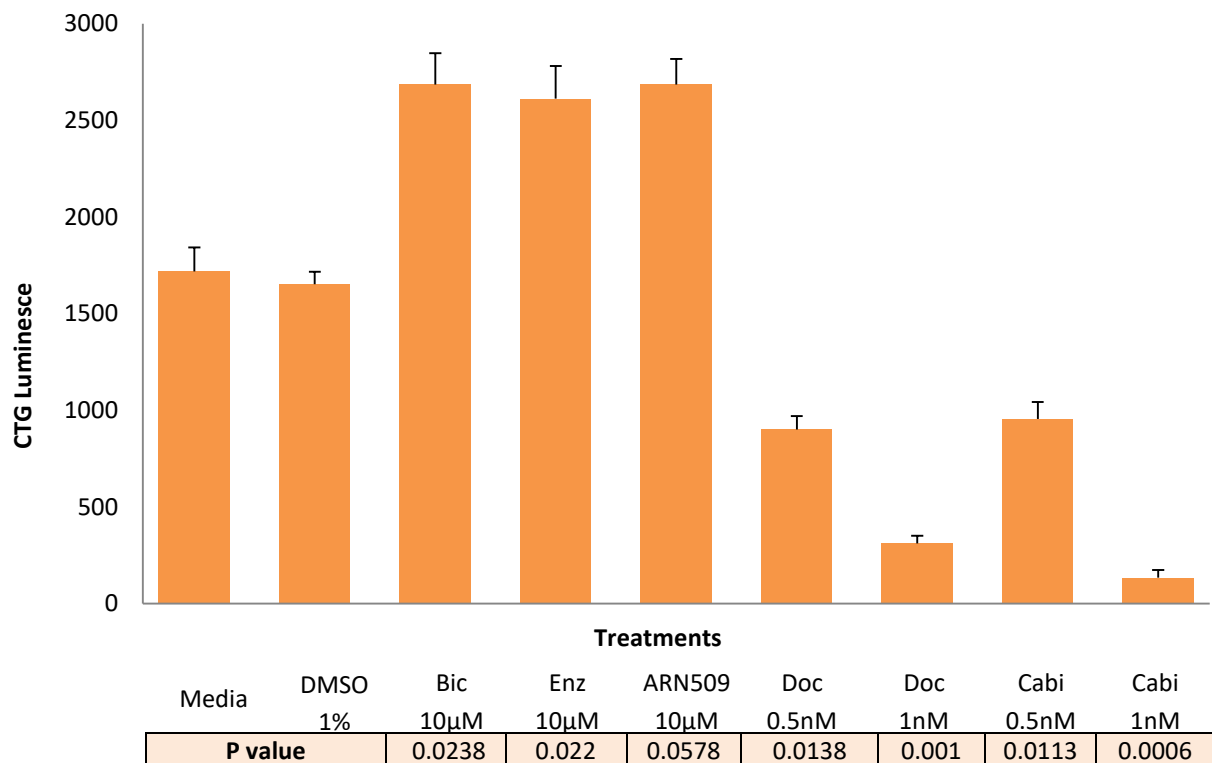
| P value | 0.39 | 0.45 | 0.2481 | 0.0058 | 0.0143 | 0.0086 | 0.021 |
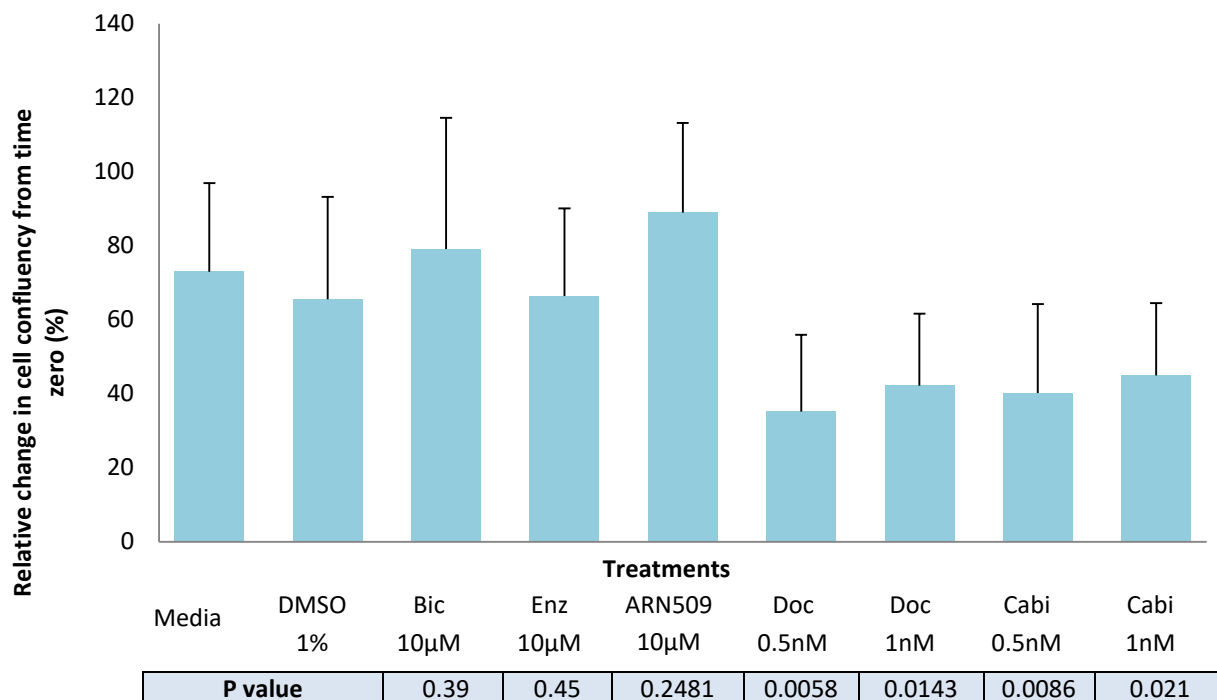
Figure 5.6 *Patient BCR002 Incucyte 2D drug screen results after 72hours of treatment*; the effect of chemotherapeutic agents on cells reached statistical significance, when compared to media alone. It appears that anti-androgen treatments had little impact on cells whereas a significant decrease was observed with chemotherapy drugs. Bic: Bicalutamide, Enz: Enzalutamide, Doc: Docetaxel, Cabi: Cabazitaxel. [n=3 technical repeats, error bars represent standard error, cells seeded at 5000 cells per well grown in HCM with 1nm DHT; statistical analysis and p values were calculated the students T-test].

Based on the 2D drug screen results (Figure 5.6), chemotherapeutic agents significantly decreased cell confluency, whereas anti–AR targeting therapeutics appeared to have little impact on cells. This may indicate an intrinsic resistance to anti-androgen therapies.

To further assess and validate this finding, 3D drug screening was performed and a change in cell viability was assessed. 3D drug testing identified a lack of antagonistic effect of anti-AR treatment on cell viability. This potentially indicates an innate resistance of tumour cells to antiandrogen therapy in this patient (Figure 5.7). It also appears that cells treated with these agents show significantly more viable cells than controls. This has potentially significant clinical implications, suggesting a potential harm to the patient should he receive these therapies. Furthermore the effect of chemotherapeutic agents reached statistical significance in both 2D and 3D drug screens, when compared to media alone (Table 5.3).

	Media	DMSO 1%	Bic 10μM	Enz 10μM	ARN509 10μM	Doc 0.5nM	Doc 1nM	Cabi 0.5nM	Cabi 1nM
P value			0.0238	0.022	0.0578	0.0138	0.001	0.0113	0.0006

Figure 5.7 *Patient BCR002 CTG cell viability 3D drug screen results after 5 days of treatment;* the effect of all treatments except ARN 509 on cells reached statistical significance when compared to media. A marked response to chemotherapy drugs is observed. In comparison there appears to be minimal effect on cells with anti-androgen treatments. Bic: Bicalutamide, Enz: Enzalutamide, Doc: Docetaxel, Cabi: Cabazitaxel. [n=3 technical repeats, error bars represent standard error, cells seeded at 5000 cells per well grown in HCM with 1nm DHT; statistical analysis and p values were calculated the students T-test].

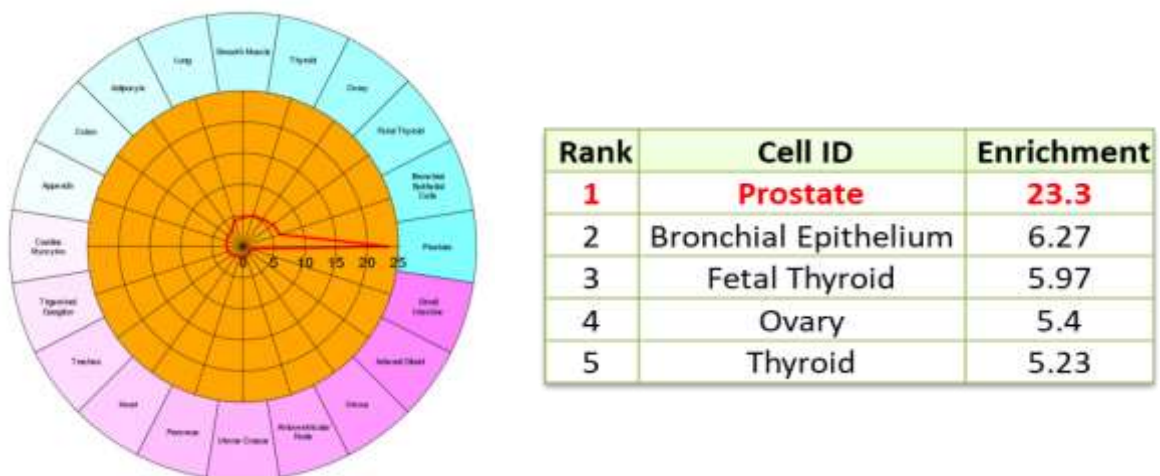**Table 5.3** *Treatment responses compared to media in both 2D and 3D culture.*

Agent	2D p value	3D p value
Bicalutamide	0.39	0.0238
Enzalutamide	0.45	0.022
ARN 509	0.2481	0.0578
Docetaxel 0.5nM	0.0058	0.0138
Docetaxel 1nM	0.0143	0.001
Cabazitaxel 0.5nM	0.0086	0.0113
Cabazitaxel 1nM	0.021	0.0006

In vitro 2D drug screening suggested a lack of effect of anti androgen and AR targeting agents and a significant response to chemotherapeutic agents, reaching statistical significance. In 3D culture, there was a significant inhibitory response to chemotherapeutic agents as well as a potentially stimulatory effect of anti androgen and AR targeting agents, reaching statistical significance.
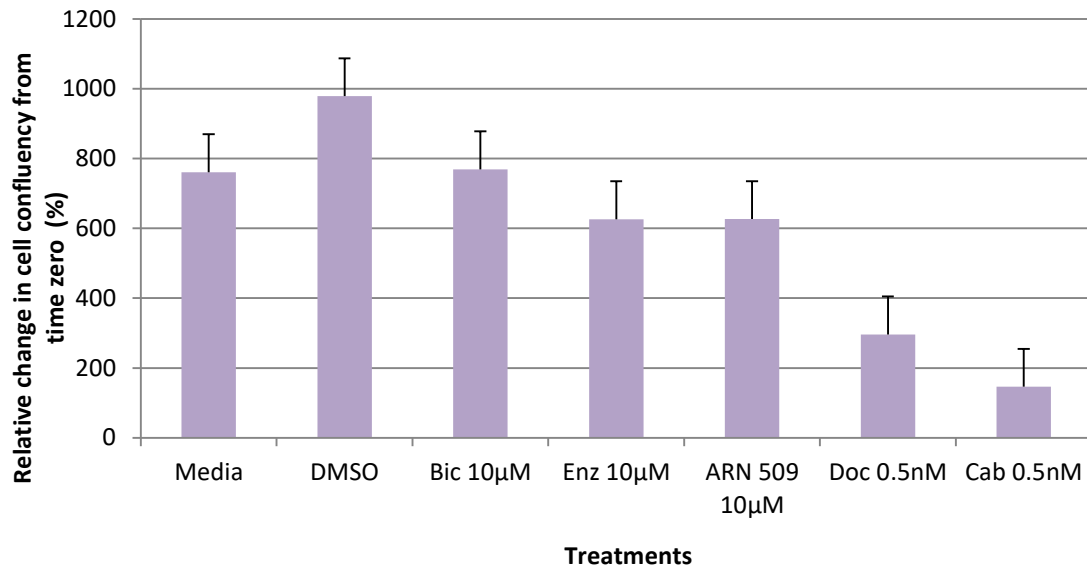
5.2.3 Patient 3

Following multidisciplinary team meeting discussions, tissue was also collected from a 74 year old gentleman (PSA 1.0 ng/ml; RRP 2003) at time of salvage lymph node dissection for a solitary PSMA avid inguinal lymph node. Tissue from the PSMA avid lymph node was obtained fresh intra operatively, with tissue retained as fresh frozen tissue for sequencing and the remainder cultured as described previously. After validation, this patient sample underwent downstream analysis. The following analysis was performed by Dr Saied Alinezhad (Post-doctoral Research Fellow in our lab) and is reproduced with permission.

RNA sequencing did not identify any clinically targetable aberration or any identifiable clinically actionable androgen receptor aberration. Based on Cten analysis described above, this patient's tissue was also identified as 'prostate' in origin (Figure 5.8). Whole exome sequencing data is pending for this patient.

Rank	Cell ID	Enrichment
1	Prostate	23.3
2	Bronchial Epithelium	6.27
3	Fetal Thyroid	5.97
4	Ovary	5.4
5	Thyroid	5.23

Figure 5.8: Patient 3 Fresh Frozen RNA enrichment map. Fresh frozen sample confirming tissue of prostatic origin.

The RNA sequencing data was once again investigated with 2D *in vitro* drug screening as a measure of functional relevance using previously described protocols in Chapter 2 and 4.

P value	0.98	0.81	0.814	0.2749	0.086

Figure 5.9 *Patient 3 derived culture 2D Incucyte drug screen results after 100hours of treatment;* when compared to DMSO control, all treatments had an apparent antagonistic effect on cultured cells; however did this not reach statistical significance. Bic: Bicalutamide, Enz: Enzalutamide, Doc: Docetaxel, Cabi: Cabazitaxel. [n=3 biological repeats, error bars represent standard error, cells seeded at 5000 cells per well grown in HCM with 1nm DHT; statistical analysis and p values were calculated the students T-test].

Based on 2D drug screen results above (Figure 5.9), all treatments had an effect on cultured cells; however, this did not reach statistical significance. The *in vitro* results above are once again reflective of the RNA sequencing data, as was the case with patient 2. With no identifiable or actionable clinical aberrations, a patient with biochemically recurrent CaP would be expected to be sensitive to all interventions when treatment naïve, as demonstrated in this case. These results are indicative of the ability of this method to result in a patient derived tumour culture that is reflective of an expected *in vivo* tumour response.

5.3 – Discussion

Successful culture of a novel patient-derived cell line with subsequent patient -specific next generation sequencing and therapeutic screening has provided proof of principle for a precision medicine approach in the mangement of early recurrent prostate cancer for the very

first time. NGS of individual patient tumours is becoming increasingly available commercially at many centers around the world. A major drawback of this technology however is identification of driver vs passenger mutations and which of the potentially targetable aberrations are acutally functional *in vivo*.

In this study NGS data of both fresh frozen tumor and cultured cells demonstrated potential functional aberrations of the androgen receptor and BRCA1 tumor suppressor gene in patient BCR002.

As mentioned above, sequencing data revealed 2 point mutations in the AR gene that may be clinically relevant. The identified point mutation occurred at codon 877 of the androgen receptor which results in a change from Threonine (T) to Alanine (A) resulting in T877A (Table 5.2). This mutation has been detected in castrate-resistant prostate cancers causing altered androgen receptor ligand binding specificity, resulting in activation of the AR with binding of antiandrogens (77). This mutation was not identified in sequencing of *in vitro* culture samples, highlighting a limitation in this culture model. If the culture alone had been relied upon then this mutation would not have been identified. The second AR mutation in the 3'UTR region of AR has was not been previously reported in the literature and as such the potential effect of this mutation is unknown and could potentially be a non-functional mutation. Further analysis is required to determine the nature of this mutation in this patient.

The low level of AR expression and the presence of the AR mutations in this tumour would predict the potential confounding of anti-androgen receptor targeting agents to impact on growth of the patients PCa cells thereby providing an intrinsic resistance to therapeutic effects. The drug screening results in patient BCR002 appear to confirm this, as tumour cells show an apparent therapeutic resistance to anti-androgen therapy in this patient. These same cells however also appear to be sensitive to chemotherapeutic drugs. This apparent inherent resistance to anti-androgen therapy would appear to be consistent with the low expression of AR and the T887A androgen receptor mutation identified.

There are significant clincal implications of these findings. Applying these results in a clinical setting would mean that this patient could benefit from up front chemotherapy as opposed to ADT or 2nd line anti-androgens following future biochemical recurrence. This would mean the patient potentially avoiding the adverse effects of ADT he would have had to endure for no

survival or disease-free benefit. Therefore by avoiding this step in the conventional treatment algorithm, there may be increased potential to improve disease free survival with the added benefit of avoiding the adverse effects the ADT.

Furthermore, sequencing of both fresh frozen tissue and cultured cells identified a BRCA 1 DNA repair gene mutation in this patient. It is unknown if this is in fact a functional mutation as we did not test a PARP inhibitor whilst carrying out *in vitro* drug screening as it was an unexpected finding. Therefore there is a potential for his to be a silent or passenger mutation. BRCA 1 (Breast-Cancer susceptibility gene 1) is a tumour suppressor gene involved in DNA repair and regulating the transcription of DNA in response to damage (79, 80). Recent studies have identified BRCA mutations and other DNA repair aberrations in patients with metastatic or castrate resistance prostate cancer (34, 35, 81). There does not appear to by any consensus on known significant BRCA 1 mutations in these patients (34, 35, 81). In a recent seminal study on the role of prostate cancer and PARP inhibitors, Mateo et al considered a patient to be biomarker-positive if a homozygous deletion or deleterious mutation was identified in a gene reported to be involved either in DNA damage repair or sensitivity to PARP inhibition (78). In this study a similar patient with a BRCA1 homozygous deletion was identified and he subsequently had a response to olaparib (78).

Poly (adenosine diphosphate [ADP]–ribose) polymerase (PARP) is involved in multiple aspects of DNA repair (78). The PARP inhibitor olaparib has demonstrated a treatment response to olaparib in patients with prostate cancer with DNA repair gene mutations such as BRCA recent phase 2 trial (78). Therefore, with evidence of potential BRCA 1 aberrations, this patient may benefit from treatment with a PARP inhibitor such as olaparib if his mutation is not silent (78, 82).

Evidence is variable regarding taxane chemotherapy efficacy and BRCA mutation status in prostate, breast and ovarian cancer (34, 82-85). Some BRCA mutant patients appear to demonstrate resistance with early progression whilst others demonstrate significant responses to treatment (86, 87). Given the *in vitro* response demonstrated in this patient's tumour, it may be that standard docetaxel chemotherapy in the recurrent disease setting (or cabazitaxel in the second line setting) remain viable therapeutic options. Platinum based chemotherapies act as alkylating agents causing crosslinking of DNA producing cell death. Mounting evidence in BRCA mutation cancers such as breast, ovarian and prostate indicate potential increased

sensitivity to platinum based chemotherapeutic agents in the setting of identified BRCA and DNA repair pathway mutations (34, 78, 82, 86, 88). Given the findings of the NGS and associated *in vitro* functional screening indicating resistance to anti-androgen therapy, it could also suggest that in a recurrent setting, early initiation of platinum based chemotherapy may be a potential treatment option for this patient. This would not be a standard of care however, and unfortunately *in vitro* therapeutic screening with platinum based chemotherapy was not performed in this study. Future BRCA mutant patients would be planned to have both Taxane and Platinum based *in vitro* therapeutic screening performed.

There are still many challenges in establishing a widespread use of the above method into clinical use, such as a relatively less aggressive tumour subtype in early recurrence and the relative large amount and quality of samples required to rapidly propagate cells to allow downstream analysis. For example, the patient sample discussed above had approximately 80% of the total lymph node involved by tumour. Our initial patient on the other hand, who did not result in an actionable model, only had approximately 50% part of a small 5cm core biopsy sample available for culture. Additionally, this methodology requires external validation and reproducibility prior to larger trials and patient application.

The method described in this thesis, potentially allows for the integration of NGS analysis of tumours as well as generation of patient derived cell models with subsequent, *in vitro* drug screening in clinically meaningful timeframes to provide personalised medicine for the treatment of prostate cancer. It appears organoids generated in 3D from patient tissue recapitulate the clinical pathologic and genetic phenotype of the original metastatic sample in order to allow therapeutic screening and demonstrate functional relevance of aberrations identified via NGS. This methodology could also be utilised to identify other potentially actionable mutations, such as other AR mutations such as AR-V7, mTOR aberrations or RAS mutations, to allow clinicians the ability to identify and test potentially relevant therapeutics and alter a patient's management, offer therapies with added efficacy and minimise the potential adverse effects of futile therapies. Thus further characterisation and testing of the methodology undertaken in this thesis could promote the ability to direct efficacious, individualised therapy based on demonstrated biologically functional, actionable tumoral aberrations. Additionally, this methodology could be attempted on other malignancies to

potentially find similar timely clinically actionable aberrations to improve outcomes for those patients.

Overall, this proof of principle study has demonstrated a methodology that can enable a clinically meaningful and timely precision medicine approach in early biochemically recurrent prostate cancer, not previously explored in the literature. Therefore, it is apparent that with further development and refinement, patients may fundamentally benefit from such an approach with less morbidity from ineffective therapies, improved disease free and overall survival and ultimately, a better quality of life.

Chapter 6 - Discussion

Up to 80% of men treated with salvage therapy fail in the longer term due to inadequate staging at the time of recurrence (5, 6) . This is because patients with distant or loco-regional disease are unrecognised due to the inability of imaging modalities to detect micro-metastatic and low volume recurrent disease, or receive unnecessary systemic therapy post external beam radiotherapy for localised failure only. The consequence of failed salvage therapy is ADT and the highly likely progression to castrate resistant disease. With developing resistance to treatment, patients are managed with second, third and fourth line systemic agents in various sequences and combinations (4, 7). These therapies are increasingly morbid and are palliative in nature with the aim to prolong survival. With the advent of precision molecular imaging in this setting, the traditional treatment landscape is being challenged by the identification of very low volume metastatic disease or "oligometastatic" disease in asymptomatic patients with PSA levels lower than previously seen (28-30). This has been demonstrated in our own clinical practice at the PAH with the adoption of PSMA PET/CT (unpublished data). It is currently unknown if directed therapy to these lesions will improve long term outcomes, however it is of significant clinical value to be able to determine which patients may benefit from specific treatments of recurrent disease whether that be local or systemic therapies.

PSMA PET imaging holds promise as the answer to meet this clinical need. Our single arm prospective trial has demonstrated how hybrid PSMA PET/MRI may be useful in staging men with biochemical recurrence, especially when PSA is low. In our study, PSMA PET/MRI has a positive predictive value of 95.2% and a sensitivity of 68.9%, with an overall detection rate of 70% and outperformed SOC imaging in accurately identifying locally recurrent disease in the pelvis, even at low PSA levels of <1.0ng/mL. This may have implications for earlier salvage treatment, avoidance of futile local therapy in patients with distant disease and change patient management which could potentially translate to better outcomes for our patients.

In our study, in suspected cases of biochemical recurrence, PSMA PET/MRI imaging provided improved detection rates and reduced the identification of false positive and false negative lesions, when compared to SOC imaging. Biochemical recurrence of prostate cancer is most commonly due to locally recurring disease in the pelvis, such as in the prostatic bed, or

recurrences at anastomotic sites. The superior anatomical definition provided by the MRI component of the hybrid scan adds valuable information to the PET component and, as demonstrated by the data above, outperforms SOC imaging (including CT) in identifying lesions. The hybrid PET/MRI scan is also co-acquired with simultaneous co-registration of the PET and MRI images, allowing the reporting physician to use both of the imaging components to full effect in determining the likelihood of true vs false positive lesions.

PSMA PET/MRI imaging allowed accurate identification of areas of recurrence and subsequently to adapt patient care. Patients with suspected local recurrence, not identified with SOC imaging, would originally have received prostatic fossa and seminal vesicle salvage radiotherapy or the initiation of ADT for patients with biochemical recurrence post radiotherapy. However, as a result of precision imaging, these patients, having PSMA PET identified low volume recurrent or metastatic disease, would have received targeted high dose radiotherapy or surgery in addition to standard of care salvage pelvic radiation. Similarly, patients with recurrent disease outside the pelvis would receive palliative therapy if the disease is wide spread or targeted treatment with radiation or surgery if oligometastatic. This imaging modality has the potential to significantly improve prostate cancer detection and allow early identification and management of recurrent disease when compared to SOC imaging. This may have implications for earlier salvage treatment, avoidance of futile local therapy when distant disease exists and change patient management to potentially allow better survival outcomes and reduce morbidity.

Assessment of the long term outcomes and potential survival benefits of the altered therapy resulting from the precision imaging conducted in this study was outside of the stated aims and timeframe of this trial. A larger cohort of patients would be required to identify if a survival benefit (overall, cancer specific and biochemical free) is obtained and would need to be performed as a dedicated long-term stand-alone trial. The results of the limited trial reported in this thesis clearly demonstrate improved sensitivity and high specificity of precision PSMA PET/MRI imaging over SOC with a very high correlation with histologic confirmation which suggests that using the novel staging modalities here provides improved clinical confidence for clinicians.

Our study also highlights that many of the investigations performed routinely for staging men with BCR are futile (especially at low PSA) and that performing PSMA PET/MRI in place of SOC

imaging in this cohort could provide substantial cost savings to the health system. A formal health economic analysis is currently underway. As an example, at our institute PSMA PET/MRI imaging costs ~$1000 per scan, including the production of the PSMA ligand and the cost of the MRI component of the scan. In this study the total cost for PSMA PET/MRI imaging was $30,000 with positive PSMA PET/MRI imaging in 21 patients that led to a significant change in the clinical management at a total cost of $21 000. Based on the April 2016 Medicare Benefits Schedule pricing, re-staging CT costs ~$480, and a whole body bone scan costs ~ $500, resulting in SOC imaging costing $980 per patient and a total cost of $29,400 in our study (89). Only 9 CT scans and 1 bone scan were positive however, with a total of $24,580 spent on negative studies (assuming all PSMA PET/MRI avid scans were due to recurrent disease), of which 12 patients were incorrectly staged as negative. In comparison, negative PSMA PET/MRI cost only $9000, providing a relative cost saving of $15,580 in order to find recurrent disease. No patients with recurrent disease would have been missed if only a PSMA PET/MRI scan had been performed instead of SOC imaging in our study. This does not also take into consideration potential on costs from futile or in appropriate therapy due to understaging.

As can be seen from the above discussion, imaging in the BCR setting with PSMA PET/MRI hybrid scans would appear to provide substantial clinical and economic benefit over the currently recommended and utilized imaging regimen. Further similar studies, along with detailed health economic analysis will be required in order for clinicians and funding bodies (such as the federal government) to formally recognize this imaging modality as the new SOC for staging men with BCR. Finally it remains to be determined if improved earlier detection of disease will ultimately improve overall clinical outcomes for our patients.

Prostate cancer cells have remained difficult to culture *in vitro*, however with the successful development and utilisation of HCM we have been able to culture patient derived prostate cancer cells to allow testing of downstream precision medicine techniques *in vitro*. Our initial experiences using established prostate cancer cell lines, led to the very first successful *in vitro* culture of established patient derived xenograft BM-18 and LuCap 35 models. Using HCM also allowed the successful genetic modification of these cell lines and their conversion back into *in vivo* tumours. This has significantly improved the utility of these PDXs and may potentially allow new and novel findings and investigations to occur. The utility of this method will be further investigated at a basic science level at our institute, allowing genetic manipulation of

these PDX models with inducible over-expression or knockdown of target genes of interest in a more complex *in vivo* model system, for the very first time. As further PDX models are generated at our institution, the potential of this technique using HCM to convert *in vivo* PDXs to *in vitro* models, for research colleagues both in our institution and others is enormous. This work is currently ongoing with collaborators in our institution.

Precision medicine aims to provide the right treatment, to the right patient for the right cancer at the right time. It is the overall concept of individualising patient management based on their specific tumour characteristics and biology as opposed to traditional histological subtypes. As previously discussed, preliminary work in the area of precision medicine has been in advanced prostate cancer. Studies in early recurrent disease are lacking currently. Published studies and institutional/commercially available NGS of prostate cancer all lack the ability to determine if identified genomic and transcriptomic aberrations are actually functional. This has been a major Achilles' heel for the field as many of the identified so called "actionable" aberrations may indeed be passenger mutations not driver mutations. Targeting such aberrations would therefore be clinically futile, expose patients to potentially toxic therapies for no benefit and potentially loose the window of opportunity for efficacious therapies through the critical wastage of time.

The potential of the novel approach described in this thesis therefore is incredibly important. The innovative approach taken by our group is to use NGS technologies to identify potential targetable aberrations and then, through the use of novel HCM organoid culture technology produce patient specific avatar *in vitro* cell lines by which to test therapeutic strategies prior to use in the patient. This is aimed to be performed in clinically meaningful time frames in order to be clinically relevant. This would prevent ineffectual targeting of identified aberrations which are not clinically important and hopefully improve patient outcomes to therapy by using only therapies to which their cancer is responsive.

Some patients in our study with lesions identified on PSMA PET/MRI were able to provide tissue for histological correlation, and to allow novel downstream analysis. These tumour recurrences, successfully identified on PET, were able to be cultured as part of a proof of principle study *in vitro* using novel HCM media. This allowed the rapid propagation of primary patient derived cell lines to allow next generation sequencing and *in vitro* drug screening in a clinically meaningful timeframe (6-8 weeks).

The patient discussed in detail in this thesis, had an isolated locally recurrent pelvic lymph node on PSMA PET/MRI. The patient progressed to have a salvage lymph node dissection, resulting at submission of this thesis, in biochemical remission for 4 months. His tumour tissue was successfully cultured *in vitro,* validated as being of prostatic origin, sequenced and *in vitro* drug screened on the basis of identified aberrations. This resulted in the identification of a potential intrinsic resistance to anti-androgen therapy resulting from a mutation of the androgen receptor. Significantly, we were also able to correlate this sequencing data from fresh frozen tissue, with *in vitro* sequencing data and drug screening results. This correlation demonstrates that genetic aberrations in tumour tissue can be retained by cells *in* vitro and therefore would allow more confidence in implementing these findings clinically.

For our patient, clinically this could mean that if this patient's disease was to recur again he might benefit from upfront chemotherapy as opposed to anti-androgen therapies, which are themselves not benign therapies, having multiple adverse side effects and appear to have significantly lower efficacy on the cancer cells in this particular patient. This patient also had a BRCA1 mutation identified in his tumour. This mutation could also be functional with impaired DNA repair pathway function leading to increased sensitivity to chemotherapeutic agents or PARP inhibitors such as olaparib. Early identification of such an aberration may allow streamline and rapid enrolment into appropriate clinical trials at an earlier time point.

There are still many challenges to overcome with this methodology, such as the relatively less aggressive tumour biology in early recurrence not resulting in rapid cell propagation *in vitro* (also limiting the potential success rate of cell line generation) and the relatively large volume and high quality of samples required to propagate cells for downstream analysis. This methodology also requires external validation and assessment of reproducibility, and efficacy and applicability of *in vitro* screening results and NGS data to the whole patient. This would need to be performed in larger trials, prior to routine application to patients. This novel study however has potentially outlined the feasibility of precision medicine in early recurrent disease, not previously explored in the literature and has enabled a timely precision medicine approach in early biochemically recurrent prostate cancer.

In conclusion, we have demonstrated that novel precision imaging using PSMA PET/MRI enables improved identification of foci of early recurrent prostate disease compared to current SOC imaging protocols. This outcome, not only allows accurate salvage treatment

implementation, but potentially allows the application of precision medicine techniques, such as *in vitro* tissue culture, NGS and drug testing, in early recurrent prostate cancer, previously proven extremely difficult to do. Combining PSMA PET/MRI with HCM technology, we have been able to culture and propagate patient-derived cells to create patient specific models of prostate cancer to allow in vitro drug screening and next generation sequencing in clinically meaningful timeframes. We have also demonstrated that genetic aberrations identified by NGS of fresh frozen tumour tissue is maintained by cells cultured using the HCM organoid culture technology *in vitro*, and as such are accurate reflections of the parental tumour, and the functional relevance of identified aberrations can be investigated by in vitro drug screening. The success of this proof of principle study combining novel imaging with novel cell culture technology demonstrates how these findings could have significant impact on defining future treatment decisions and outcomes for patients with early recurrent prostate cancer.

Overall, our results suggest a promising potential role for PSMA PET/MRI as a superior staging modality in men with biochemical recurrence of prostate cancer, especially when PSA is low, outperforming SOC imaging especially in identifying locally recurrent disease. Furthermore combining this imaging modality with precision medicine techniques demonstrates that this management approach in early recurrent disease is feasible and may enable the identification of functional, targetable aberrations that could potentially direct effective treatment of individuals and have significant beneficial impact on patient outcomes.

Chapter 7 - References

1. ABO. Underlying causes of death (Australia) Australia: Australian Bureau of Statistics; 2016 [cited 2016 10/3/2016]. Available from: http://www.aihw.gov.au/deaths/leading-causes-of-death/#leading-sex.
2. AIHW. Australian Cancer Incidence and Mortality (ACIM) books: prostate cancer. Canberra: Australian Institute of Health and Welfare; 2016.
3. Lozano R, Naghavi M, Foreman K, Lim S, Shibuya K, Aboyans V, et al. Global and regional mortality from 235 causes of death for 20 age groups in 1990 and 2010: a systematic analysis for the Global Burden of Disease Study 2010. The Lancet.380(9859):2095-128.
4. Mottet N, Bellmunt J, Briers E, Van den Bergh R, Bolla M, Van Casteren N, et al. Guidelines on Prostate Cancer 2015 [cited 2016]. Available from: https://uroweb.org/guideline/prostate-cancer/.
5. Lee RJ, Tzou KS, Heckman MG, Hobbs CJ, Rawal B, Diehl NN, et al. Proposed prognostic scoring system evaluating risk factors for biochemical recurrence of prostate cancer after salvage radiation therapy. BJU Int. 2016;118(2):236-42.
6. Steigler A, Denham JW, Lamb DS, Spry NA, Joseph D, Matthews J, et al. Risk Stratification after Biochemical Failure following Curative Treatment of Locally Advanced Prostate Cancer: Data from the TROG 96.01 Trial. Prostate cancer. 2012;2012:814724.
7. Heidenreich A, Bastian PJ, Bellmunt J, Bolla M, Joniau S, van der Kwast T, et al. EAU guidelines on prostate cancer. Part II: Treatment of advanced, relapsing, and castration-resistant prostate cancer. European Association of Urology. 2014;65(2):467-79.
8. George D. Natural History of Prostate Cancer in 2010. Urology 2013;82.
9. Kane CJ, Amling CL, Johnstone PAS, Pak N, Lance RS, Thrasher JB, et al. Limited value of bone scintigraphy and computed tomography in assessing biochemical failure after radical prostatectomy. Urology. 2003;61(3):607-11.
10. Sarkar S, Das S. A review of imaging methods for prostate cancer detection. Biomedical Engineering and Computational Biology. 2016;7(Suppl 1):1-15.
11. Joshi A, Nicholson C, Rhee H, Gustafson S, Miles K, Vela I. Incidental Malignancies Identified During Staging for Prostate Cancer With 68Ga Prostate-specific Membrane Antigen HBED-CC Positron Emission Tomography Imaging. Urology. 2017;104:e3-e4.
12. Liu IJ, Zafar MB, Lai Y-H, Segall GM, Terris MK. Fluorodeoxyglucose positron emission tomography studies in diagnosis and staging of clinically organ-confined prostate cancer. Urology.57(1):108-11.
13. Takahashi N, Inoue T, Lee J, Yamaguchi T, Shizukuishi K. The roles of PET and PET/CT in the diagnosis and management of prostate cancer. Oncology. 2007;72(3-4):226-33.
14. Beer AJ, Eiber M, Souvatzoglou M, Schwaiger M, Krause BJ. Radionuclide and hybrid imaging of recurrent prostate cancer. The Lancet Oncology.12(2):181-91.
15. Bertagna F, Sadeghi R, Giovanella L, Treglia G. Incidental uptake of 18F-fluorodeoxyglucose in the prostate gland. Systematic review and meta-analysis on prevalence and risk of malignancy. Nuklearmedizin Nuclear medicine. 2014;53(6):249-58.
16. Ceci F, Herrmann K, Castellucci P, Graziani T, Bluemel C, Schiavina R, et al. Impact of 11C-choline PET/CT on clinical decision making in recurrent prostate cancer: results from a retrospective two-centre trial. European Journal of Nuclear Medicine and Molecular Imaging. 2014;41(12):2222-31.

17. Umbehr MH, Muntener M, Hany T, Sulser T, Bachmann LM. The role of 11C-choline and 18F-fluorocholine positron emission tomography (PET) and PET/CT in prostate cancer: a systematic review and meta-analysis. Eur Urol. 2013;64(1):106-17.

18. Poulsen MH, Bouchelouche K, Hoilund-Carlsen PF, Petersen H, Gerke O, Steffansen SI, et al. [18F]fluoromethylcholine (FCH) positron emission tomography/computed tomography (PET/CT) for lymph node staging of prostate cancer: a prospective study of 210 patients. BJU Int. 2012;110(11):1666-71.

19. Afshar-Oromieh A, Babich JW, Kratochwil C, Giesel FL, Eisenhut M, Kopka K, et al. The Rise of PSMA Ligands for Diagnosis and Therapy of Prostate Cancer. Journal of Nuclear Medicine. 2016;57(Supplement 3):79S-89S.

20. Maurer T, Eiber M, Schwaiger M, Gschwend JE. Current use of PSMA-PET in prostate cancer management. Nat Rev Urol. 2016;13(4):226-35.

21. Silver DA, Pellicer I, Fair WR, Heston WD, Cordon-Cardo C. Prostate-specific membrane antigen expression in normal and malignant human tissues. Clinical Cancer Research. 1997;3(1):81-5.

22. Sweat SD, Pacelli A, Murphy GP, Bostwick DG. Prostate-specific membrane antigen expression is greatest in prostate adenocarcinoma and lymph node metastases. Urology.52(4):637-40.

23. Ghosh A, Heston WD. Tumor target prostate specific membrane antigen (PSMA) and its regulation in prostate cancer. Journal of Cellular Biochemistry. 2004;91(3):528-39.

24. Tagawa ST, Beltran H, Vallabhajosula S, Goldsmith SJ, Osborne J, Matulich D, et al. Anti-Prostate Specific Membrane Antigen-based Radioimmunotherapy for Prostate Cancer. Cancer. 2010;116(4 Suppl):1075-83.

25. Eder M, Schäfer M, Bauder-Wüst U, Hull W-E, Wängler C, Mier W, et al. 68Ga-Complex Lipophilicity and the Targeting Property of a Urea-Based PSMA Inhibitor for PET Imaging. Bioconjugate Chemistry. 2012;23(4):688-97.

26. Afshar-Oromieh A, Avtzi E, Giesel FL. The diagnostic value of PET/CT imaging with the (68)Ga-labelled PSMA ligand HBED-CC in the diagnosis of recurrent prostate cancer. Eur J Nucl Med Mol Imaging. 2015;42.

27. Eiber M, Maurer T, Souvatzoglou M, Beer AJ, Ruffani A, Haller B, et al. Evaluation of hybrid 68Ga-PSMA-ligand PET/CT in 248 patients with biochemical recurrence after radical prostatectomy. Journal of Nuclear Medicine. 2015.

28. Meredith G, Wong D, Yaxley J, Coughlin G, Thompson L, Kua B, et al. The use of 68 Ga-PSMA PET CT in men with biochemical recurrence after definitive treatment of acinar prostate cancer. BJU International. 2016;118:49-55.

29. Perera M, Papa N, Christidis D, Wetherell D, Hofman MS, Murphy DG, et al. Sensitivity, Specificity, and Predictors of Positive 68Ga–Prostate-specific Membrane Antigen Positron Emission Tomography in Advanced Prostate Cancer: A Systematic Review and Meta-analysis. European Urology. 2016;70(6):926-37.

30. von Eyben FE, Picchio M, von Eyben R, Rhee H, Bauman G. 68Ga-Labeled Prostate-specific Membrane Antigen Ligand Positron Emission Tomography/Computed Tomography for Prostate Cancer: A Systematic Review and Meta-analysis. European Urology Focus. 2016.

31. Afshar-Oromieh A, Zechmann CM, Malcher A, Eder M, Eisenhut M, Linhart HG, et al. Comparison of PET imaging with a 68Ga-labelled PSMA ligand and 18F-choline-based PET/CT for the diagnosis of recurrent prostate cancer. European Journal of Nuclear Medicine and Molecular Imaging. 2013;41(1):11-20.

32. Graziani T, Ceci F, Castellucci P, Polverari G, Lima GM, Lodi F, et al. (11)C-Choline PET/CT for restaging prostate cancer. Results from 4,426 scans in a single-centre patient series. Eur J Nucl Med Mol Imaging. 2016;43(11):1971-9.

33. Afshar-Oromieh A, Haberkorn U, Schlemmer HP, Fenchel M, Eder M, Eisenhut M, et al. Comparison of PET/CT and PET/MRI hybrid systems using a 68Ga-labelled PSMA ligand for the diagnosis of recurrent prostate cancer: initial experience. European Journal of Nuclear Medicine and Molecular Imaging. 2014;41(5):887-97.

34. Robinson D, Van Allen EM, Wu YM, Schultz N, Lonigro RJ, Mosquera JM, et al. Integrative clinical genomics of advanced prostate cancer. Cell. 2015;161(5):1215-28.

35. Beltran H, Eng K, Mosquera JM, Sigaras A, Romanel A, Rennert H, et al. Whole-exome sequencing of metastatic cancer and biomarkers of treatment response. JAMA oncology. 2015;1(4):466-74.

36. Roychowdhury S, Chinnaiyan AM. Advancing Precision Medicine for Prostate Cancer Through Genomics. Journal of Clinical Oncology. 2013;31(15):1866-73.

37. Antonarakis ES, Lu C, Wang H, Luber B, Nakazawa M, Roeser JC, et al. AR-V7 and Resistance to Enzalutamide and Abiraterone in Prostate Cancer. New England Journal of Medicine. 2014;371(11):1028-38.

38. Yadav SS, Li J, Lavery HJ, Yadav KK, Tewari AK. Next-generation sequencing technology in prostate cancer diagnosis, prognosis, and personalized treatment. Urologic Oncology. 2015;33(6):267 e1-13.

39. Sharma A, Yeow W-S, Ertel A, Coleman I, Clegg N, Thangavel C, et al. The retinoblastoma tumor suppressor controls androgen signaling and human prostate cancer progression. The Journal of Clinical Investigation.120(12):4478-92.

40. Beltran H, Rickman DS, Park K, Chae SS, Sboner A, MacDonald TY, et al. Molecular Characterization of Neuroendocrine Prostate Cancer and Identification of New Drug Targets. Cancer Discovery. 2011;1(6):487-95.

41. Barbieri CE, Chinnaiyan AM, Lerner SP, Swanton C, Rubin MA. The Emergence of Precision Urologic Oncology: A Collaborative Review on Biomarker-driven Therapeutics. Eur Urol. 2017;71(2):237-46.

42. Horoszewicz JS, Leong SS, Kawinski E, Karr JP, Rosenthal H, Chu TM, et al. LNCaP model of human prostatic carcinoma. Cancer Research. 1983;43(4):1809-18.

43. Kaighn ME, Narayan KS, Ohnuki Y, Lechner JF, Jones LW. Establishment and characterization of a human prostatic carcinoma cell line (PC-3). Investigative urology. 1979;17(1):16-23.

44. Korenchuk S, Lehr JE, L MC, Lee YG, Whitney S, Vessella R, et al. VCaP, a cell-based model system of human prostate cancer. In vivo (Athens, Greece). 2001;15(2):163-8.

45. Navone NM, Olive M, Ozen M, Davis R, Troncoso P, Tu SM, et al. Establishment of two human prostate cancer cell lines derived from a single bone metastasis. Clinical Cancer Research. 1997;3(12):2493-500.

46. Sramkoski RM, Pretlow TG, Giaconia JM, Pretlow TP, Schwartz S, Sy M-S, et al. A new human prostate carcinoma cell line, 22Rv1. In Vitro Cellular & Developmental Biology - Animal.35(7):403-9.

47. Lee YG, Korenchuk S, Lehr J, Whitney S, Vessela R, Pienta KJ. Establishment and characterization of a new human prostatic cancer cell line: DuCaP. In vivo (Athens, Greece). 2001;15(2):157-62.

48. Sobel RE, Sadar MD. CELL LINES USED IN PROSTATE CANCER RESEARCH: A COMPENDIUM OF OLD AND NEW LINES—PART 1. The Journal of Urology. 2005;173(2):342-59.

49. Stone KR, Mickey DD, Wunderli H, Mickey GH, Paulson DF. Isolation of a human prostate carcinoma cell line (DU 145). International Journal of Cancer. 1978;21(3):274-81.
50. Gao D, Vela I, Sboner A, Iaquinta PJ, Karthaus WR, Gopalan A, et al. Organoid cultures derived from patients with advanced prostate cancer. Cell. 2014;159(1):176-87.
51. Drost J, Karthaus WR, Gao D, Driehuis E, Sawyers CL, Chen Y, et al. Organoid culture systems for prostate epithelial and cancer tissue. Nature Protocols. 2016;11(2):347-58.
52. Baca SC, Prandi D, Lawrence MS, Mosquera JM, Romanel A, Drier Y, et al. Punctuated evolution of prostate cancer genomes. Cell. 2013;153(3):666-77.
53. Barbieri CE, Baca SC, Lawrence MS, Demichelis F, Blattner M, Theurillat J-P, et al. Exome sequencing identifies recurrent SPOP, FOXA1 and MED12 mutations in prostate cancer. Nature Genetics. 2012;44(6):685-9.
54. Taylor BS, Schultz N, Hieronymus H, Gopalan A, Xiao Y, Carver BS, et al. Integrative genomic profiling of human prostate cancer. Cancer cell. 2010;18(1):11-22.
55. Shen MM, Abate-Shen C. Molecular genetics of prostate cancer: new prospects for old challenges. Genes & Development. 2010;24(18):1967-2000.
56. Hayflick L. The limited in vitro lifetime of human diploid cell strains. Experimental cell research. 1965;37:614-36.
57. Vela I, Chen Y. Prostate cancer organoids: a potential new tool for testing drug sensitivity. Expert review of anticancer therapy. 2015;15(3):261-3.
58. Karthaus WR, Iaquinta PJ, Drost J, Gracanin A, van Boxtel R, Wongvipat J, et al. Identification of multipotent luminal progenitor cells in human prostate organoid cultures. Cell. 2014;159(1):163-75.
59. Eder M, Schafer M, Bauder-Wust U, Hull WE, Wangler C, Mier W, et al. 68Ga-complex lipophilicity and the targeting property of a urea-based PSMA inhibitor for PET imaging. Bioconjugate Chemistry. 2012;23(4):688-97.
60. Kim KA, Kakitani M, Zhao J, Oshima T, Tang T, Binnerts M, et al. Mitogenic influence of human R-spondin1 on the intestinal epithelium. Science (New York, NY). 2005;309(5738):1256-9.
61. Komiya Y, Habas R. Wnt signal transduction pathways. Organogenesis. 2008;4(2):68-75.
62. Clevers H. Wnt/beta-catenin signaling in development and disease. Cell. 2006;127(3):469-80.
63. Chen B, Dodge ME, Tang W, Lu J, Ma Z, Fan CW, et al. Small molecule-mediated disruption of Wnt-dependent signaling in tissue regeneration and cancer. Nature chemical biology. 2009;5(2):100-7.
64. Livak KJ, Schmittgen TD. Analysis of relative gene expression data using real-time quantitative PCR and the 2(-Delta Delta C(T)) Method. Methods (San Diego, Calif). 2001;25(4):402-8.
65. Krueger F. TrimGalore 2012 [Available from: http://www.bioinformatics.babraham.ac.uk/projects/trim_galore/.
66. Dobin A, Davis CA, Schlesinger F, Drenkow J, Zaleski C, Jha S, et al. STAR: ultrafast universal RNA-seq aligner. Bioinformatics (Oxford, England). 2013;29(1):15-21.
67. Li B, Dewey CN. RSEM: accurate transcript quantification from RNA-Seq data with or without a reference genome. BMC bioinformatics. 2011;12:323.
68. Robinson MD, Oshlack A. A scaling normalization method for differential expression analysis of RNA-seq data. Genome biology. 2010;11(3):R25.
69. Robinson MD, McCarthy DJ, Smyth GK. edgeR: a Bioconductor package for differential expression analysis of digital gene expression data. Bioinformatics (Oxford, England). 2010;26(1):139-40.

70. Edmondson R, Broglie JJ, Adcock AF, Yang L. Three-Dimensional Cell Culture Systems and Their Applications in Drug Discovery and Cell-Based Biosensors. Assay and Drug Development Technologies. 2014;12(4):207-18.
71. Afshar-Oromieh A, Haberkorn U, Hadaschik B, Habl G, Eder M, Eisenhut M, et al. PET/MRI with a 68Ga-PSMA ligand for the detection of prostate cancer. Eur J Nucl Med Mol Imaging. 2013;40(10):1629-30.
72. Eiber M, Weirich G, Holzapfel K, Souvatzoglou M, Haller B, Rauscher I, et al. Simultaneous 68Ga-PSMA HBED-CC PET/MRI Improves the Localization of Primary Prostate Cancer. European Urology. 2016;70(5):829-36.
73. Zacho HD, Nielsen JB, Haberkorn U, Stenholt L, Petersen LJ. 68Ga-PSMA PET/CT for the detection of bone metastases in prostate cancer: a systematic review of the published literature. Clinical Physiology and Functional Imaging.n/a-n/a.
74. McCulloch DR, Opeskin K, Thompson EW, Williams ED. BM18: A novel androgen-dependent human prostate cancer xenograft model derived from a bone metastasis. Prostate. 2005;65(1):35-43.
75. Corey E, Quinn JE, Buhler KR, Nelson PS, Macoska JA, True LD, et al. LuCaP 35: a new model of prostate cancer progression to androgen independence. Prostate. 2003;55(4):239-46.
76. Shoemaker JE, Lopes TJ, Ghosh S, Matsuoka Y, Kawaoka Y, Kitano H. CTen: a web-based platform for identifying enriched cell types from heterogeneous microarray data. BMC Genomics. 2012;13(1):460.
77. Brooke GN, Gamble SC, Hough MA, Begum S, Dart DA, Odontiadis M, et al. Antiandrogens act as selective androgen receptor modulators at the proteome level in prostate cancer cells. Molecular & cellular proteomics : MCP. 2015;14(5):1201-16.
78. Mateo J, Carreira S, Sandhu S, Miranda S, Mossop H, Perez-Lopez R, et al. DNA-Repair Defects and Olaparib in Metastatic Prostate Cancer. N Engl J Med. 2015;373(18):1697-708.
79. Venkitaraman AR. Functions of BRCA1 and BRCA2 in the biological response to DNA damage. Journal of Cell Science. 2001;114(20):3591.
80. Yoshida K, Miki Y. Role of BRCA1 and BRCA2 as regulators of DNA repair, transcription, and cell cycle in response to DNA damage. Cancer Science. 2004;95(11):866-71.
81. Beltran H, Yelensky R, Frampton GM, Park K, Downing SR, MacDonald TY, et al. Targeted Next-generation Sequencing of Advanced Prostate Cancer Identifies Potential Therapeutic Targets and Disease Heterogeneity. European urology. 2013;63(5):920-6.
82. Kumar-Sinha C, Chinnaiyan AM. Precision oncology in the age of integrative genomics. Nature Biotechnology. 2018;36:46.
83. Kriege M, Jager A, Hooning MJ, Huijskens E, Blom J, van Deurzen CH, et al. The efficacy of taxane chemotherapy for metastatic breast cancer in BRCA1 and BRCA2 mutation carriers. Cancer. 2012;118(4):899-907.
84. Akashi-Tanaka S, Watanabe C, Takamaru T, Kuwayama T, Ikeda M, Ohyama H, et al. BRCAness Predicts Resistance to Taxane-Containing Regimens in Triple Negative Breast Cancer During Neoadjuvant Chemotherapy. Clinical Breast Cancer. 2015;15(1):80-5.
85. Tan DSP, Yap TA, Hutka M, Roxburgh P, Ang J, Banerjee S, et al. Implications of BRCA1 and BRCA2 mutations for the efficacy of paclitaxel monotherapy in advanced ovarian cancer. European Journal of Cancer. 2013;49(6):1246-53.
86. Godet I, Gilkes DM. BRCA1 and BRCA2 mutations and treatment strategies for breast cancer. Integrative cancer science and therapeutics. 2017;4(1):10.15761/ICST.1000228.
87. Zheng R, Han S, Duan C, Chen K, You Z, Jia J, et al. Role of taxane and anthracycline combination regimens in the management of advanced breast cancer: a meta-analysis of randomized trials. Medicine. 2015;94(17):e803.

88. Mylavarapu S, Das A, Roy M. Role of BRCA Mutations in the Modulation of Response to Platinum Therapy. Frontiers in Oncology. 2018;8:16.

89. Department of Health. MBS online - The April 2016 Medicare Benefits Schedule [Internet]. : Health.gov.au; 2016 [Available from: http://www.health.gov.au/internet/mbsonline/publishing.nsf/Content/Downloads-201604.

Chapter 8 Appendix

Appendix 1 – R Spondin Conditioned Media validation results

Figure A1 demonstrates how wells with added R-Spondin conditioned media enhance the Wnt3a substrate and luminesce brighter than Wnt3a alone and controls to a maximum response for this assay (seen for the response to 5% CM onwards).

Table A1 R-Spondin Conditioned Media (CM) validation plate setup.

Media	MC	Wnt3a	2.5% CM	5% CM	10% CM	15% CM
Media	MC	Wnt3a	2.5% CM	5% CM	10% CM	15% CM
Media	MC	Wnt3a	2.5% CM	5% CM	10% CM	15% CM

Media only (M), Media + cells only (MC), Media with cells an Wnt3a (Wnt3a), Media + cells + Wnt3a+ 2.5%, 5%, 10%, 15% R Spondin Media
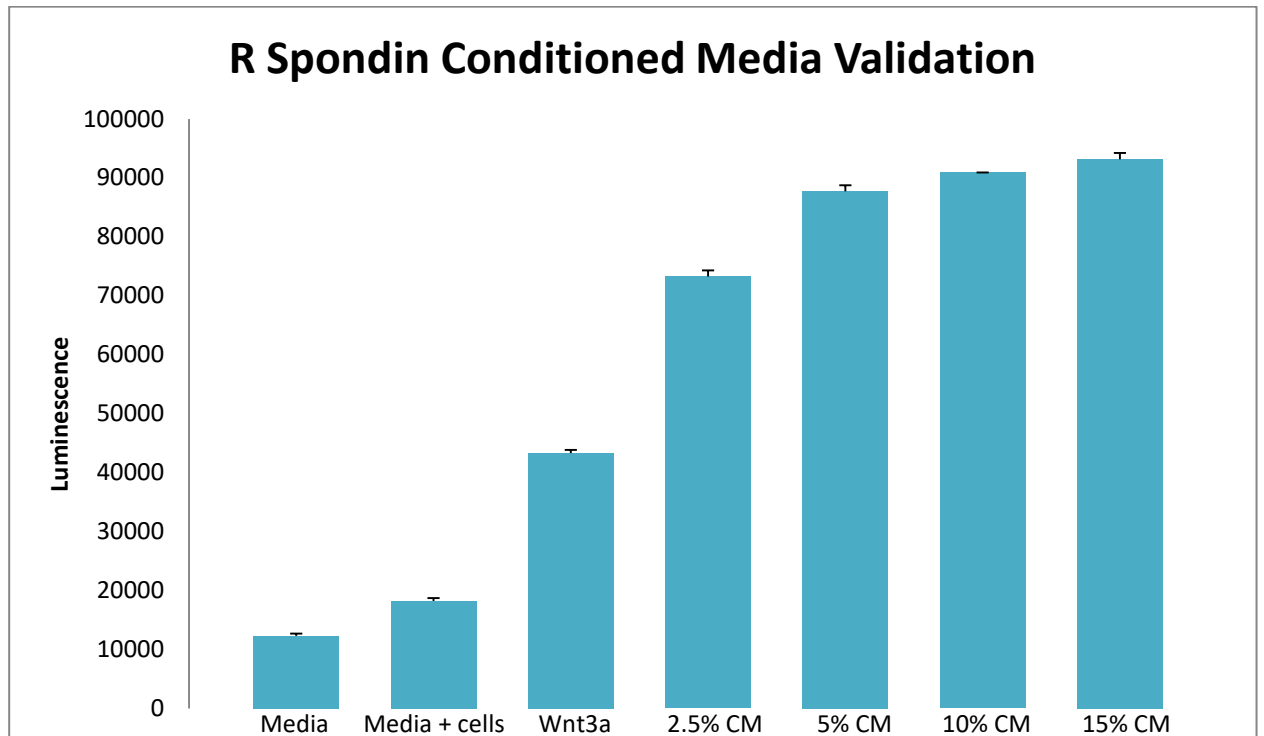
Figure A1 Validation of R-Spondin Conditioned Media (CM). R-Spondin conditioned media significantly increase luminescence when compared to media and Wnt3a substrate alone. CM: conditioned media [n = 3 technical repeats, error bars represent standard error].

Appendix 2 – Noggin Conditioned Media validation results

Noggin conditioned media was validated using a Western blot comparing Recombinant Noggin to various dilutions of conditioned media.

Noggin Human Recombinant produced in E.Coli has a total molecular mass of approximately 46.2 kDa (Noggin Human, ProSpec, 2017). Figure A2 outlines successful validation of Noggin CM. Our cell line Noggin protein has a slightly higher weight than Recombinant Noggin likely due to protein folding and post translational modification of the Noggin protein in our system.

Table A2 *Noggin Conditioned Media (CM) validation plate setup.*

Ladder	RN	RN	CM 25%	CM 25%	CM 50%	CM 50%	CM 75%	CM 75%	CM 100%

ThermoFischer Scientific Page Ruler Plus Pre-stained protein ladder, Recombinant Noggin (RN), Various dilutions of Noggin CM
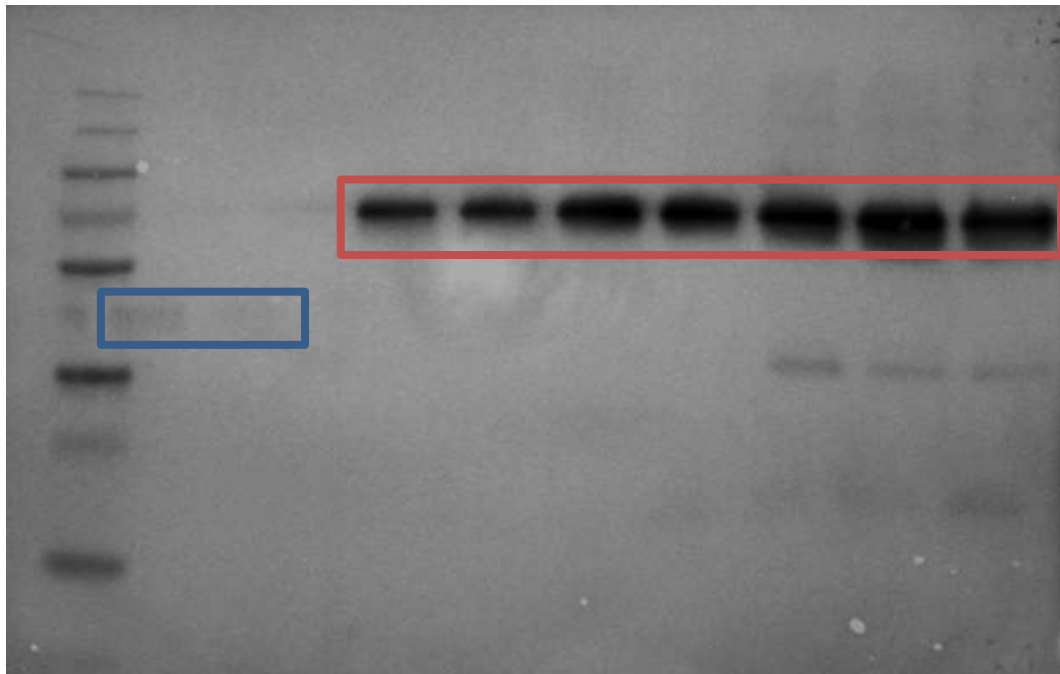
Figure A2 *Validation of Noggin Conditioned Media (CM)..* Our cell line Noggin protein has a slightly higher weight than Recombinant Noggin likely due to protein folding and post translational modification of the Noggin protein in our system. This overall represents successful validation of Noggin conditioned media. Recombinant Noggin (Blue, ~46.2kDa), Conditioned media with increasing concentrations per Table A2 (Orange).

Appendix 3 – Forward and Reverse Primers of Genes of Interest

Table A3 *Forward and reverse primers of genes of interest*

Gene	Primer	Sequence
RPL32	Forward	5'-GCACCAGTCAGACCGATATG-3'
	Reverse	5'-ACTGGGCAGCATGTGCTTTG-3'
AR	Forward	5'-CTGGACACGACAACAACCAG-3'
	Reverse	5'-CAGATCAGGGGCGAAGTAGA-3'
PSA	Forward	5'-AGTGCGAGAAGCATTCCCAAC-3'
	Reverse	5'-CCAGCAAGATCACGCTTTTGTT-3'
FKBP5	Forward	5'-AAAAGGCCACCTAGCTTTTTGC-3'
	Reverse	5'-CCCCCTGGTGAACCATAATACA-3'
TMPRSS2	Forward	5'-CCATTTGCAGGATCCGTCTG-3'
	Reverse	5'-GGATGTGTCTTGGGGGAGCAA-3'
COX IV	Forward	5'-GAGAAAGTCGAGTTGTATCGCA-3'
	Reverse	5'-GCTTCTGCCACATGATAACGA-3'

SOP - Culturing LNCaP cells and treatment with androgens / anti-androgens

(modified from APCRC-Q/MRTA, version 25-Jun-2014)

LNCaP stock   Clone FGC, purchased from ATCC in 2010 @ passage 18 (CRL-1740, LOT:

58431008)

Mycoplasma & XMRV negative LN2 stocks @ passage 23-27 available from the

APCRC-Q

Passage   Discard after passage 50

TC vessels   Corning brand

Culture   37°C, 5% CO_2, humidified incubator

- **NO antibiotics** are to be used for routine culture

- **Monthly** routine testing for **Mycoplasma** (SOP: Mycoplasma test) and **XMRV** (SOP: XMRV test) contamination.

- Additional testing during experiments: Mycoplasma from culture supernatant before harvest, XMRV on extracted RNA.

Routine Culture

1. Pre-warm media, PBS and Trypsin to 37°C

2. Aspirate media from flask

3. Rinse very carefully with PBS

4. Add 1x Trypsin-EDTA/PBS, gently tilt/swirl to evenly cover cells, return to incubator

5. After 3 min observe the cells with an inverted microscope

6. Add HCM , use gentle pipetting to remove cells from surface of flask

7. Transfer to a centrifuge tube and pellet @ 300 xg for 3 min at RT

8. Aspirate supernatant and add 1 ml HCM using a 1 ml pipette, carefully pipette up and down 10-20 times

9. Transfer desired amount of cell suspension into fresh TC vessel containing HCM

10. Passage twice/week @1:2 to 1:4, recommended seeding density for continuous culture around 20% ~ 20,000 cells/cm^2, max 4 days between medium changes

Preparation for androgen/anti-androgen treatment - starting one week before the experiment

1. *Day 0:*   Check visually that resuspended culture is primarily single cells. Count cells & use Trypan Blue staining to assure viability >90%. Plate cells in HCM

2. *Day 3*:   Change media

3. *Day 5*:   Change media

Setting up cultures for androgen/anti-androgen treatment

1. *Day 7:*   Plate cells in TC dish/plate in RPMI + 5% FBS and Incubate cells for 72 hours in HCM

2. *Day 10*: Add treatments to cells as per experimental protocol

   Final concentrations in culture: 10 µM Enzalutamide, Bicalutamide, ARN509

Appendix 5 – Representative Images from all positive scans by patient
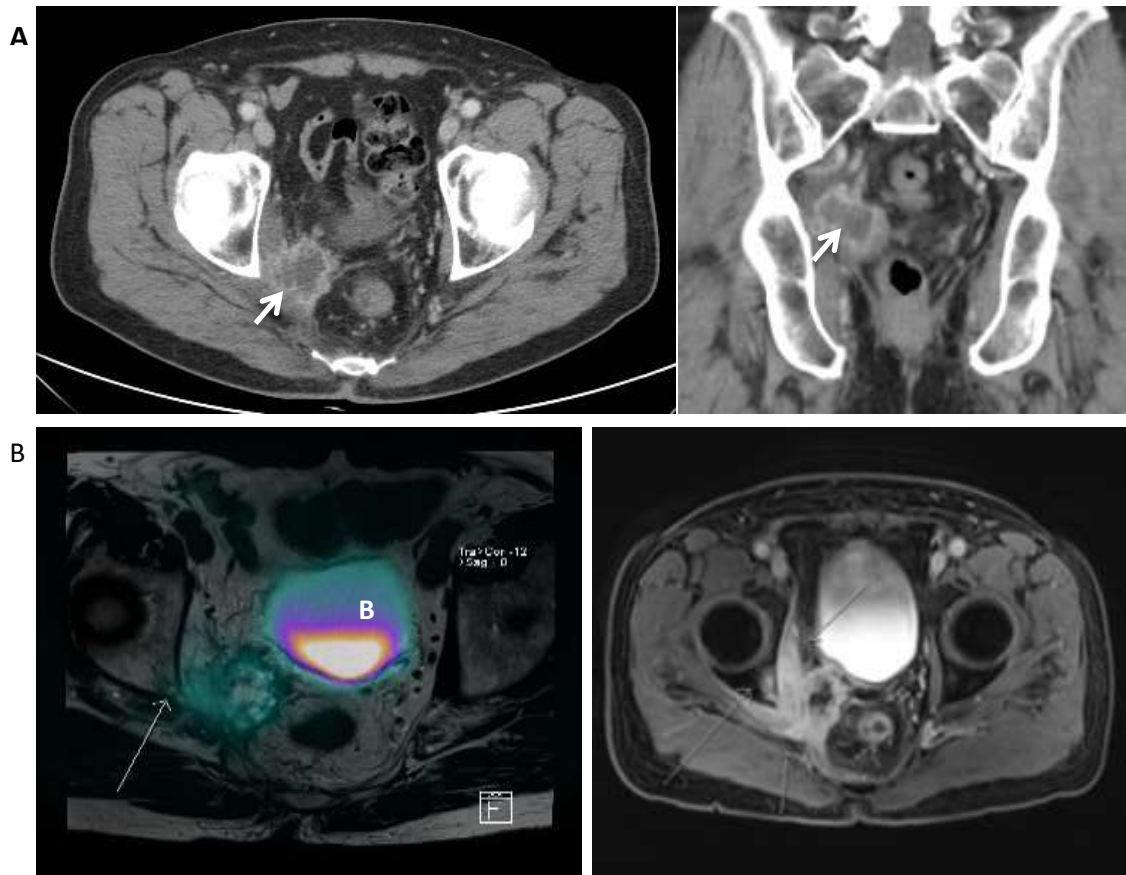
Figure A3 *Invasion recurrent disease demonstrated on CT and PSMA PET imaging for patient BCR001;* (A) Stan4dard CT image showing axial [left panel] and coronal [right panel] views of a right pelvic sidewall mass (white arrows). (B) PSMA PET/MRI demonstrating PSMA avidity of same lesion (white arrow) [left panel]; lesion on T2 weighted MRI demonstrating degree of invasion, not identifiable in (A) (white arrows) [right panel] B: bladder.
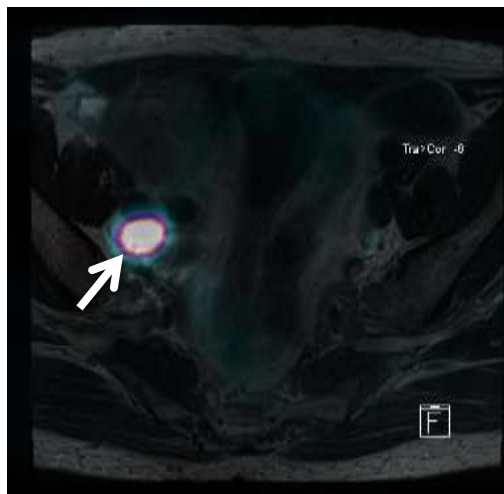
Figure A4 *PSMA PET/MRI imaging for BCR002 demonstrating an isolated PSMA avid right external iliac lymph node* (white arrow)
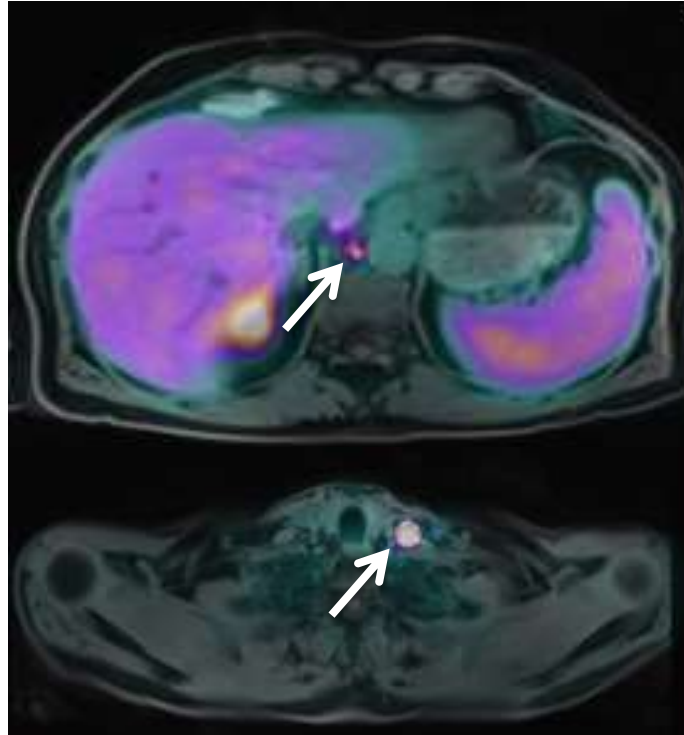
Figure A5 *Patient BCR003 PSMA PET/MRI imaging showing retroperitoneal (top) and supraclavicular (bottom) lymphadenopathy* (white arrow).
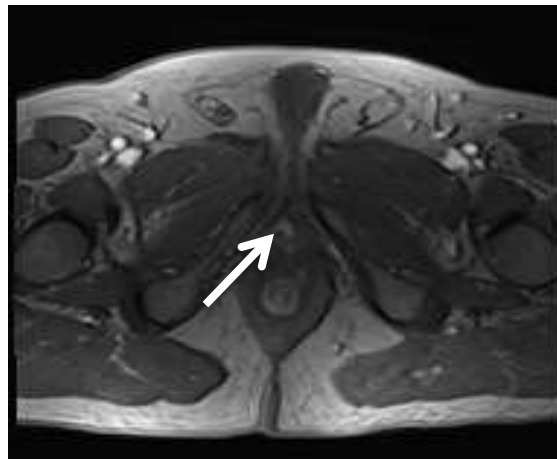
Figure A6 *Axial dynamic contrast-enhanced MRI image showing tumour recurrence at vesicourethral anastomosis in patient BCR004* (white arrow).
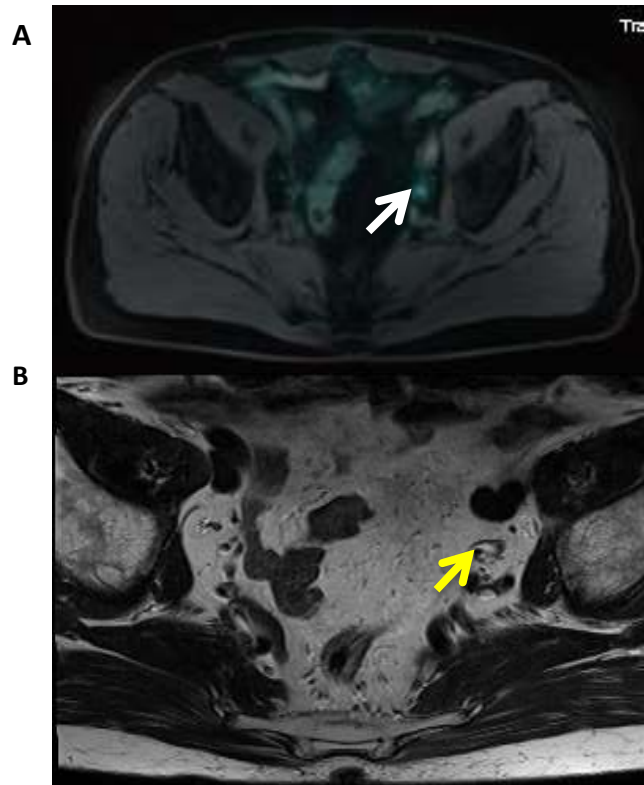
Figure A7 Imaging in patient BCR005 demonstrating the added benefit of T2 MRI component of the PSMA PET/MRI; (A) PSMA PET/MRI demonstrating PSMA avidity in left pelvic side wall (white arrow) (B) T2 weighted MRI correlating avidity with urine in a dilated left ureter (yellow arrow).
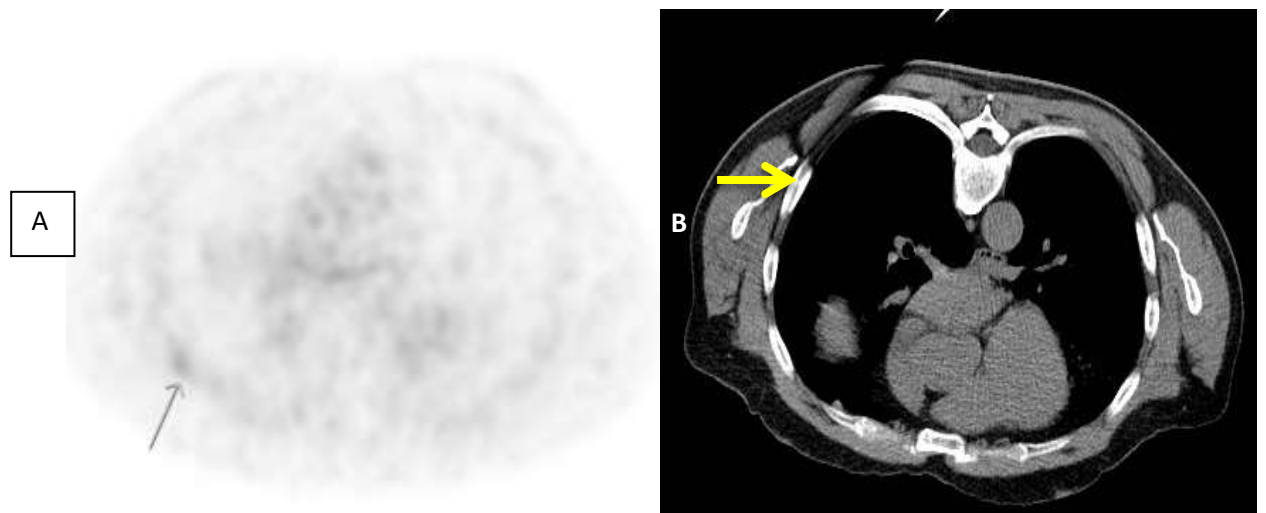
Figure A8 Imaging for BCR006 demonstrating a biopsied PSMA avid rib lesion; (A) Axial PSMA PET/MRI showing an avid Rib lesion (black arrow) (B) CT guided biopsy of avid lesion (yellow arrow pointing to intended biopsy target on CT at time of biopsy).
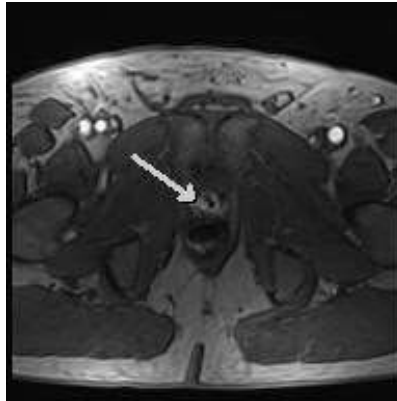
Figure A9 An example of locoregional recurrence at prostatectomy site demonstrated on Axial dynamic contrast-enhanced MRI imaging in patient BCR007 (white arrow).
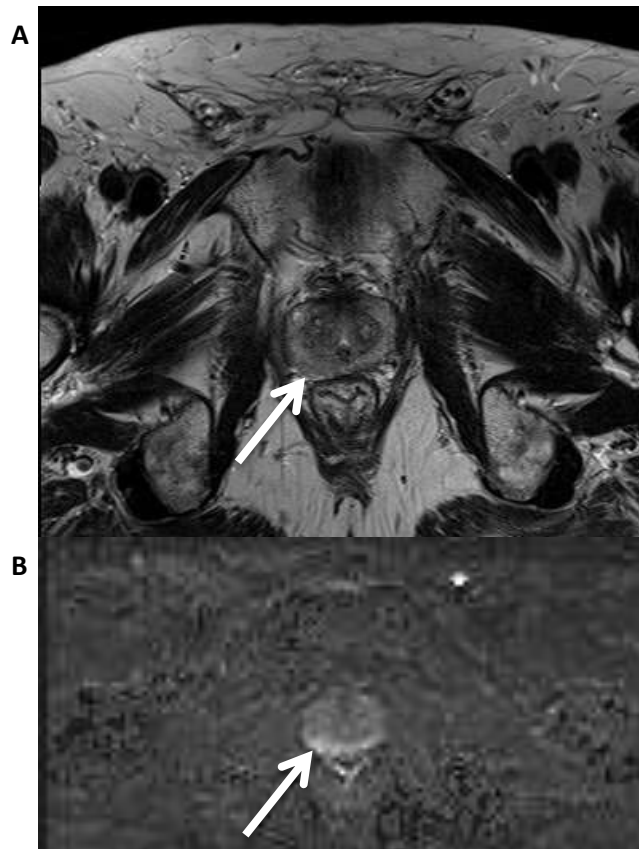
Figure A10 Imaging for patient BCR012 demonstrating intraprostatic recurrence; (A) T2 weight MRI image and (B) DWI demonstrating local recurrence in the right peripheral zone of the prostate (white arrow).
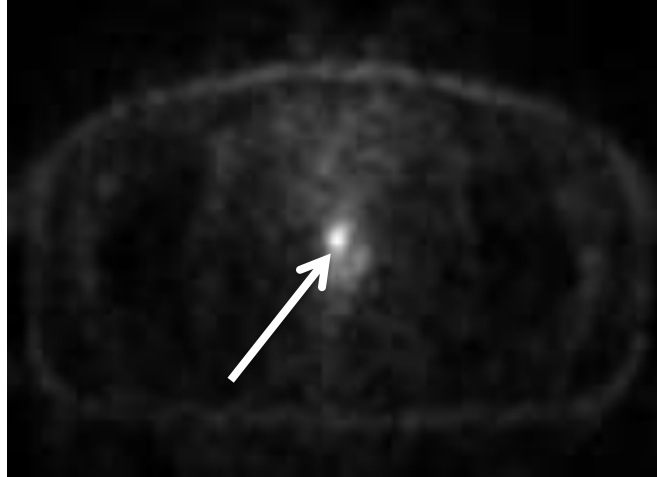
Figure A11 **MRI-based attenuation correction (MRAC) PSMA PET series demonstrating an area of recurrence next to prostate in patient BCR013** (white arrow).
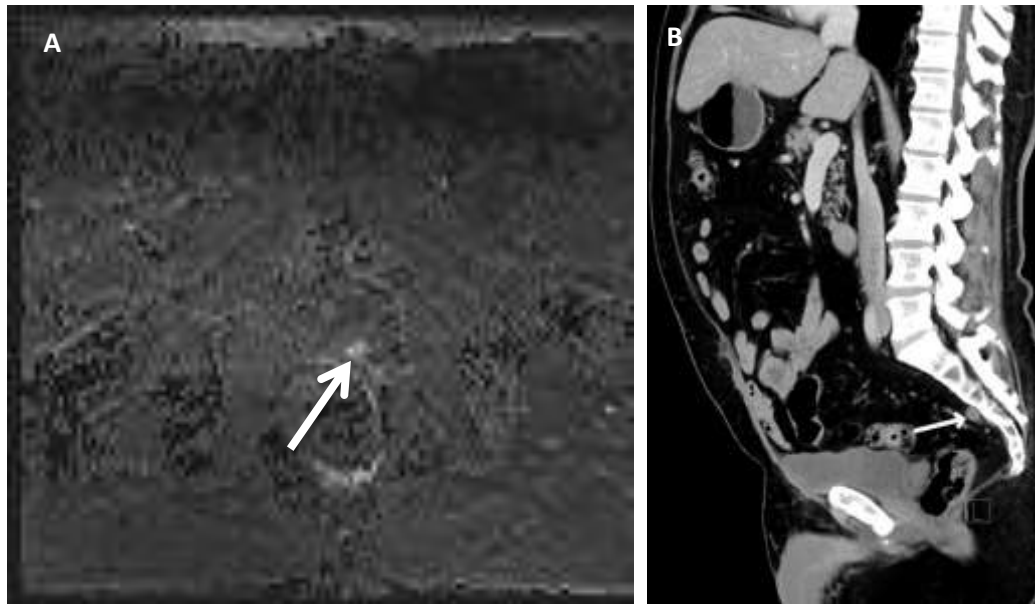
Figure A12 **Biochemical recurrence in patient BCR014 secondary to local recurrence; (**A) DWI MRI demonstrating local left seminal vesicle recurrence (B) SOC CT demonstrating a pre sacral node which did not have PSMA avidity on PSMA PET MRI.

Figure A13 Patient BCR015 demonstrating evidence of local recurrence on imaging; (A) Extensive recurrence within prostate gland, demonstrated on PSMA PET MRI (B) T2 weighted MRI component showing concordance with PSMA PET, demonstrating recurrent lesion (white arrows).
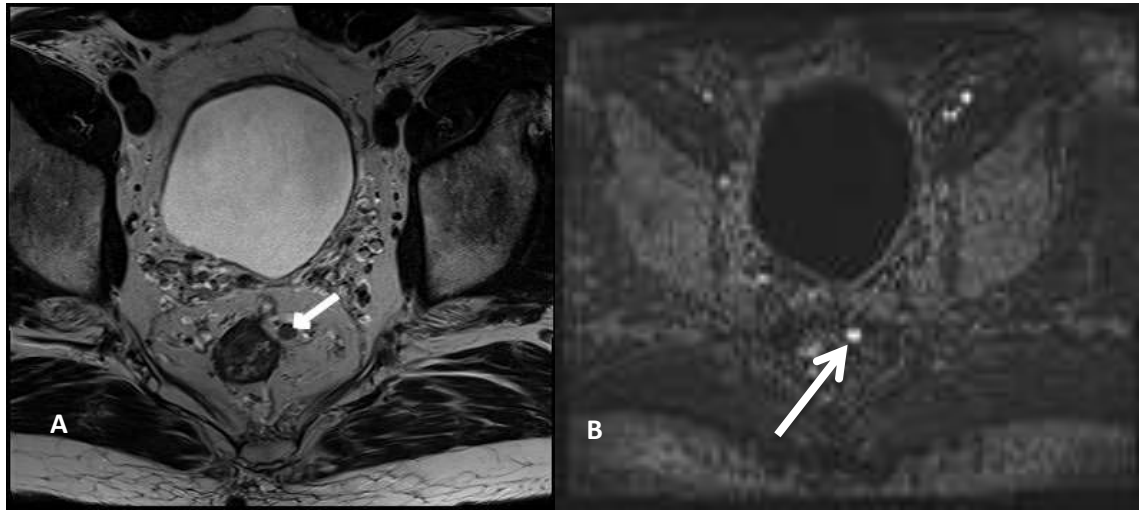
Figure A14 Presacral nodal recurrence, demonstrated on T2 weight MRI (A) and DWI MRI (B) in patient BCR016 (white arrows).
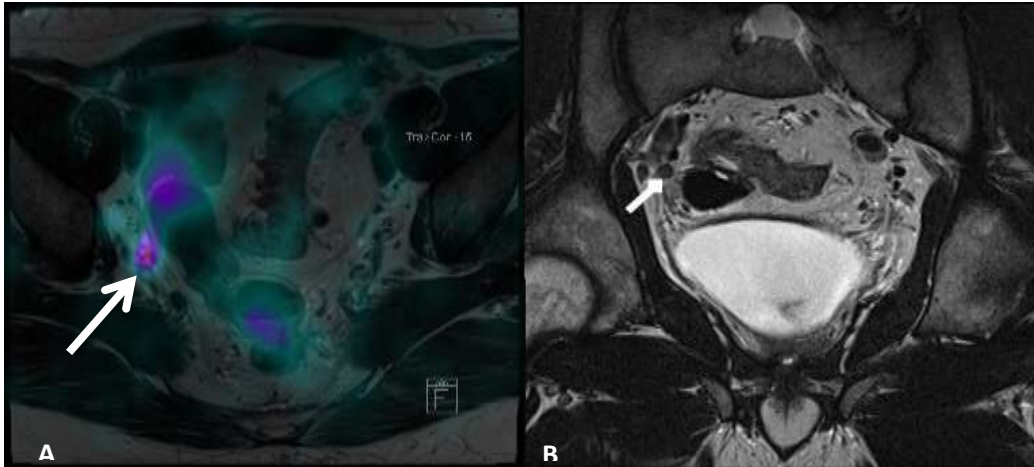
Figure A15 **Right iliac nodal recurrence demonstrated in patient BCR017;** (A) PSMA PET MRI demonstrating PSMA avid right iliac node (B) Right iliac node on T2 weighted MRI (white arrows).
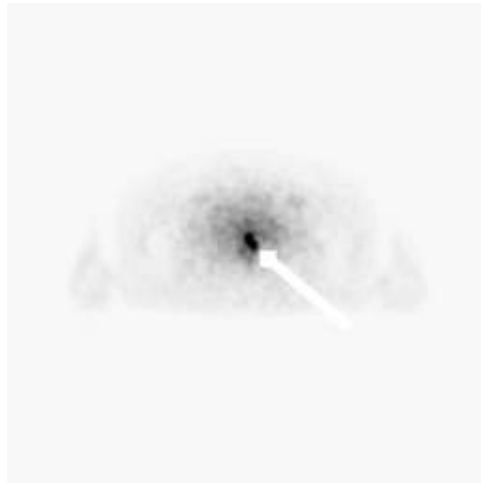
Figure A16 **Local recurrence to left of the prostatic bed demonstrated on MRAC PSMA PET series images in patient BCR018**(white arrow)
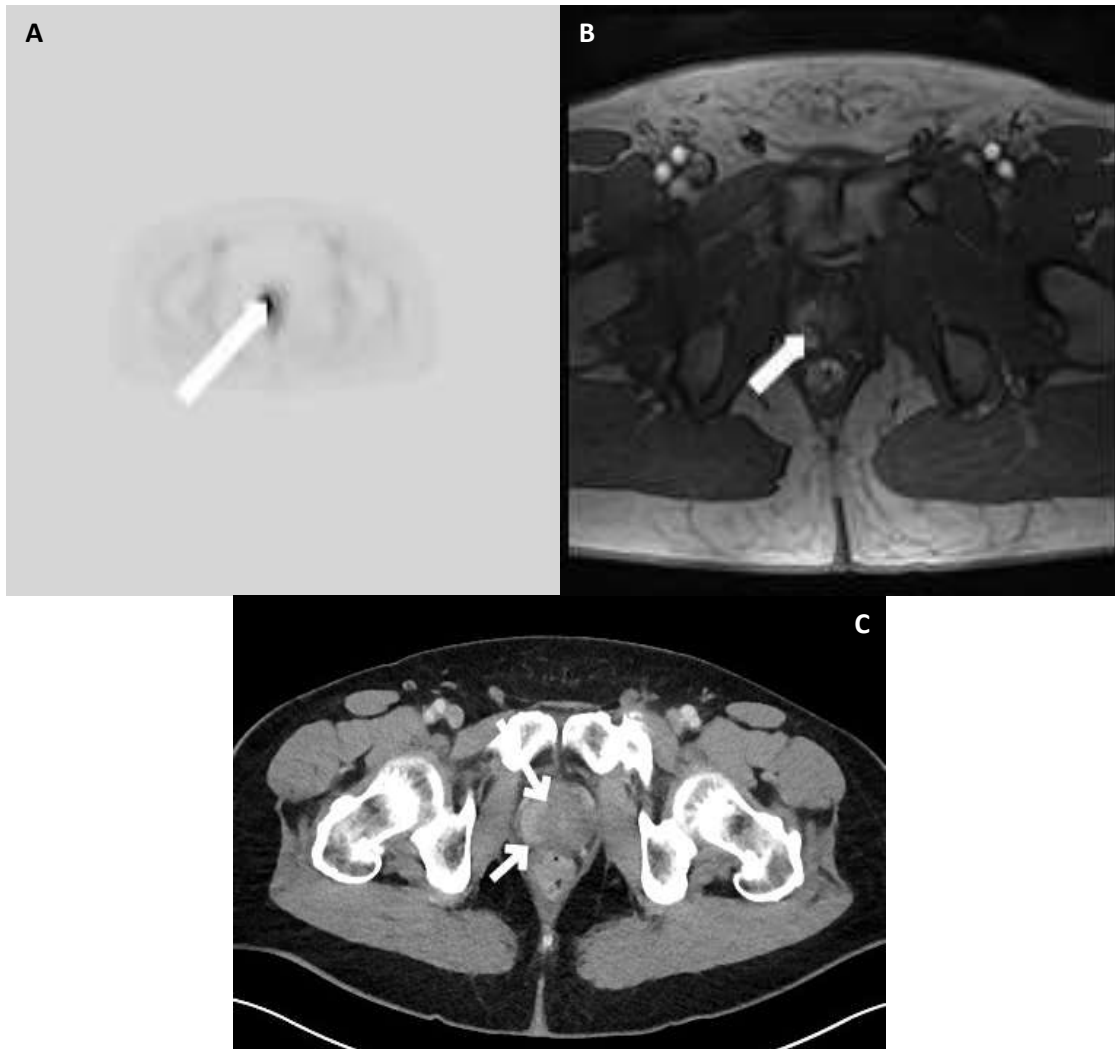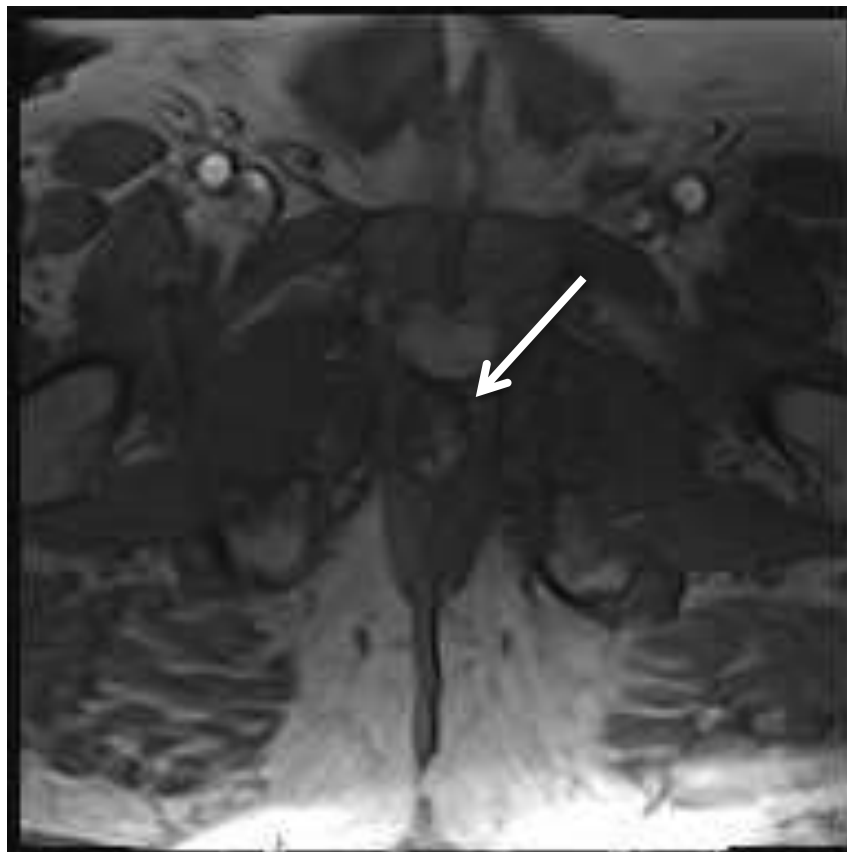
Figure A17 **Intraprostatic recurrent disease identified in patient BCR020;** (A) PSMA avid recurrent intra-prostatic disease in the right peripheral zone on MRAC PET (B) Area of enhancement on dynamic MRI series correlating with PET (C) disease visible on SOC contrast CT correlating with PSMA PET findings (white arrows).
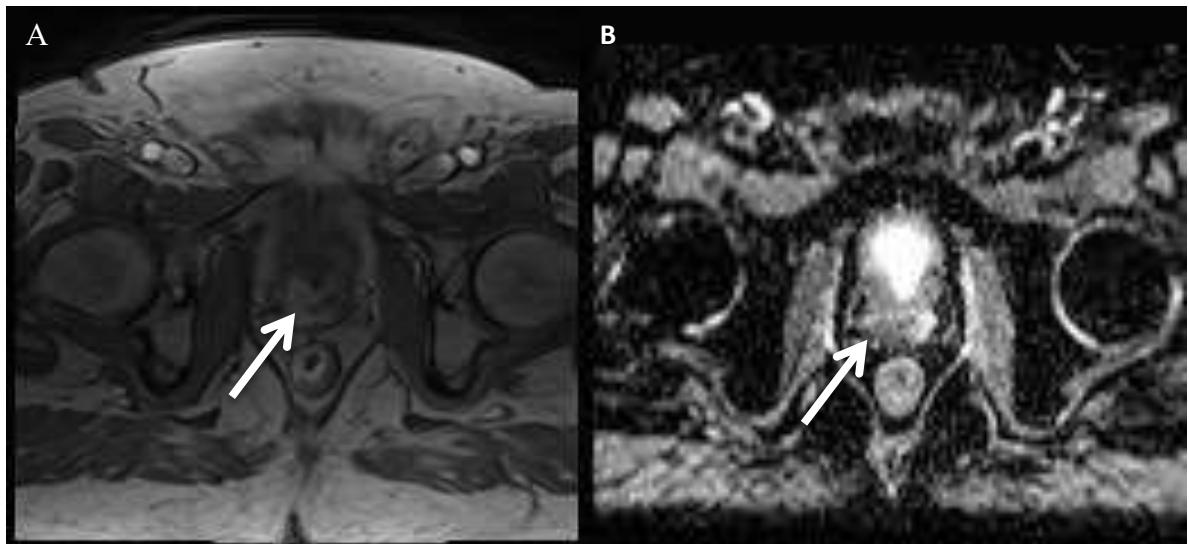
Figure A18 **PSMA PET avid Seminal vesical invasive disease identified in patient BCR021;** (A) PSMA avid lesion involving the base of right prostate gland transition zone on Dynamic MRI (B) Invasion into right seminal vesicles demonstrated on DWI MRI (white arrows).


Figure A19 **PSMA avidity in the left prostate gland suggesting recurrent disease in patient BCR022 demonstrated on DWI MRI** (white arrow).
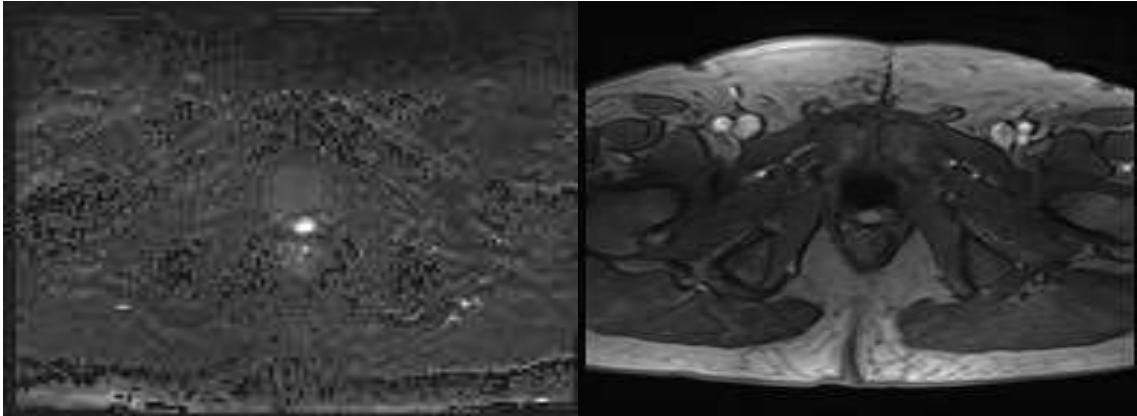
Figure A20 **Focal PSMA avid soft tissue recurrence at the prostatic bed best characterised on DWI (A) and Dynamic MRI (B) in patient BCR023** (white arrows).
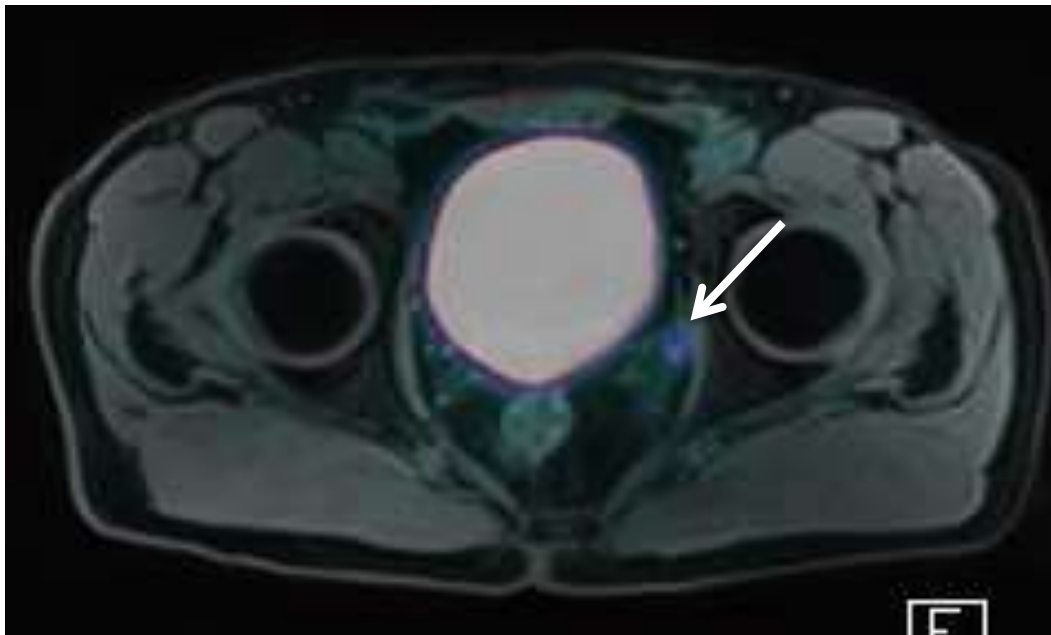
Figure A21 **PSMA avid non-enlarged left pelvic sidewall lymph node on PSMA PET MRI imaging for patient BCR025** (white arrow).
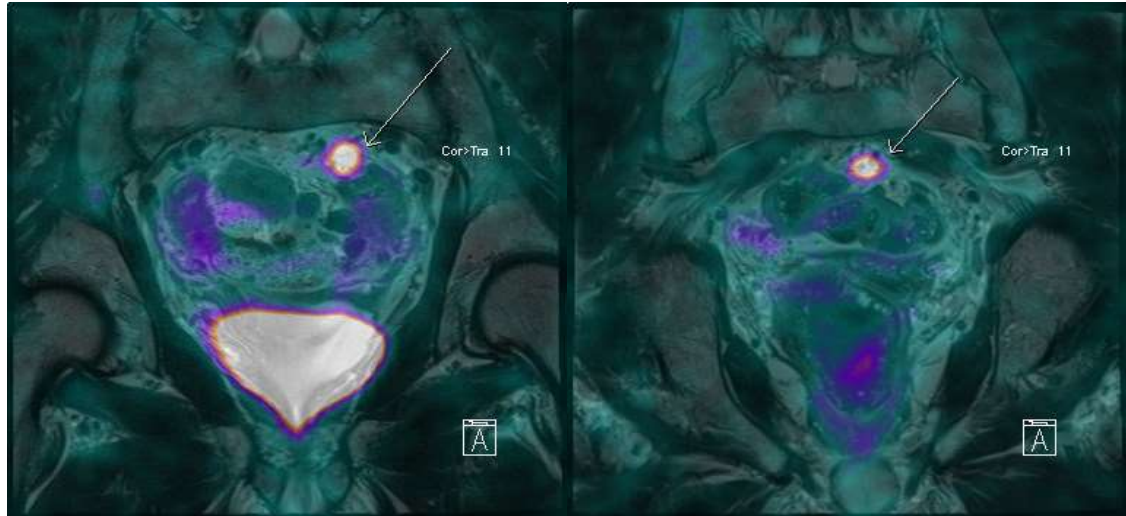
Figure A22 Multiple PSMA avid enlarged pelvic and presacral lymph nodes identified in patient
BCR028 on PSMA PET MRI (white arrows).
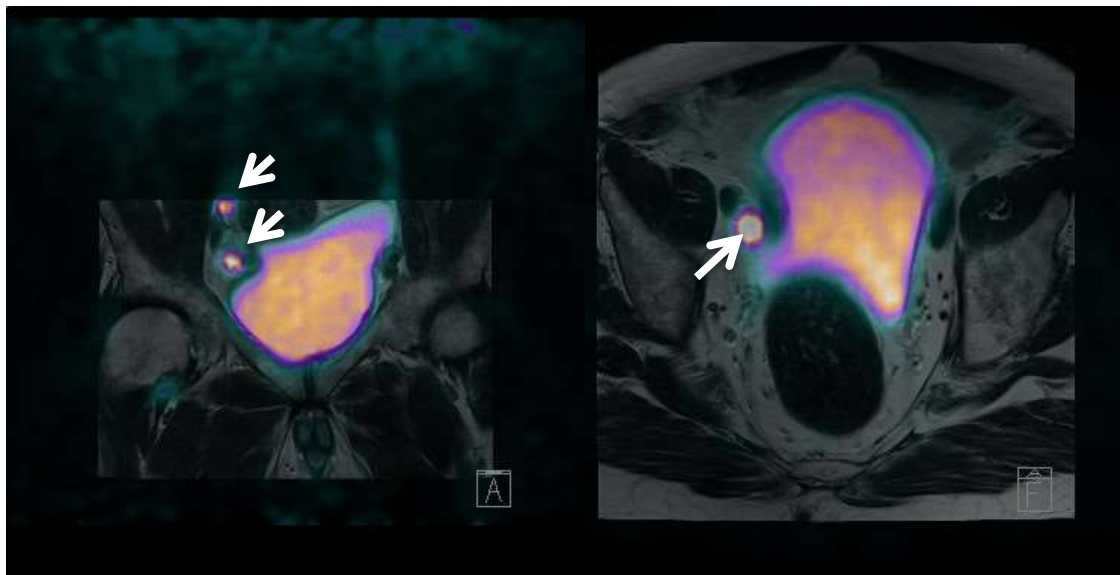
Figure A23 Multiple PSMA avid enlarged right pelvic and iliac lymph nodes demonstrated PSMA PET
MRI imaging in patient BCR029 (white arrows).